U.S. DEPARTMENT OF ENERGY | National Energy Technology Laboratory

OFFICE OF FOSSIL ENERGY

# Guidance for NETL's Oxycombustion R&D Program: Chemical Looping Combustion Reference Plant Designs and Sensitivity Studies

December 19, 2014

**DOE/NETL – 2014/1643**

# Disclaimer

This report was prepared as an account of work sponsored by an agency of the United States Government. Neither the United States Government nor any agency thereof, nor any of their employees, makes any warranty, express or implied, or assumes any legal liability or responsibility for the accuracy, completeness, or usefulness of any information, apparatus, product, or process disclosed, or represents that its use would not infringe privately owned rights. Reference therein to any specific commercial product, process, or service by trade name, trademark, manufacturer, or otherwise does not necessarily constitute or imply its endorsement, recommendation, or favoring by the United States Government or any agency thereof. The views and opinions of authors expressed therein do not necessarily state or reflect those of the United States Government or any agency thereof.

All exhibits have been created by NETL unless otherwise noted.

**Author List:**

**National Energy Technology Laboratory (NETL)**

*Robert Stevens*
**General Engineer, Performance Division**

**Energy Sector Planning and Analysis (ESPA)**

*Richard Newby, Vasant Shah, Norma Kuehn, Dale Keairns*
**Booz Allen Hamilton, Inc.**

This report was prepared by Energy Sector Planning and Analysis (ESPA) for the United States Department of Energy (DOE), National Energy Technology Laboratory (NETL). This work was completed under DOE NETL Contract Number DE-FE0004001. This work was performed under ESPA Task 341.03.15.

The authors wish to acknowledge the excellent guidance, contributions, and cooperation of the NETL staff, particularly:

Robert Stevens, NETL Technical Monitor, and Kristin Gerdes

**DOE Contract Number DE-FE0004001**

This page intentionally left blank.

# Table of Contents

# Exhibits

# Acronyms and Abbreviations

| | |
|---|---|
| $Al_2O_3$ | Aluminum oxide |
| Ar, AR | Argon |
| ASU | Air separation unit |
| BBR | Bituminous Baseline report |
| BFW | Boiler feed water |
| BH | Baghouse |
| BOP | Balance of plant |
| Btu/lb | British thermal unit per pound |
| $CaCO_3$ | Calcium carbonate |
| CaO | Calcium oxide |
| CaS | Calcium sulfide |
| $CaSO_4$ | Calcium sulfate |
| CCS | Carbon capture and sequestration |
| $CH_4$ | Methane |
| $CH_y$ | General fuel symbol |
| CLC | Chemical looping combustion |
| CO | Carbon monoxide |
| $CO_2$ | Carbon dioxide |
| COE | Cost of electricity |
| COS | Carbonyl sulfide |
| DOE | Department of Energy |
| ESPA | Energy Sector Planning and Analysis |
| FD | Forced draft |
| $Fe_2O_3$ | Hematite |
| $Fe_3O_4$ | Magnetite |
| FGD | Flue gas desulfurization |
| ft/s | Feet per second |
| FY | First year |
| GJ/hr | Gigajoule |
| gpm | Gallon per minute |
| h, hr | Hour |
| $H_2$ | Hydrogen |
| $H_2O$ | Water |
| $H_2S$ | Hydrogen sulfide |
| HCl | Hydrogen chloride |
| Hg | Mercury |
| HHV | Higher heating value |
| HR | High-risk |
| HRSG | Heat recovery steam generator |
| ID | Induced draft |
| IGCC | Integrated gasification combined cycle |
| ISO | Independent system operator |
| $kg/m^3$ | Kilogram per cubic meter |
| kgmol/hr | Kilogram-mole per hour |
| kJ/kg | Kilojoule per kilogram |
| kWe | Kilowatt electric |
| kWh | Kilowatt-hour |
| kWth | Kilowatt thermal |
| $lb/ft^3$ | Pound per cubic foot |
| lb/hr | Pounds per hour |
| lbmol/hr | Pound moles per hour |
| LR | Low-risk |
| $m^3/min$ | Cubic meter per minute |
| mm | millimeter |
| MMBtu/hr | Million British thermal units per hour |
| mole% | Molar compositing in percent |
| MOx | Oxygen carrier symbol |
| MPa | Millions of pascals |
| MW | Megawatt electric |
| MWh | Megawatt-hour |
| N/A | Not applicable |
| $N_2$ | Nitrogen |
| NETL | National Energy Technology Laboratory |
| $NO_X$ | Nitrogen oxide |
| $NH_3$ | Ammonia |
| $O_2$ | Oxygen |
| O&M | Operating and maintenance |
| PC | Pulverized coal |
| ppmv | Parts per million by volume |
| psi | Pound per square inch differential |
| psia | Pound per square inch absolute |
| psig | Pound per square inch gauge |
| QGESS | Quality Guidelines for Energy Systems Studies |
| R&D | Research and development |
| SC | Supercritical steam |
| SCR | Selective catalytic reduction |
| $SO_2$ | Sulfur dioxide |
| TASC | Total as-spent cost |
| TGA | Thermogravimetric analysis |
| TOC | Total overnight cost |
| TPC | Total plant cost |
| T&S | Transport and storage |
| U.S. | United States |

| | | | |
|---|---|---|---|
| $/MWh | Dollars per megawatt-hour | °F | Degrees Fahrenheit |
| °C | Degrees Celsius | | |

# Executive Summary

An emerging, coal-fired power plant technology, chemical looping combustion (CLC), is assessed in this report. CLC technology is, in essence, an oxycombustion technology being developed with focus on its potential for improved performance and reduced cost. Its benefits are measured against performance and cost of the conventional pulverized coal (PC) power plant using amine-based $CO_2$ absorption for post-combustion carbon capture. This study develops National Energy Technology Laboratory (NETL) reference CLC plant configurations and assumptions that are used to evaluate CLC system performance and cost.

In CLC, the oxygen carrier particles replace the oxygen source, air or air separation unit (ASU)-derived oxygen, used in the conventional PC plant or in the oxy-combustion PC plant. A key variable in the CLC technology is the type of oxygen carrier applied in the process reactors. CLC reference plant configurations for two types of oxygen carriers are assessed in this document. The two oxygen carrier types considered are an iron-based carrier, $Fe_2O_3$ supported on alumina, and $CaSO_4$ generated by limestone sulfation. These two oxygen carriers represent alternative approaches to CLC, the first using highly reactive, but expensive, metal oxide applied on a fabricated particle structure, and the second using lower-reactivity, but cheaper, oxygen carrier material.

The Reference CLC power plants are described in Section 3. Key operating conditions and configuration features for the chemical looping processes are summarized in Exhibit ES-1.

**Exhibit ES-1 Comparison of reference plant reactor conditions and configuration features**

| Oxygen Carrier Type | $Fe_2O_3$ | $CaSO_4$ |
|---|---|---|
| Reducer reactor type | Circulating fluid bed | Circulating fluid bed |
| Reducer outlet gas velocity (ft/s) | 30 | 29 |
| Reducer temperature (°F) | 1,745 | 1,800 |
| Reducer pressure drop (psi) | 21.4 | 2.9 |
| Solids flow to Reducer (1000 lb/hr) | 94,374 | 17,183 |
| Oxidizer reactor type | Circulating fluid bed | Circulating fluid bed |
| Oxidizer outlet gas velocity (ft/s) | 31 | 26 |
| Oxidizer temperature (°F) | 1,800 | 2,000 |
| Reducer off-gas $H_2$ and CO (mole%) | 0.05 | 1.5 |
| Oxidizer pressure drop (psi) | 1.8 | 0.4 |
| Oxygen carrier flow to Oxidizer (1000 lb/hr) | 93,566 | 16,363 |
| Oxidizer off-gas $O_2$ (mole%) | 3.5 | 3.5 |
| Location of solids cooler | Solids stream to Reducer | Solids stream to Oxidizer |
| Use of fuel recovery/$CO_2$ purification | None needed | Used for fuel recovery |

Several CLC process concepts were considered for the reference plant design including bubbling fluidized beds, circulating fluidized beds, and moving beds. A circulating fluid bed CLC process design was selected. The Reducer and Oxidizer reactors are circulating fluidized beds operated with high gas velocities and with temperatures, pressure drops, solids circulation rates, and off-gas compositions characteristic of the oxygen carrier properties. The significance of these characteristics is described in this document.

Reference CLC power plant performance and cost have been estimated for these two oxygen carriers by means of process simulation to generate power plant energy and material balances. The reference CLC plant concept includes a supercritical steam cycle and conventional carbon dioxide compression technology. Plant material and energy balance results are reported in Section 4. Integrated with the process simulation has been CLC reactor modeling to estimate main reactor performance and dimensions, as outlined in Section 7.

Exhibit ES-2 compares the overall performance and cost of CLC power generation using the two oxygen carriers to the performance and cost of conventional PC power generation using amine-based post-combustion carbon capture. [1] The performance and cost values are calculated using a common basis, described in Section 2, to ensure that the comparisons can produce valid conclusions. The cost of electricity (COE) for the CLC plant concepts assumes the high-risk financial structure.

**Exhibit ES-2 Comparison of CLC reference plant results to conventional PC plant**

| Oxygen Carrier Type | $Fe_2O_3$ | $CaSO_4$ | Conventional PC BBR Case 12 |
|---|---|---|---|
| Plant Net Capacity (MW) | 550 | 550 | 550 |
| Plant Efficiency (%, HHV) | 35.1 | 32.6 | 28.4 |
| Carbon Capture Efficiency (%) | 95.8 | 91.4 | 90 |
| $CO_2$ Product Purity (mole% $CO_2$) | 98.9 | 99.7 | 100 |
| Total Plant Cost ($/kW; $2011) | 2,379 | 2,597 | 3,563 |
| Cost of Electricity ($/MWh; 1st-year w/o T&S) | 115.2 | 104.7 | 137.3 |
| Reduction in COE (%) [Reference IGCC w CCS @ 133 $/MWh] | 13.4 | 21.3 | -3.2 |
| Cost of Captured $CO_2$ ($/tonne) [Reference SC PC plant @ 81.0 $/MWh] | 40.1 | 26.8 | 56.5 |

It is seen from the exhibit results that, although the $Fe_2O_3$ oxygen carrier CLC power plant has higher plant efficiency and lower plant capital cost, the $CaSO_4$ oxygen carrier CLC power plant has lower COE. This lower COE is a direct result of the expected higher price of the makeup $Fe_2O_3$ oxygen carrier relative to the lower price for a $CaSO_4$ oxygen carrier makeup limestone.

The impact of the cost of oxygen carrier makeup is shown in the COE breakdown in Exhibit ES-3. Both CLC reference power plants show a sizable COE advantage over the comparable conventional PC power plant with amine-based carbon capture.

**Exhibit ES-3 Cost of electricity breakdown comparison**

| Cost | $Fe_2O_3$ ($/MWh) | $CaSO_4$ ($/MWh) | Conventional PC BBR Case 12 |
|---|---|---|---|
| Capital | 49.6 | 53.4 | 73.1 |
| Fixed | 11.3 | 12.2 | 15.7 |
| Variable | 25.7 | 8.4 | 13.2 |
| Maintenance materials | 3.2 | 3.5 | 4.7 |
| Water | 0.4 | 0.4 | 0.9 |
| Oxygen carrier makeup * | 18.7 | 1.1 | N/A |
| Other chemicals & catalyst | 1.9 | 1.7 | 6.4 |
| Waste disposal | 1.4 | 1.7 | 1.3 |
| Fuel | 28.4 | 30.8 | 35.3 |
| Total | 115.1 | 104.7 | 137.3 |

*$Fe_2O_3$ oxygen carrier makeup: 132 tons/day @ $2,000 per ton; Limestone carrier makeup: 439 tons/day @ $33.5 per ton

The carbon capture efficiency of the $CaSO_4$ oxygen carrier CLC plant, at 91.4 percent, is less than that of the $Fe_2O_3$ oxygen carrier CLC plant due to $CO_2$ losses in the CLC processing that ensures that fuel constituents (CO and $H_2$) are not lost and the $CO_2$ product stream is sufficiently pure. Alternative processing can be applied that will produce a lower purity $CO_2$ product stream while yielding lower $CO_2$ losses.

The CLC reference plant assessments have identified the status and potential issues associated with the CLC technology:

- The development status of CLC power generation is at a laboratory/bench-scale; insufficient test data and data correlation are available to project plant performance and cost with any degree of certainty.
- The Reducer reactor is complex and is the major developmental component in the CLC process.
- The Reducer reactor is a simultaneous coal gasifier and oxygen carrier reducer, and it operates at temperatures where char gasification reaction rates are relatively slow.
- The Reducer reactor char gasification efficiency may limit the CLC power plant performance.
- To minimize the Reducer reactor size and meet the carbon capture requirement, a char-oxygen carrier separation process must also be developed as part of the Reducer system.

- The char-oxygen carrier separation process requires processing very large amounts of solids, an 18 to 100 million lb/hr mixture of coal ash and oxygen carrier particles having a small content of char particles, to extract and recycle at least eighty percent of the char.
- The Reducer off-gas (the raw $CO_2$ stream) may contain substantial $H_2$ and CO, and purification with fuel recovery may be needed to maintain the plant efficiency and to meet $CO_2$ product purity specifications.
- $CO_2$ capture efficiency as high as ninety percent may be difficult to achieve, depending on how high the Reducer reactor carbon gasification efficiency can be maintained and how low the Reducer off-gas $H_2$ and CO content will be.

There is significant uncertainty in the CLC process performance and cost for the initial set of operating conditions and design parameters selected, and sensitivity studies have been performed to assess how sensitive the CLC power plant performance and cost is to the major operating conditions and design parameters. Sensitivity studies around the CLC reference plant designs have been completed for the major CLC process operating conditions, design parameters, and cost parameter, and are reported in Section 6.

It is found that increased temperature results in reduced Oxidizer vessel height and reduced forced draft (FD) fan auxiliary power consumption. While these are helpful trends, these improvements will not result in significant improvements in the CLC plant performance or cost. It is concluded that the best operating temperature for the Reducer and Oxidizer vessels with respect to operational reliability and oxygen carrier durability needs to be identified experimentally. The benefits of temperature increases above this best-temperature can then be considered relative to the detrimental impacts of these increases.

As the Reducer velocity increases, the vessel shell diameter decreases, but does not approach a vessel size that could be shop fabricated. Increasing velocity also results in greatly increased Reducer vessel height with a moderate increase in the off-gas $H_2$ and CO content. There is certainly no clear benefit resulting from increased Reducer velocity for either of the two oxygen carrier types. The impact on reactor footprint versus reactor vessel height needs to be assessed for given plant sites to provide further perspective and a basis for judging these sensitivity results.

A similar trend is shown for the Oxidizer velocity sensitivity. Increasing the Oxidizer velocity for both types of oxygen carriers yields a reduction in the Oxidizer shell diameter, which is beneficial. This is accompanied by an increase in the Oxidizer vessel height and the Oxidizer FD fan power consumption due to higher Oxidizer vessel pressure drop. Again, it is concluded that there is no clear benefit to be shown for increasing the Oxidizer velocity. It should also be noted that operating velocities above 30 ft/s enter a region of limited commercial operational experience in circulating fluid beds and would require significant development effort.

The benefit of the char-oxygen carrier separator appears to be clear. Without char-oxygen carrier separation the Reducer vessel height and vessel cost are dramatically increased to a point where the Reducer would not be a feasible reactor to construct and install. In the Reference plants, it is assumed that 80 percent of the unconverted carbon transported from the Reducer is separated and recycled to the Reducer for an overall carbon conversion efficiency of 96 percent.

When using char-oxygen carrier separation, increased carbon gasification efficiency results in moderately greater Reducer vessel heights and vessel costs, with slightly decreased off-gas $H_2$

and CO content. Increased carbon gasification efficiency will only serve to increase the plant $CO_2$ capture efficiency and will not impact the power plant thermal efficiency significantly since all of the carbon not gasified in the Reducer will be burned in the Oxidizer reactor. There appears to be little need for Reducer carbon gasification efficiency greater than that needed to achieve 90 percent carbon capture efficiency.

The real need is to develop technically feasible and affordable char-oxygen carrier separation approaches for achieving even this limited level of carbon gasification efficiency. The technology challenge is the very high rate of solids flow having very small content of char that is characteristic of these CLC processes.

Lower levels of oxygen carrier conversion will result in higher reactivity oxygen carrier, and lower Reducer off-gas $H_2$ and CO contents. Lower levels of oxygen carrier conversion also result in moderately higher Oxidizer FD fan power consumption, and a very large increase in the oxygen carrier circulation rate.

With the $Fe_2O_3$ oxygen carrier, the oxygen carrier is inherently of high reactivity, and higher conversions can be applied to avoid the huge oxygen carrier circulation rates that would result at low oxygen carrier conversion. The reference plant conversion level of about sixty-nine percent appears to be a good design choice.

The $CaSO_4$ oxygen carrier is a low reactivity material, with inherently low oxygen carrier circulation rates. Operating at lower levels of oxygen carrier conversion results in a relatively high reactivity in the Reducer, and also gives oxygen carrier circulation rates that are low compared to those found for the $Fe_2O_3$ oxygen carrier. Again, the $CaSO_4$ oxygen carrier Reference plant conversion of about nineteen percent appears to be a good design choice.

Large oxygen carrier circulation rates are relatively easy to accommodate when using circulating fluidized bed reactors, because the Reducer and Oxidizer off-gases are the transport gases for the circulating solids and can generate high circulation rates if required. High rates are more costly and consume more auxiliary power with other reactor types of reactors, such as bubbling fluidized beds or moving beds. In these types of reactors the oxygen carrier circulation system is a completely independent equipment system, and a separate transport gas system is needed.

The $Fe_2O_3$ oxygen carrier has an expected price of $1/lb to $5/lb, and with high makeup rates the COE could exceed the COE of the conventional PC plant. For the $Fe_2O_3$ oxygen carrier CLC power plant to have lower COE than the $CaSO_4$ oxygen carrier CLC power plant the $Fe_2O_3$ makeup rate will need to be quite low. Minimizing $Fe_2O_3$ oxygen carrier losses is a priority for process development.

The $CaSO_4$ oxygen carrier, even if at a relatively high limestone price, can accommodate high makeup rates and maintain a COE significantly lower than the conventional PC plant. At the lower price assumed in the reference plant design, the limestone makeup rate is not a significant consideration.

In the reference plant evaluations, the hypothetical char-oxygen carrier separation system was assumed to have zero cost. To understand how sensitive the CLC plant COE is to the potential capital cost of the char-carrier separation system, a range of char-carrier costs has been applied that are equivalent to as much as ten times the cost of the Reducer reactor. It is found that the capital cost of the char-carrier separation system is not likely to have a significant impact on the

CLC power plant COE. The performance and reliability of the char-carrier separation system, though, will be critically important.

At this early stage of development of CLC technology, the uncertainties in its performance and cost are great. The process simulations in this report have shown the possibility that CLC could provide sizable performance and cost advantages over conventional PC power plants using conventional, amine-based $CO_2$ capture technology. These findings may be optimistic given that the CLC plant operability and availability are assumed in this report to be the same as that of the conventional PC power plant. Operability and reliability issues are likely to represent the major challenges to be dealt with in continued, larger-scale development of CLC technology.

# 1 Introduction

Chemical looping combustion (CLC) is an emerging technology current undergoing bench and early pilot testing. The main characteristic of chemical looping combustion that is being taken advantage of is its inherent oxycombustion of fuels without the need to include an air separation process in the plant. It is expected that the elimination of the air separation process might result in a power plant having performance and cost advantages over a conventional plant applying oxycombustion or post-combustion carbon capture. This is the application of chemical looping combustion that is evaluated in this document.

This oxycombustion application is accomplished by splitting the fuel combustion operation into a pair of coupled reactors, the Reducer and the Oxidizer. In the ideal, simplified description of CLC, within the Reducer the fuel reduces a solids reactant to a lower oxidation state while converting the fuel to primarily $CO_2$ and $H_2O$. The ideal reaction describing this is:

$$\mathbf{CH_y\ (fuel) + (2+y/2) \bullet MO_x => CO_2 + y/2 \bullet H_2O + (2+y/2) \bullet MO_{x-1}}$$

The Reducer off-gas represents the raw $CO_2$ product stream that is then dehydrated and compressed for sequestration.

The reduced solid reactant is transported to an adjacent reactor, the Oxidizer, and is reacted with air to return it to its fully oxidized state:

$$\mathbf{MO_{x-1} + 1/2 \bullet O_2 => MO_x}$$

The Oxidizer off-gas represents the plant flue gas, containing nitrogen and excess oxygen. Steam is generated by heat recovery from the off-gas streams and from solids cooling, and this steam is used for conventional steam turbine power generation.

In reality, with a real fuel such as coal, the actual reaction mechanisms are much more complex, and the reaction steps do not proceed to completion, with intermediate reaction products and fuel contaminant forms also generated. The Reducer and Oxidizer reactors are modeled in this evaluation to estimate their behavior and performance, but the reactor mechanisms and behavior are not fully understood at this point in their development, and the modeling results are very uncertain.

One of the major areas of research activity has been on the development of effective oxygen carriers, and a multitude of metal oxides and metal sulfates have been proposed and tested under laboratory conditions. Oxygen characteristics such as reactivity, oxygen capacity, durability, and price have been considered, but there is currently not sufficient, long-term pilot testing and commercial assessment to select an optimum oxygen carrier. In this document, two oxygen carrier types are evaluated, a metal oxide-based, supported $Fe_2O_3$ carrier, and a limestone-based $CaSO_4$ carrier. These represent two significantly differing types of oxygen carriers that have received much research interest, and have been speculated to have promising characteristics.

The application considered in this report is a base-load, utility, coal-fueled CLC power plant. It's estimated performance and cost is compared to that of a conventional pulverized coal (PC) power plant that uses amine-based, post-combustion $CO_2$ capture.

# 2 CLC Plant Design, Modeling, and Cost Estimation Bases

Chemical looping combustion reference power plant designs, with estimates of performance and cost, are developed in this document for two specific oxygen carriers, a $Fe_2O_3$-based oxygen carrier and a $CaSO_4$-based oxygen carrier. The general design basis for the power plants is identical to the design basis described in detail in the National Energy Technology Laboratory (NETL) Bituminous Baseline report (BBR) for comparable, conventional, PC power plants. [1] The essential aspects of the design basis are presented in this report.

The chemical looping combustion power plant contains two unique reactors, the Reducer and Oxidizer that require significant modeling efforts to estimate their design features and performance. The general modeling approach applied is outlined in this section.

Most equipment components in the CLC power plant are conventional, and their performance and cost can be estimated by scaled from the Bituminous Baseline report performance and cost estimates for conventional PC power plants. Other equipment components, the Reducer and Oxidizer and their associated subsystems, are developmental in nature, and their costs must be estimated by approximate sizing of the equipment and application of general cost correlations. The cost estimation approach applied is summarized in this section.

## 2.1 Design Basis

This is a base-load, electric utility, power generation application. The reference CLC power plant is assumed to be located at a generic Midwestern United States (U.S.) plant site and the ambient conditions and site characteristics correspond to Midwest Independent System Operator (ISO) conditions listed in the Quality Guidelines for Energy System Studies (QGESS) process modeling parameters document. [2] The key features of the design basis are:

- ambient conditions: ISO
- nominal net plant capacity: 550 MW
- design coal: Illinois No. 6
- steam conditions: supercritical {3,500 psig (24 MPa), 1100°F (593°C),1100°F (593°C)}
- carbon capture requirement: at least 90 percent
- $CO_2$ product purity requirement: at least 95 percent $CO_2$ mole content
- $CO_2$ product delivery pressure: 2200 psig

The Illinois No.6 coal as described in the QGESS coal feedstock specification [2] was used in the present study.

Assumptions for the performance of major equipment components within the plants that are consistent with those used in the Bituminous Baseline report are applied. Some major items are:

- fan efficiency: 75% (polytropic)
- compressor efficiency: 86% (polytropic)
- electric motor efficiency: 97%
- generator efficiency: 98.5%

Pressure drops and auxiliaries representative of conventional equipment components in the CLC power plant are scaled directly from the comparable equipment components characterized in the BBR Case 12. Such equipment components are:

- coal handling
- coal pulverizers
- limestone handling
- ash handling
- forces and induced draft fans
- gas cleaning (baghouses, flue gas desulfurization [FGD], selective catalytic reduction [SCR])
- steam turbine cycle
- cooling water system

## 2.2 Cost Estimation Basis

Cost estimation for the CLC Reference plants are maintained consistent with the BBR, with the costs being updated to 2011-dollars. Major costing premises are:

- plant capacity factor: 85 percent
- plant financial classification: High-risk
- capital charge factor : 12.43 percent per year
- fixed and variable operating and maintenance (O&M) costs: Estimated analogously with BBR Case 12 [1]

Conventional equipment costs are scaled from the BBR Case 12 analogous equipment costs. Such equipment components are:

- coal handling system
- coal preparation and feed systems
- feedwater and miscellaneous balance of plant (BOP) systems
- gas cleaning
- steam turbine generator system
- cooling water system
- accessory electric plant
- instrumentation and control
- improvements to site
- buildings and structures

For novel equipment or equipment unique to the CLC application, as listed below, approximate equipment sizing and general cost correlations must be applied:

- reducer reactor
- oxidizer reactor
- cyclones
- high-temperature piping
- solids cooling steam generator
- fuel recovery/$CO_2$ purification and compression

## 2.3 Reactor Modeling Basis

The behavior and performance of the Reducer and Oxidizer reactors is controlled by the characteristics of the oxygen carrier reaction kinetics, the coal gasification kinetics, and the fluidized bed hydrodynamics and mass transfer. Specific assumptions have been selected to represent each of these for the reference CLC plant and these are summarized in Exhibit 2-1.

The two oxygen carrier types considered in the reference plant design have characteristics and properties extracted from the literature on chemical looping combustion. Exhibit 2-1 summarizes the main characteristics of the oxygen carriers assumed and also addresses coal gasification aspect of the Reducer reactor modeling basis. A large literature exists on $Fe_2O_3$-based oxygen carrier CLC reaction behavior observed in laboratory testing, and a key reference has been applied that provides reaction kinetics correlations for a specific $Fe_2O_3$ oxygen carrier. [3] Alstom has previously conducted laboratory and bench-scale studies for CLC using $CaSO_4$ oxygen carrier, [4] but has not reported reaction kinetic correlations. Several literature resources on $CaSO_4$ laboratory reaction kinetics have been applied, as listed in the exhibit, all testing only pure calcium anhydrite; however, none of these tested limestone-based $CaSO_4$. Section 7 of this report reviews some details relating to the oxygen carrier reaction kinetics applied in this evaluation.

The Reducer reactor is, in reality, a coal gasifier with the oxygen carrier generating $CO_2$ and $H_2O$ from reaction with the coal gasification product $H_2$ and CO. Because the rate of char gasification at the relatively low Reducer temperature is very small, the gasification rate controlled the volume of the Reducer reactor needed. Section 7 of this document reviews the coal gasification assumptions applied and shows how the char gasification kinetics and the oxygen carrier reaction kinetics inter-relate within the Reducer reactor.

With respect to the oxygen carrier delivered price, the $Fe_2O_3$ oxygen carrier is expected to be a relatively expensive fabricated material, in the range of $2,000 to $10,000 per ton, while the $CaSO_4$ makeup material will be low-cost limestone, having a delivered price of $30 to $300 per ton. A cost sensitivity study in Section 6.5 also considers the influence of the $Fe_2O_3$ oxygen carrier price on the CLC power plant cost of electricity if cheaper forms of $Fe_2O_3$-based oxygen carrier were used, such as a natural ore (e.g., hematite) or a waste material (e.g., red mud).

**Exhibit 2-1 Reactor modeling basis**

| Modeling Factor | $Fe_2O_3$ | $CaSO_4$ |
|---|---|---|
| **Oxygen Carrier Characteristics** | | |
| Oxygen carrier type | Supported metal oxide | Natural quarry material |
| Makeup carrier composition | 45 wt% $Fe_2O_3$ on $Al_2O_3$ support | Limestone |
| Particle size, mm (in) | 0.28 (0.01) | 0.5 (0.02) |
| Particle density, $kg/m^3$ ($lb/ft^3$) | 3250 (203) | 1571 (98) |
| Reduction and oxidation kinetics | Rapid; shrinking grain model behavior | Slow; shrinking grain model behavior |
| Reaction kinetic sources | Abad [3] | Song, et al [6], Tian, H., and Q. Guo [7], Qilei Song [8] |
| Oxygen carrier reactivity with coal contaminants | Yes, with $SO_2$, $H_2S$, HCl | Yes, with $SO_2$, $H_2S$, HCl |
| Oxygen carrier price (delivered $/ton) | High (2,000-10,000 $/ton) | Low (100 – 300 $/ton) |
| **Coal Gasification Characteristics** | | |
| Coal devolatilization rate | Very fast (about 0.5 second gas residence time) | |
| Char gasification rate | Very slow compared to oxygen carrier reactor rates | |
| Char gasification kinetics sources | Johnson [9] | |
| **Fluidized Bed Characteristics** | | |
| Oxygen carrier Fluidization Class [5] at reactor conditions | B | B |
| Type of Reducer fluidized bed regime | Turbulent at bottom and fast, circulating bed at top | Turbulent at bottom and fast, circulating bed at top |
| Type of Oxidizer fluidized bed regime | Fast, circulating bed | Fast, circulating bed |
| Fluid bed reactor model sources | Kunii, D., and O. Levenspiel [10] and Abba, et al [5] | |

Section 7 addresses the modeling approach and the resulting design equations applied for the CLC, circulating fluid bed Reducer and Oxidizer reactors.

# 3 Chemical Looping Combustion Reference Plant Descriptions

The general configurations of the chemical looping combustion plants using the two oxygen carrier types are very similar. The major subsystems and features of the CLC plants are:

- Reducer circulating fluid bed reactor and associated cyclones, with char/oxygen carrier separation and char recycle to the Reducer to minimize $CO_2$ losses and to reduce the Reducer reactor volume
- Oxidizer circulating fluid bed reactor and associated cyclones, with possible need for ash/oxygen carrier separation to minimize carrier losses
- Reducer reactor off-gas heat recovery, particulate, Hg control, and FGD
- Oxidizer off-gas heat recovery, particulate control, and possible SCR
- Circulating solids heat recovery unit
- Integrated $CO_2$ product stream compression, and purification, with recovered fuel constituents fed to the Oxidizer
- Steam turbine power cycle (supercritical)

This section describes the CLC power plant configuration, equipment functions, and stream conditions. The operating conditions and reactor performances differ significantly between the $Fe_2O_3$ and $CaSO_4$ oxygen carrier cases.

## 3.1 General CLC Power Plant Configuration

Exhibit 3-1 is a block flow diagram of the $Fe_2O_3$ oxygen carrier-based power plant, but it will also serve to describe the $CaSO_4$-based CLC power plant configuration. The heart of the power plant is the Reducer and Oxidizer reactors coupled with circulating oxygen carrier. Coal is delivered to the base of the Reducer using conversional coal handling and coal feeding equipment. A stream of makeup oxygen carrier ($Fe_2O_3$ or $CaSO_4$) is also fed at the Reducer base. Steam and $CO_2$ recycled from the fuel recovery and compression system provide initial fluidization and coal devolatilization reactants for the Reducer. The $CO_2$ recycle is a slip-stream from the Reducer's raw-$CO_2$ stream that has passed through the first compression stage of the $CO_2$ compression system. It contains primarily $CO_2$, but also may contain some unconverted fuel constituents.

The Reducer is a circulating fluidized bed reactor, and a set of four parallel cyclones capture the entrained stream of oxygen carrier, coal char, and coal ash particles, and three recycle them to the base of the Reducer. One of the cyclones captures of the Reducer entrained solids and transports it to the Oxidizer reactor. Because this is a circulating bed reactor, no separate solids transport system is needed.

The off-gas from the Reducer represents the raw $CO_2$ stream to be sequestered. It contains primarily $CO_2$ and $H_2O$, but also has portions of particulate, $H_2$, CO, and coal contaminants ($SO_2$, $H_2S$, HCl, Hg, etc.). The particulate and coal contaminants must be removed from the raw $CO_2$ stream using conventional cleaning equipment (baghouse, FGD, and mercury removal by activated carbon injected into the baghouse). A heat recovery steam generator (HRSG) precedes the gas cleanup equipment, producing a portion of the plant steam turbine system steam.

**Exhibit 3-1 Reference CLC power plant block flow configuration**

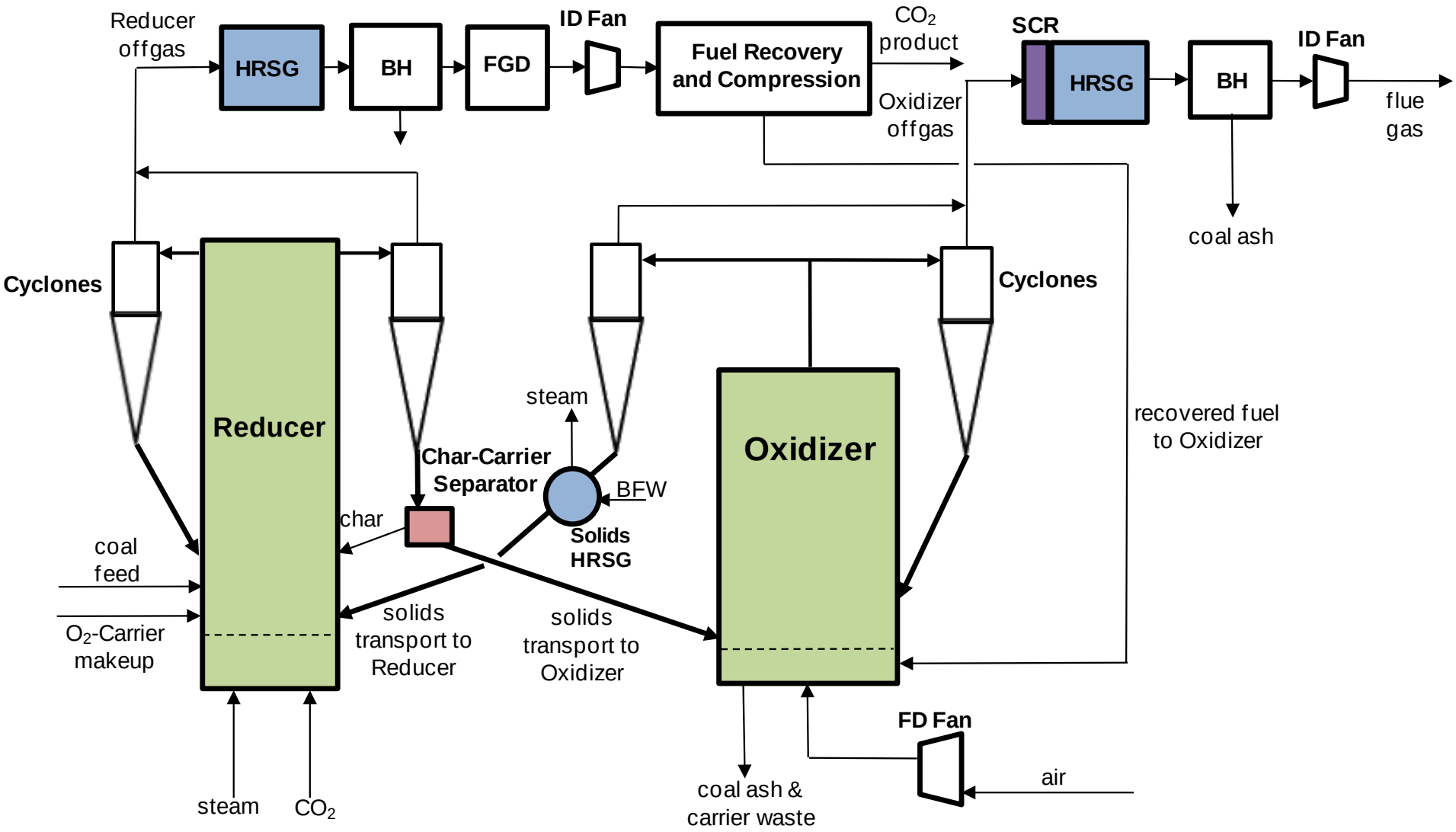

The unconverted fuel constituents (primarily $H_2$ and CO) may need to be separated from the raw $CO_2$ stream and fed to the Oxidizer for utilization. This is a function of the fuel recovery and compression system, which is a near-term, low-temperature, phase separation technique for purification and compression of the $CO_2$ stream. [11] The $Fe_2O_3$ oxygen carrier is sufficiently reactive that the $H_2$ and CO content of the Reducer off-gas is low, and fuel recovery is not needed. In this case, conventional $CO_2$ stream dehydration and compression is applied. In contrast, the $CaSO_4$ oxygen carrier, having relatively low reactivity, results in a significant amount of $H_2$ and CO in the Reducer off-gas, and fuel recovery/$CO_2$ purification is applied to yield a more pure $CO_2$ product and to utilize all of the fuel constituents.

The Reducer reactor is the most complex of the two reactors, and conducts simultaneous coal gasification and the partial reduction of the oxygen carrier ($Fe_2O_3$ carrier to $Fe_3O_4$; or $CaSO_4$ to CaS) within a circulating fluidized bed environment. Because coal gasification is slow at the temperature of the Reducer, a significant amount of char may be unconverted and fed to the Oxidizer with the oxygen carrier solids circulation stream. It is expected that the carbon transferred to the Oxidizer would be significant enough to result in unacceptable power plant carbon capture. Thus, a device is inserted into the Reducer solids transport stream to separate char from the ash and oxygen carrier and recycle it to the Reducer. The separation will result in a more compact Reducer reactor by increasing the content and residence time of char particles in the Reducer reactor, and will yield acceptable carbon capture efficiency. The char-carrier-ash separator device is undeveloped and is a conceptual unit operation in the reference plant design. There are many char-carrier-ash separation mechanisms that can be attempted, such as:

- particle segregation due to particle density differences
- particle segregation due to particle size differences
- particle separation based on differences in magnetic properties

In the reference plant this device is treated as a separator block that separates out eighty percent of the unconverted char and recycles this char back to the Reducer.

The Oxidizer reactor is a much simpler reactor than the Reducer reactor. In it, air reacts with the partially-reduced oxygen carrier particles from the Reducer, converting them back to a nearly fully oxidized form of the oxygen carrier. The oxygen carrier stream from the Reducer delivers the partially-reduced oxygen carrier to the base of the Oxidizer vessel. This stream must be stripped of fuel gas constituents, and its flow is controlled by L-valve aeration. The Oxidizer is also a circulating bed reactor and uses eight parallel cyclones in the same way the Reducer reactor does: six for recycle of entrained solids back into the Oxidizer and the remaining two to transport a portion of the total entrained solids to the Reducer vessel, with this solids transport stream being stripped of air and controlled by aerated L-valves.

Because of the high particle velocities existing in the Oxidizer, and the limited volume of the Oxidizer reactor, no in-bed heat transfer surface is used. Instead, an external solids heat recovery unit (solids HRSG) is placed on the solids stream transported to the Reducer for the $Fe_2O_3$ oxygen carrier and on the solids transport stream leading to the Oxidizer for the $CaSO_4$ oxygen carrier. This is a moving bed heat exchanger, and solid heat exchangers of this type are currently commercially available at smaller capacities. [12]

The off-gas from the Oxidizer primarily contains nitrogen with excess oxygen, $H_2O$, particulate, some $CO_2$, and small amounts of coal contaminants, as well as the possibility for some NOx. It is

expected that Oxidizer off-gas cleaning requirements will be limited to particulate control using a conventional baghouse and SCR (not shown). The baghouse is preceded by an HRSG. A conventional forced draft fan to supply the Oxidizer air flow and conventional induced draft fans are utilized.

The power plant must maintain a coal ash inventory balance within the reactors. This is normally performed in fluidized bed reactors by draining a portion of the Oxidizer reactor bed mass, which is a mixture of coal ash and oxygen carrier particles. In the reference plant configuration for $Fe_2O_3$ oxygen carrier it is assumed that the coal ash material balance is maintained by cyclone ash losses through the Reducer and Oxidizer cyclones. This is assumed to be accomplished by using moderately efficient cyclone designs that allow the lighter and smaller ash particles to penetrate the cyclones while capturing the larger, denser oxygen carrier particles. The reference plant configuration for $Fe_2O_3$ oxygen carrier requires no Oxidizer bed drain, with all the oxygen carrier losses also being through cyclone penetration, and the makeup oxygen carrier being based on these losses.

In contrast, with the $CaSO_4$ oxygen carrier it is assumed that high-efficiency cyclones are utilized that permit very little of the relatively low-density ash and oxygen carrier particles to penetrate. Oxidizer bed drainage is applied to maintain the plant coal ash material balance, and the $CaSO_4$ oxygen carrier makeup is fed to the Reducer to account for the oxygen carrier lost with the drained coal ash from the Oxidizer.

In cases where the plant ash material balance is maintained by Oxidizer bed drainage, large oxygen carrier losses may result. If this is the case, and if it results in an unacceptable operating cost for makeup oxygen carrier, an additional device will be needed to separate oxygen carrier from the bed ash to minimized oxygen carrier losses. Such a device is not required for the reference plants due to the assumptions applied.

## 3.2 Reference Plant Stream Conditions

The major reactor conditions and plant configuration features for the two oxygen carrier types are compared in Exhibit 3-2. The $Fe_2O_3$ oxygen carrier reactors operate at lower temperatures than the $CaSO_4$ oxygen carrier reactors. Much higher solids circulation rates and bed pressure drops result with the $Fe_2O_3$ oxygen carrier than with the $CaSO_4$ oxygen carrier. Better Reducer performance results with the $Fe_2O_3$ oxygen carrier than with the $CaSO_4$ oxygen carrier as indicated by the Reducer off-gas $H_2$ and CO content. This results in no need for fuel recovery/$CO_2$ purification with the $Fe_2O_3$ oxygen carrier; with the $CaSO_4$ oxygen carrier it is assumed that purification is required so that the fuel constituents in the raw $CO_2$ stream can be utilized.

Exhibit 3-4 lists stream conditions for the $Fe_2O_3$ oxygen carrier reference plant, referring to the selected streams numbered in the Exhibit 3-3 block flow diagram. Similarly, Exhibit 3-6 lists stream conditions for the $CaSO_4$ oxygen carrier reference plant, referring to the selected streams numbered in the Exhibit 3-5 block flow diagram. Due to the assumptions applied, stream 14 in Exhibit 3-4 has negligible flow and is not included in the stream table.

**Exhibit 3-2 Comparison of reference plant reactor conditions and configuration features**

| Oxygen Carrier Type | $Fe_2O_3$ | $CaSO_4$ |
|---|---|---|
| Reducer reactor type | Circulating fluid bed | Circulating fluid bed |
| Reducer outlet gas velocity (ft/s) | 30 | 29 |
| Reducer temperature (°F) | 1,745 | 1,800 |
| Reducer pressure drop (psi) | 21.4 | 2.9 |
| Solids flow to Reducer (1000 lb/hr) | 94,374 | 17,183 |
| Oxidize reactor type | Circulating fluid bed | Circulating fluid bed |
| Oxidizer outlet gas velocity (ft/s) | 31 | 26 |
| Oxidizer temperature (°F) | 1,800 | 2,000 |
| Reducer off-gas $H_2$ and CO (mole%) | 0.05 | 1.5 |
| Oxidizer pressure drop (psi) | 1.8 | 0.4 |
| Oxygen carrier flow to Oxidizer (1000 lb/hr) | 93,566 | 16,363 |
| Oxidizer off-gas $O_2$ (mole%) | 3.5 | 3.5 |
| Location of solids cooler | Solids stream to Reducer | Solids stream to Oxidizer |
| Use of fuel recovery / $CO_2$ purification | None needed | Used for fuel recovery |

**Exhibit 3-3 $Fe_2O_3$-based chemical looping combustion power plant stream flow diagram**

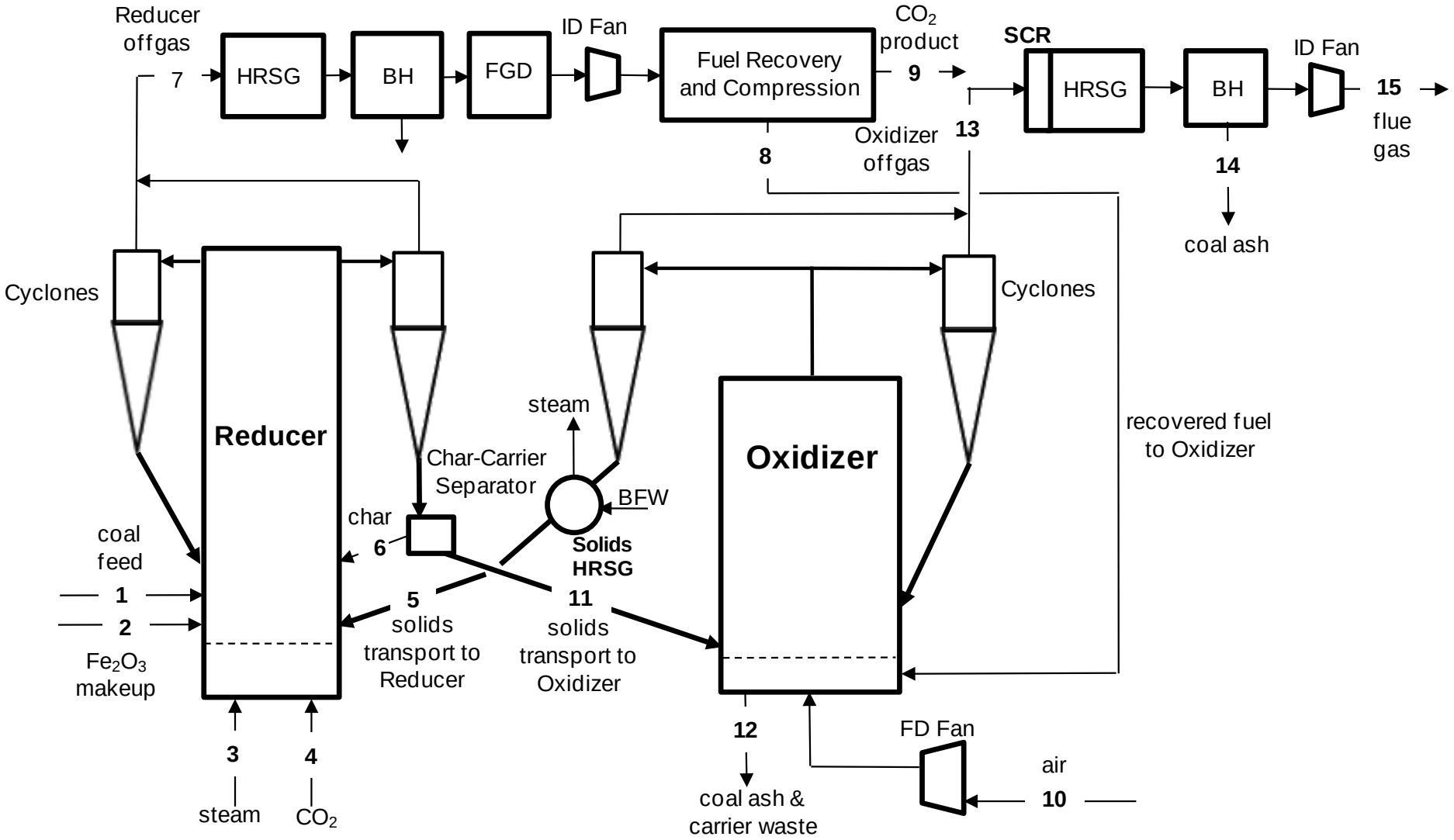

## Exhibit 3-4 $Fe_2O_3$-based chemical looping combustion power plant stream table

| | 1 | 2 | 3 | 4 | 5 | 6 | 7 | 8 | 9 | 10 | 11 | 12 | 13 | 14 | 15 |
|---|---|---|---|---|---|---|---|---|---|---|---|---|---|---|---|
| **Gas Composition (mole fraction)** | | | | | | | | | | | | | | | |
| **AR** | 0 | 0 | 0 | 0 | 0 | 0 | 0 | 0 | 0 | 0.009 | 0 | 0 | 0.011 | 0 | 0.011 |
| **$CH_4$** | 0 | 0 | 0 | 0 | 0 | 0 | 0 | 0 | 0 | 0 | 0 | 0 | 0 | 0 | 0 |
| **CO** | 0 | 0 | 0 | 1.53E-05 | 0 | 0 | 7.93E-06 | 0 | 1.5516E-05 | 0 | 0 | 0 | 0 | 0 | 1.702E-05 |
| **$CO_2$** | 0 | 0 | 0 | 0.972 | 0 | 0 | 0.505 | 0 | 0.989 | 0.0003 | 0 | 0 | 0.0075 | 0 | 0.0075 |
| **$H_2$** | 0 | 0 | 0 | 9.93E-06 | 0 | 0 | 5.16E-06 | 0 | 1.01E-05 | 0 | 0 | 0 | 0 | 0 | 0 |
| **$H_2O$** | 0 | 0 | 1 | 0.017 | 0 | 0 | 0.482 | 0 | 0 | 0.010 | 0 | 0 | 0.018 | 0 | 0.019 |
| **$H_2S$** | 0 | 0 | 0 | 0 | 0 | 0 | 0 | 0 | 0 | 0 | 0 | 0 | 0 | 0 | 0 |
| **$N_2$** | 0 | 0 | 0 | 0.010 | 0 | 0 | 0.005 | 0 | 0.010 | 0.773 | 0 | 0 | 0.928 | 0 | 0.927 |
| **$NH_3$** | 0 | 0 | 0 | 0 | 0 | 0 | 0.0004 | 0 | 0 | 0 | 0 | 0 | 0 | 0 | 0 |
| **$O_2$** | 0 | 0 | 0 | 0 | 0 | 0 | 0 | 0 | 0 | 0.207 | 0 | 0 | 0.035 | 0 | 0.035 |
| **$SO_2$** | 0 | 0 | 0 | 0.001 | 0 | 0 | 0.007 | 0 | 0.001 | 0 | 0 | 0 | 1.70E-05 | 0 | 0 |
| **Total** | 0 | 0 | 1 | 1 | 0 | 0 | 1 | 0 | 1 | 1 | 1 | 0 | 1 | 0 | 1 |
| | | | | | | | | | | | | | | | |
| **Gas Flowrate (kgmol/hr)** | 0 | 0 | 4,894 | 340 | 0 | 1,606 | 21,609 | 0 | 10,710 | 73,334 | 0 | 0 | 61,119 | 0 | 61,147 |
| **Gas Flowrate (kg/hr)** | 0 | 0 | 88,175 | 14,775 | 0 | 3,323 | 681,736 | 0 | 469,796 | 2,116,191 | 0 | 0 | 1,725,006 | 0 | 1,725,469 |
| **Solids Flowrate (kg/hr)** | 207,745 | 4,667 | 0 | 0 | 42,807,449 | 23,690 | 424 | 0 | 0 | 0 | 42,439,819 | 0 | 24,401 | 24,401 | 0 |
| | | | | | | | | | | | | | | | |
| **Temperature (°C)** | 15 | 15 | 138 | 38 | 960 | 952 | 951 | --- | 52 | 15 | 951 | --- | 982 | 149 | 148 |
| **Pressure (MPa, abs)** | 0.101 | 0.101 | 0.276 | 0.341 | 0.101 | 0.101 | 0.101 | --- | 15.27 | 0.101 | 0.101 | --- | 0.101 | 0.097 | 0.102 |
| **Enthalpy (kJ/kg)** | --- | --- | 2,751.4 | 46.3 | --- | 3,602.2 | 2,009.6 | --- | -158.6 | 30.2 | -7,510.6 | --- | 1,115.2 | --- | 178.2 |
| **Density ($kg/m^3$)** | --- | --- | 1.5 | 5.8 | --- | 0 | 0.3 | --- | 632.1 | 1.2 | 0 | --- | 0.3 | --- | 0.8 |
| **Gas Molecular Weight** | --- | --- | 18.0 | 43.4 | --- | 0 | 31.5 | --- | 43.9 | 28.9 | 0 | --- | 28.2 | --- | 28.2 |
| | | | | | | | | | | | | | | | |
| **Gas Flowrate (lbmol/hr)** | 0 | 0 | 10,790 | 750 | 0 | 0 | 47,640 | 0 | 23,611 | 161,673 | 0 | 0 | 134,745 | 0 | 134,806 |
| **Gas Flowrate (lb/hr)** | 0 | 0 | 194,392 | 32,572 | 0 | 0 | 1,502,971 | 0 | 1,035,722 | 4,665,403 | 0 | 0 | 3,802,988 | 0 | 3,804,007 |
| **Mass flow coal ash (lb/hr)** | 0 | 0 | 0 | | 399,547 | 5,217 | 4 | | | 0 | 443,969 | 0 | 44,397 | 44,397 | 0 |
| **Mass flow $O_2$-carrier (lb/hr)** | 0 | 10,290 | 0 | | 93,974,722 | 47,010 | 931 | | | 0 | 93,119,817 | 0 | 9,398 | 9,398 | 0 |
| **Solids Flowrate (lb/hr)** | 458,000 | 10,290 | 0 | 0 | 94,374,269 | 52,228 | 936 | 0 | 0 | 0 | 93,563,785 | 0 | 53,795 | 53,795 | 0 |
| | | | | | | | | | | | | | | | |
| **Temperature (°F)** | 59 | 59 | 280 | 100 | 1761 | 1745 | 1744 | --- | 125 | 59 | 1744 | --- | 1800 | 300 | 298 |
| **Pressure (psia)** | 14.7 | 14.7 | 40 | 49.5 | 14.7 | 14.7 | 14.7 | --- | 2,214.5 | 14.7 | 14.7 | --- | 14.7 | 14.1 | 14.8 |
| **Enthalpy (Btu/lb)** | --- | --- | 1,182.9 | 19.9 | --- | 1,548.7 | 864.0 | --- | -68.2 | 13.0 | -3,229.0 | --- | 479.5 | --- | 76.6 |
| **Density ($lb/ft^3$)** | --- | --- | 0.09 | 0.36 | --- | 0 | 0.02 | --- | 39.46 | 0.08 | 0 | --- | 0.02 | --- | 0.05 |
| | | | | | | | | | | | | | | | |
| **$O_2$-Carrier Flowrate (lbmol/hr)** | | | | | | | | | | | | | | | |
| **Support $Al_2O_3$** | 0 | 71 | 0 | 0 | 647,760 | 0 | 6 | 0 | 0 | 0 | 647,824 | 0 | 65 | 65 | 0 |
| **$Fe_2O_3$** | 0 | 29 | 0 | 0 | 246,824 | 0 | 1 | 0 | 0 | 0 | 82,614 | 0 | 25 | 25 | 0 |
| **$Fe_3O_4$** | 0 | 0 | 0 | 0 | 12,164 | 0 | 1 | 0 | 0 | 0 | 121,655 | 0 | 1 | 1 | 0 |
| **Char carbon** | 0 | 0 | 0 | 0 | 10 | 3,889 | 0 | 0 | 0 | 0 | 972 | 0 | 0 | 0 | 0 |

**Exhibit 3-5 $CaSO_4$-based chemical looping combustion power plant stream flow diagram**

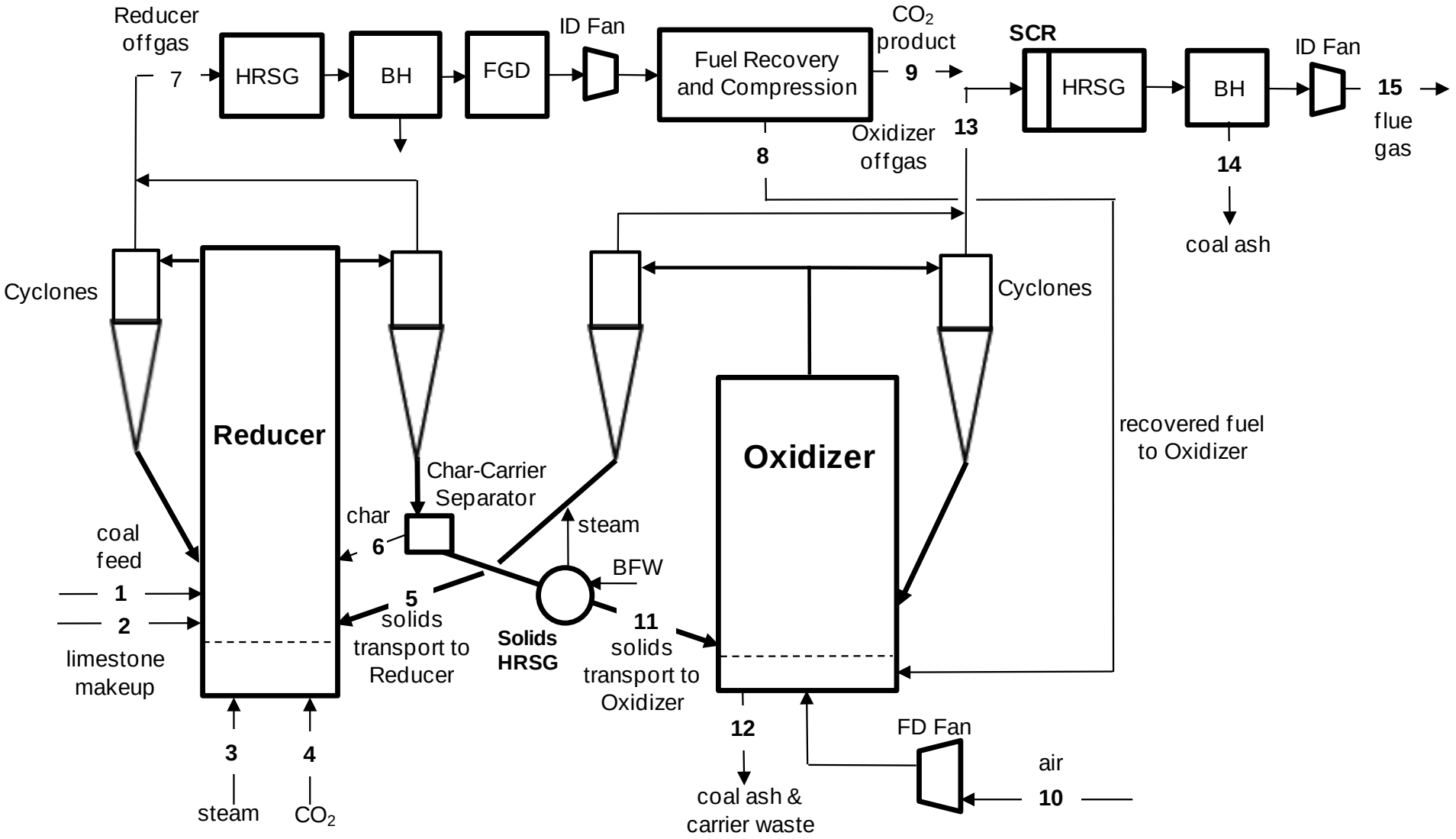

## Exhibit 3-6 $CaSO_4$-based chemical looping combustion power plant stream table

| | 1 | 2 | 3 | 4 | 5 | 6 | 7 | 8 | 9 | 10 | 11 | 12 | 13 | 15 |
|---|---|---|---|---|---|---|---|---|---|---|---|---|---|---|
| **Gas Compostion (mole fraction)** | | | | | | | | | | | | | | |
| **AR** | 0 | 0 | 0 | 0 | 0 | 0 | 0 | 0 | 0 | 0.009 | 0 | 0 | 0.011 | 0.011 |
| **$CH_4$** | 0 | 0 | 0 | 0 | 0 | 0 | 0 | 0 | 0 | 0 | 0 | 0 | 0 | 0 |
| **CO** | 0 | 0 | 0 | 0.014 | 0 | 0 | 0.008 | 0.263 | 0 | 0 | 0 | 0 | 0 | 0 |
| **$CO_2$** | 0 | 0 | 0 | 0.944 | 0 | 0 | 0.503 | 0.335 | 0.997 | 0 | 0 | 0 | 0.016 | 0.016 |
| **$H_2$** | 0 | 0 | 0 | 0.014 | 0 | 0.998 | 0.007 | 0.254 | 0 | 0 | 0.998 | 0 | 0 | 0 |
| **$H_2O$** | 0 | 0 | 1 | 0.017 | 0 | 0 | 0.471 | 0 | 0 | 0.010 | 0 | 0 | 0.021 | 0.021 |
| **H2S** | 0 | 0 | 0 | 0 | 0 | 0 | 0.005 | 0 | 0 | 0 | 0 | 0 | 0 | 0 |
| **$N_2$** | 0 | 0 | 0 | 0.008 | 0 | 0.002 | 0.004 | 0.148 | 0 | 0.773 | 0.002 | 0 | 0.918 | 0.918 |
| **$NH_3$** | 0 | 0 | 0 | 0 | 0 | 0 | 0 | 0 | 0 | 0 | 0 | 0 | 0 | 0 |
| **$O_2$** | 0 | 0 | 0 | 0 | 0 | 0 | 0 | 0 | 0 | 0.207 | 0 | 0 | 0.035 | 0.035 |
| **$SO_2$** | 0 | 0 | 0 | 0.003 | 0 | 0 | 0.002 | 0 | 0.003 | 0 | 0 | 0 | 0 | 0 |
| **Total** | 0 | 0 | 1 | 0 | 0 | 0 | 0 | 0 | 0 | 1 | 0 | 0 | 1 | 1 |
| | | | | | | | | | | | | | | |
| **Gas Flowrate (kgmol/hr)** | 0 | 0 | 5,279 | 485 | 0 | 1,729 | 23,257 | 644 | 11,055 | 78,139 | 432 | 0 | 65,932 | 65,949 |
| **Gas Flowrate (kg/hr)** | 0 | 0 | 95,103 | 20,722 | 0 | 3,559 | 726,769 | 17,236 | 487,217 | 2,254,867 | 890 | 0 | 1,867,586 | 1,867,851 |
| **Solids Flowrate (kg/hr)** | 223,689 | 16,069 | 0 | 0 | 7,794,191 | 25,508 | 0 | 0 | 0 | 0 | 7,422,116 | 33,331 | 0 | 0 |
| | | | | | | | | | | | | | | |
| **Temperature (°C)** | 15 | 15 | 127 | 38 | 1,093 | 15 | 982 | 129 | 52 | 15 | 980 | 1,093 | 1,093 | 158 |
| **Pressure (MPa, abs)** | 0.101 | 0.101 | 0.172 | 0.341 | 0.101 | 0.101 | 0.101 | 0.234 | 15.268 | 0.101 | 0.101 | 0.101 | 0.101 | 0.102 |
| **Enthalpy (kJ/kg)** | --- | --- | 2,733.6 | 47.0 | --- | 314.1 | 2,053.3 | 155.6 | -163.8 | 30.2 | -1,439.3 | --- | 1,266.2 | 192.4 |
| **Density (kg/m3)** | --- | --- | 0.9 | 5.7 | --- | 0.1 | 0.3 | 1.9 | 651.5 | 1.2 | 0.0 | --- | 0.3 | 0.8 |
| **Gas Molecular Weight** | --- | --- | 18.0 | 42.7 | --- | 2.1 | 31.3 | 26.8 | 44.1 | 28.9 | 2.1 | --- | 28.3 | 28.3 |
| | | | | | | | | | | | | | | |
| **Gas Flowrate (lbmol/hr)** | 0 | 0 | 11,638 | 1,070 | 0 | 3,811 | 51,272 | 1,419 | 24,373 | 172,268 | 953 | 0 | 145,356 | 145,393 |
| **Gas Flowrate (lb/hr)** | 0 | 0 | 209,667 | 45,685 | 0 | 7,847 | 1,602,250 | 37,998 | 1,074,130 | 4,971,131 | 1,962 | 0 | 4,117,322 | 4,117,906 |
| **Mass flow coal ash (lb/hr)** | 0 | 0 | 0 | | 11,141,616 | 5,618 | 0 | | | 0 | 11,189,452 | 47,647 | | |
| **Mass flow $O_2$-carrier (lb/hr)** | 0 | 35,425 | 0 | | 6,041,635 | 50,618 | 0 | | | 0 | 5,173,514 | 25,836 | | |
| **Solids Flowrate (lb/hr)** | 493,150 | 35,425 | 0 | 0 | 17,183,251 | 56,236 | 0 | 0 | 0 | 0 | 16,362,966 | 73,483 | 0 | 0 |
| | | | | | | | | | | | | | | |
| **Temperature (°F)** | 59 | 59 | 260 | 100 | 1,999 | 59 | 1,799 | 264 | 125 | 59 | 1,796 | 2,000 | 2,000 | 317 |
| **Pressure (psia)** | 14.7 | 14.7 | 25.0 | 49.5 | 14.7 | 14.7 | 14.7 | 34.0 | 2,214.5 | 14.7 | 14.7 | 14.7 | 14.7 | 14.8 |
| **Enthalpy (Btu/lb)** | --- | --- | 1,175.2 | 20.2 | --- | 135.0 | 882.8 | 66.9 | -70.4 | 13.0 | -618.8 | --- | 544.4 | 82.7 |
| **Density (lb/ft3)** | --- | --- | 0.059 | 0.358 | --- | 0.005 | 0.019 | 0.117 | 40.672 | 0.076 | 0.001 | --- | 0.016 | 0.051 |
| | | | | | | | | | | | | | | |
| **$O_2$-Carrier Flowrate (lbmol/hr)** | | | | | | | | | | | | | | |
| **$CaSO_4$** | 0 | 0 | 0 | | 14,328 | 0 | 0 | | | 0 | 0 | 61 | | |
| **CaS** | 0 | 0 | 0 | | 0 | 0 | 0 | | | 0 | 14,391 | 0 | | |
| **CaO** | 0 | 0 | 0 | | 65,458 | 0 | 0 | | | 0 | 65,395 | 280 | | |
| **$CaCO_3$** | 0 | 336 | 0 | | 0 | 0 | 0 | | | 0 | 336 | 0 | | |
| **Char carbon** | 0 | 0 | 0 | | 21 | 4,188 | 0 | | | 0 | 1,047 | 0 | | |

# 4 Chemical Looping Combustion Reference Plant Performance

Exhibit 4-1 lists the major Reducer reactor dimensions and some of its most important design characteristics. The Reducer operating velocity is high, but is within normal experience for circulating fluidized beds. There is a significant increase in the gas velocity across the Reducer reactor. Smaller oxygen carrier makeup rate is needed with $Fe_2O_3$ than with $CaSO_4$, but the $Fe_2O_3$ oxygen carrier has a much greater price. The Reducer vessel dimensions are similar for the two oxygen carrier types, this similarity resulting from the higher operating temperature assumed for the less reactive $CaSO_4$ oxygen carrier. Four very large cyclones are required to support the Reducer operation.

**Exhibit 4-1 Reducer reactor characteristics and vessel dimensions**

| Oxygen Carrier Type | $Fe_2O_3$ | $CaSO_4$ |
|---|---|---|
| Inlet velocity (ft/s) | 20 | 20 |
| Outlet velocity (ft/s) | 30 | 29 |
| Oxygen carrier circulation rate (1000 lb/hr) | 94,374 | 17,183 |
| Oxygen carrier makeup rate (lb/hr) | 10,290 | 35,425 |
| Pressure drop (psi) | 21.4 | 2.9 |
| Carbon gasification efficiency (%) | 96 | 96 |
| Reducer off-gas $H_2$ and CO (mole%) | 0.05 | 1.5 |
| Reducer vessel shell diameter (ft) | 39 | 41 |
| Reducer vessel height (ft) | 115 | 87 |
| Reducer cyclone number | 4 | 4 |
| Reducer cyclone shell diameter (ft) | 19 | 20 |
| Reducer cyclone height (ft) | 90 | 94 |
| Estimated bed structure (see Section 7) | | |
| Solids content, % of total solids volume: oxygen carrier, char, ash | 92.8, 6.1, 1.1 | 25.3, 13.3, 61.4 |
| Volume % solids in bed Core region ($f_c$,%) | 2.3 | 1.5 |
| Volume of Core region ($\delta_c$,% of bed) | 68.1 | 76.8 |

Some aspects of the circulating fluid bed average structure are included. These indicate that the $Fe_2O_3$ Reducer reactor solids have high oxygen carrier content relative to char and coal ash, while the $CaSO_4$ Reducer reactor solids have very high char and coal ash contents. Both Reducer reactors have low solids volumetric contents, with a large central core region containing small volume fractions of solids. These characteristics are representative of circulating fluidized bed.

Exhibit 4-2 lists the Oxidizer reactor dimensions and some of its most important design characteristics. Like the reducer reactor, the Oxidizer reactor operates with high gas velocity. The $Fe_2O_3$ Oxidizer is more compact than the $CaSO_4$ Oxidizer reactor, both having relatively low pressure drops. Again, a large number of parallel cyclones are required. The Oxidizer circulating fluid bed structure has characteristics similar to those in the Reducer fluid bed.

**Exhibit 4-2 Oxidizer reactor characteristics and vessel dimensions**

| Oxygen Carrier Type | $Fe_2O_3$ | $CaSO_4$ |
|---|---|---|
| Inlet velocity (ft/s) | 32 | 30 |
| Outlet velocity (ft/s) | 31 | 26 |
| Pressure drop (psi) | 1.8 | 0.4 |
| Oxidizer vessel shell diameter (ft) | 52 | 63 |
| Oxidizer vessel height (ft) | 39 | 54 |
| Oxidizer cyclone number | 8 | 8 |
| Oxidizer cyclone shell diameter (ft) | 23 | 25 |
| Oxidizer cyclone height (ft) | 108 | 117 |
| Estimated bed structure (see Section 7) | | |
| Solids content, % of total solids volume: oxygen carrier, ash | 98.7, 1.3 | 26.1, 73.9 |
| Volume % solids in bed Core region ($f_c$,%) | 0.9 | 0.25 |
| Volume of Core region ($\delta_c$,% of bed) | 63.9 | 79.0 |

Exhibit 4-3 presents the CLC power plant performance and the breakdown of the auxiliary loads in the plants. Note that the $Fe_2O_3$ oxygen carrier process requires no flue recovery, using conventional raw-$CO_2$ dehydration and compression, while the $CaSO_4$ oxygen carrier process requires fuel recovery. Comparison with a conventional PC power plant using amine absorber for carbon capture is included.

**Exhibit 4-3 Reference power plant performance comparison**

| Plant Performance Factors | $Fe_2O_3$ | $CaSO_4$ | Conventional PC BBR Case 12 |
|---|---|---|---|
| **Plant Output (kW)** | | | |
| Steam Turbine Power | 641,800 | 671,100 | 662,800 |
| **Auxiliary Load (kW)** | | | |
| Coal Handling | 460 | 480 | 510 |
| Pulverizers | 3,110 | 3,350 | 3,850 |
| Sorbent & Oxygen Carrier Handling | 1,530 | 1,860 | 1,250 |
| Ash and Carrier Waste Handling | 720 | 980 | 740 |
| Forced Draft Fans | 6,450 | 4,410 | 2,300 |
| Induced Draft Fans | 3,880 | 6,010 | 11,120 |
| SCR | 50 | 60 | 70 |
| Baghouses | 120 | 90 | 100 |
| Wet FGD | 6,440 | 4090 | 4,110 |
| $CO_2$ Removal | 0 | 0 | 20,600 |
| Fuel Recovery & Compression | 55,920 | 86,170 | 44,890 |
| Miscellaneous Balance or Plant | 2,000 | 2,000 | 2,000 |
| Steam Turbine Auxiliaries | 400 | 400 | 400 |
| Condensate Pumps | 870 | 890 | 560 |
| Circulating Water Pumps | 4,970 | 5,160 | 10,100 |
| Ground Water Pumps | 0 | 0 | 910 |
| Cooling Tower Fans | 2,570 | 2,670 | 5,230 |
| Transformer Losses | 2,170 | 2,340 | 2,290 |
| **Plant Performance** | | | |
| Net Auxiliary Load, kW | 91,660 | 120,960 | 112,830 |
| Net Plant Power, kW | 550,140 | 550,140 | 549,970 |
| Net Plant Efficiency, % (HHV) | 35.1 | 32.6 | 28.4 |
| Coal Feed Flowrate, kg/hr (lb/hr) | 207,745 (458,000) | 223,689 (493,150) | 256,652 (565,820) |
| Thermal Input, kWth | 1,565,887 | 1,686,064 | 1,923,519 |
| Condenser Duty, GJ/hr (MMBtu/hr) | 2,424 (2,298) | 2,521 (2,389) | 1,737 (1,646) |
| Carbon Capture Efficiency, % | 95.8 | 91.4 | 90.0 |

Higher plant thermal efficiency results with the CLC plants primarily due to the much lower extracted steam usage in these plants compared to the conventional amine absorber PC plant. The $Fe_2O_3$ oxygen carrier CLC plant has very high thermal efficiency resulting from the high Reducer performance with no need for fuel recovery or $CO_2$ purification.

Exhibit 4-4 shows tabulated material balances for the $Fe_2O_3$ oxygen carrier CLC power plant.

**Exhibit 4-4 Material balances for $Fe_2O_3$ oxygen carrier CLC reference plant**

**Carbon Balance**

| Carbon In | | Carbon Out | |
|---|---|---|---|
| | kg/hr (lb/hr) | | kg/hr (lb/hr) |
| Coal | 132,427 (291,951) | Stack Gas | 5,532 (12,197) |
| Air ($CO_2$) | 288 (634) | FGD Product | 21 (46) |
| FGD Reagent | 33 (73) | $CO_2$ Product | 127,189 (280,404) |
| | | | |
| | | Convergence Tolerance | 6 (13) |
| Total | 132,748 (292,659) | Total | 132,748 (292,659) |

**Sulfur Balance**

| Sulfur In | | Sulfur Out | |
|---|---|---|---|
| | kg/hr (lb/hr) | | kg/hr (lb/hr) |
| Coal | 5,207 (11,479) | FGD Product | 4,855 (10,704) |
| | | Stack Gas | 0 (0) |
| | | $CO_2$ Product | 352 (776) |
| | | $O_2$-Carrier/Ash | 0 (0) |
| | | | |
| Total | 5,207 (11,479) | Total | 5,207 (11,479) |

**Water Consumption**

| Water Use | Water Demand | Internal Recycle | Raw Water Withdrawal | Process Water Discharge | Raw Water Consumption |
|---|---|---|---|---|---|
| | $m^3$/min (gpm) | $m^3$/min (gpm) | $m^3$/min (gpm) | $m^3$/min (gpm) | $m^3$/min (gpm) |
| BFW Makeup | 1.47 (389) | 0.0 (0) | 1.47 (389) | 0.00 (0) | 1.47 (389) |
| Cooling Tower | 19.4 (5,117) | 3.14 (830) | 16.2 (4,287) | 4.36 (1,151) | 11.87 (3,136) |
| **Total** | **20.8 (5,506)** | **3.14 (830)** | **17.7 (4,676)** | **4.36 (1,151)** | **13.34 (3,525)** |

Exhibit 4-5 shows tabulated material balances for the $CaSO_4$ oxygen carrier CLC power plant.

**Exhibit 4-5 Material balances for $CaSO_4$ oxygen carrier CLC reference plant**

**Carbon Balance**

| Carbon In | | Carbon Out | |
|---|---|---|---|
| | kg/hr (lb/hr) | | kg/hr (lb/hr) |
| Coal | 142,590 (314,357) | Stack Gas | 12,315 (27,151) |
| Air ($CO_2$) | 307 (676) | FGD Product | 0 (0) |
| FGD Reagent | 20 (45) | $CO_2$ Product | 132,381 (291,851) |
| | | | |
| | | Convergence Tolerance | -1,780 (-3,923) |
| Total | 142,917 (315,078) | Total | 142,917 (315,078) |

**Sulfur Balance**

| Sulfur In | | Sulfur Out | |
|---|---|---|---|
| | kg/hr (lb/hr) | | kg/hr (lb/hr) |
| Coal | 5,607 (12,360) | FGD Product | 4,642 (10,234) |
| | | Stack Gas | 0 (0) |
| | | $CO_2$ Product | 73 (162) |
| | | $O_2$-Carrier/Ash | 891 (1,965) |
| | | | |
| Total | 5,607 (12,360) | Total | 5,607 (12,360) |

**Water Consumption**

| Water Use | Water Demand | Internal Recycle | Raw Water Withdrawal | Process Water Discharge | Raw Water Consumption |
|---|---|---|---|---|---|
| | $m^3$/min (gpm) | $m^3$/min (gpm) | $m^3$/min (gpm) | $m^3$/min (gpm) | $m^3$/min (gpm) |
| BFW Makeup | 1.59 (419) | 0.0 (0) | 1.59 (419) | 0.00 (0) | 1.59 (419) |
| Cooling Tower | 20.1 (5,313) | 4.05 (1069) | 16.1 (4,244) | 4.52 (1,195) | 11.54 (3,050) |
| **Total** | **21.7 (5,732)** | **4.05 (1069)** | **17.7 (4,664)** | **4.52 (1,195)** | **13.13 (3,469)** |

Exhibit 4-6 shows the plant emissions for the $Fe_2O_3$ CLC power plant.

**Exhibit 4-6 Emissions for $Fe_2O_3$ oxygen carrier CLC reference plant**

| | kg/GJ (lb/MMBtu) | Tonne/year (tons/year) | kg/MWh (lb/MWh) |
|---|---|---|---|
| $SO_2$ | 0.000 (0.000) | 0 (0) | 0.000 (.00) |
| $NO_x$ | 0.030 (0.070) | 1,263 (1,392) | 0.264 (.583) |
| Particulate | 0.006 (0.0130) | 235 (259) | 0.049 (.108) |
| Hg | 4.91E-7 (1.14E-6) | 0.021 (0.023) | 4.32E-6 (9.51E-6) |
| $CO_2$ | 3.6 (8.4) | 150,939 (166,381) | 32 (70) |

Exhibit 4-7 shows the plant emissions for the $CaSO_4$ CLC power plant.

**Exhibit 4-7 Emissions for $CaSO_4$ oxygen carrier CLC reference plant**

| | kg/GJ (lb/MMBtu) | Tonne/year (tons/year) | kg/MWh (lb/MWh) |
|---|---|---|---|
| $SO_2$ | 0.000 (0.000) | 0 (0) | 0.000 (.00) |
| $NO_x$ | 0.030 (0.070) | 1,360 (1,499) | 0.272 (.600) |
| Particulate | 0.006 (0.0130) | 253 (278) | 0.051 (.111) |
| Hg | 4.91E-7 (1.14E-6) | 0.022 (0.024) | 4.44E-6 (9.80E-6) |
| $CO_2$ | 7.4 (17.3) | 336,000 (370,376) | 67 (148) |

# 5 Chemical Looping Combustion Reference Plant Cost

Exhibit 5-1 shows the equipment cost breakdown for the two CLC power plants. Fuel recovery is not needed for the $Fe_2O_3$ oxygen carrier process, but is used with the $CaSO_4$ process.

**Exhibit 5-1 Total plant cost breakdown comparison**

| Cost | $Fe_2O_3$ ($/kW) | $CaSO_4$ ($/kW) |
|---|---|---|
| Coal Handling, Prep & Feed Systems | 88 | 92 |
| Coal Prep & Feed Systems | 44 | 44 |
| Feedwater & Misc BOP Systems | 181 | 185 |
| Chemical Looping Combustion System | 729 | 785 |
| Reducer Reactor | 13 | 12 |
| Reducer Cyclones | 13 | 14 |
| Reducer High-temperature Piping | 5 | 5 |
| Char-carrier Separator | 0 | 0 |
| Oxidizer Reactor | 10 | 18 |
| Oxidizer Cyclones | 37 | 44 |
| Oxidizer High-temperature Piping | 9 | 9 |
| Solids HRSG & Convective HRSGs | 326 | 351 |
| CLC BOP (w/ FD and ID fans) | 315 | 331 |
| Gas Cleanup (FGD, Baghouses, SCR) | 161 | 229 |
| Fuel Recovery & Compression | 159 | 202 |
| HRSG, Ducting & Stack | 79 | 80 |
| Steam Turbine Generator | 292 | 301 |
| Cooling Water System | 83 | 85 |
| Ash & Carrier Waste Handling System | 133 | 144 |
| Accessory Electric Plant | 170 | 186 |
| Instrumentation & Control | 58 | 61 |
| Improvements to Site | 31 | 31 |
| Buildings & Structures | 170 | 171 |
| Total Plant Cost (TPC) | 2,379 | 2,597 |
| Total Overnight Cost (TOC) | 2,975 | 3,204 |
| Total As-Spent Cost (TASC) | 3,392 | 3,653 |

These results indicate that the primary reactor vessel and cyclones represent a small cost contribution the total CLC power plant cost. More significant costs are associated with the heat recovery units and the forced draft (FD) and induced draft (ID) fans.

Exhibit 5-2 displays the initial and annual O&M expenses for the $Fe_2O_3$ CLC power plant. A relatively high cost is associated with the cost of makeup $Fe_2O_3$ oxygen carrier. Similarly, Exhibit 5-3 displays the initial and annual O&M expenses for the $CaSO_4$ CLC power plant.

## Exhibit 5-2 $Fe_2O_3$ CLC initial and annual O&M expenses

| INITIAL & ANNUAL O&M EXPENSES | | | | | Cost Base (Jun): | 2011 |
|---|---|---|---|---|---|---|
| FE Case - $Fe_2O_3$ Chemical Looping (1x550 MWnet) with $CO_2$ Capture | | | | | Heat Rate-net (Btu/kWh): | 9,712 |
| | | | | | MWe-net: | 550 |
| | | | | | Capacity Factor (%): | 85 |
| OPERATING & MAINTENANCE LABOR | | | | | | |
| Operating Labor | | | | | | |
| Operating Labor Rate(base): | 39.70 | $/hour | | | | |
| Operating Labor Burden: | 30.00 | % of base | | | | |
| Labor O-H Charge Rate: | 25.00 | % of labor | | | | |
| Operating Labor Requirements(O.J.)per Shift: | 1 unit/mod. | | Total Plant | | | |
| Skilled Operator | 2.0 | | 2.0 | | | |
| Operator | 11.3 | | 11.3 | | | |
| Foreman | 1.0 | | 1.0 | | | |
| Lab Tech's, etc. | 2.0 | | 2.0 | | | |
| TOTAL-O.J.'s | 16.3 | | 16.3 | | | |
| | | | | | Annual Cost $ | Annual Unit Cost $/kW-net |
| Annual Operating Labor Cost | | | | | $7,384,208 | $13.422 |
| Maintenance Labor Cost | | | | | $8,849,699 | $16.086 |
| Administrative & Support Labor | | | | | $4,058,477 | $7.377 |
| Property Taxes and Insurance | | | | | $26,173,671 | $47.576 |
| **TOTAL FIXED OPERATING COSTS** | | | | | **$46,466,055** | $84.462 |
| VARIABLE OPERATING COSTS | | | | | | |
| | | | | | | $/kWh-net |
| **Maintenance Material Cost** | | | | | **$13,274,549** | **$0.00324** |
| Consumables | Consumption Initial Fill | /Day | Unit Cost | Initial Fill Cost | | |
| **Water(/1000 gallons)** | 0 | 3,400 | 1.67 | **$0** | **$1,766,069** | **$0.00043** |
| **Chemicals** | | | | | | |
| MU & WT Chem.(lbs) | 0 | 16,461 | 0.27 | $0 | $1,367,825 | $0.00033 |
| Limestone (ton) | 0 | 293 | 33.48 | $0 | $3,040,413 | $0.00074 |
| Carbon (Mercury Removal) lb | 0 | 1,491 | 1.63 | $0 | $751,814 | $0.00018 |
| $FE_2O_3$ Oxygen Transport (ton) | 0 | 123 | 2,000 | $0 | $76,617,888 | $0.01870 |
| NaOH (tons) | 0 | 0 | 671.16 | $0 | $0 | $0.00000 |
| $H_2SO_4$ (tons) | 0 | 0 | 214.78 | $0 | $0 | $0.00000 |
| Corrosion Inhibitor | 0 | 0 | 0 | $115,072 | $5,480 | $0.00000 |
| Activated Carbon (lb) | 0 | 0 | 1.63 | $0 | $0 | $0.00000 |
| Ammonia (19% $NH_3$) ton | 0 | 16 | 330.00 | $0 | $1,599,523 | $0.00039 |
| **Subtotal Chemicals** | | | | **$115,072** | **$83,382,943** | **$0.02036** |
| **Other** | | | | | | |
| Supplemental Fuel (MBtu) | 0 | 0 | 0.00 | $0 | $0 | $0.00000 |
| SCR Catalyst ($m^3$) | w/equip. | 0.38 | 8,938.80 | $0 | $1,041,791 | $0.00025 |
| Emission Penalties | 0 | 0 | 0.00 | $0 | $0 | $0.00000 |
| **Subtotal Other** | | | | **$0** | **$1,041,791** | **$0.00025** |
| **Waste Disposal** | | | | | | |
| Fly Ash (ton) | 0 | 657 | 25.11 | $0 | $5,116,465 | $0.00125 |
| Bottom Ash (ton) | 0 | 107 | 25.11 | $0 | $830,382 | $0.00020 |
| **Subtotal Waste Disposal** | | | | **$0** | **$5,946,847** | **$0.00145** |
| **By-products & Emissions** | | | | | | |
| Gypsum (tons) | 0 | 585 | 0.00 | $0 | $0 | $0.00000 |
| **Subtotal By-products** | | | | **$0** | **$0** | **$0.00000** |
| **TOTAL VARIABLE OPERATING COSTS** | | | | **$115,072** | **$105,412,199** | **$0.02573** |
| **Fuel (ton)** | 0 | 5,496 | 68.60 | **$0** | **$116,972,192** | **$0.02856** |

## Exhibit 5-3 $CaSO_4$ CLC initial and annual O&M expenses

| INITIAL & ANNUAL O&M EXPENSES | | | | | Cost Base (Jun): | 2011 |
|---|---|---|---|---|---|---|
| CA Case - $CaSO_4$ Chemical Looping (1x550 MWnet) with $CO_2$ Capture | | | | | Heat Rate-net (Btu/kWh): | 10,457 |
| | | | | | MWe-net: | 550 |
| | | | | | Capacity Factor (%): | 85 |
| OPERATING & MAINTENANCE LABOR | | | | | | |
| Operating Labor | | | | | | |
| Operating Labor Rate(base): | 39.70 | $/hour | | | | |
| Operating Labor Burden: | 30.00 | % of base | | | | |
| Labor O-H Charge Rate: | 25.00 | % of labor | | | | |
| Operating Labor Requirements(O.J.)per Shift: | 1 unit/mod. | | Total Plant | | | |
| Skilled Operator | 2.0 | | 2.0 | | | |
| Operator | 11.3 | | 11.3 | | | |
| Foreman | 1.0 | | 1.0 | | | |
| Lab Tech's, etc. | 2.0 | | 2.0 | | | |
| TOTAL-O.J.'s | 16.3 | | 16.3 | | | |
| | | | | | Annual Cost | Annual Unit Cost |
| | | | | | $ | $/kW-net |
| Annual Operating Labor Cost | | | | | $7,384,208 | $13.422 |
| Maintenance Labor Cost | | | | | $9,629,603 | $17.504 |
| Administrative & Support Labor | | | | | $4,253,453 | $7.732 |
| Property Taxes and Insurance | | | | | $28,578,510 | $51.948 |
| **TOTAL FIXED OPERATING COSTS** | | | | | **$49,845,774** | $90.606 |
| VARIABLE OPERATING COSTS | | | | | | |
| | | | | | | $/kWh-net |
| **Maintenance Material Cost** | | | | | **$14,444,405** | **$0.00353** |
| Consumables | Consumption Initial Fill | /Day | Unit Cost | Initial Fill Cost | | |
| **Water(/1000 gallons)** | 0 | 3,392 | 1.67 | **$0** | **$1,761,443** | **$0.00043** |
| **Chemicals** | | | | | | |
| MU & WT Chem.(lbs) | 0 | 16,417 | 0.27 | $0 | $1,364,242 | $0.00033 |
| Limestone (ton) | 0 | 66 | 33.48 | $0 | $688,590 | $0.00017 |
| Carbon (Mercury Removal) lb | 0 | 1,546 | 1.63 | $0 | $779,694 | $0.00019 |
| Limestone/Oxygen Transport (ton) | 0 | 425 | 33.48 | $0 | $4,415,606 | $0.00108 |
| NaOH (tons) | 64 | 6 | 671.16 | $43,283 | $1,342,862 | $0.00033 |
| $H_2SO_4$ (tons) | 0 | 0 | 214.78 | $0 | $0 | $0.00000 |
| Corrosion Inhibitor | 0 | 0 | 0 | $123,903 | $5,900 | $0.00000 |
| Activated Carbon (lb) | 0 | 0 | 1.63 | $0 | $0 | $0.00000 |
| Ammonia (19% $NH_3$) ton | 0 | 17 | 330.00 | $0 | $1,722,281 | $0.00042 |
| **Subtotal Chemicals** | | | | **$167,186** | **$10,319,175** | **$0.00252** |
| **Other** | | | | | | |
| Supplemental Fuel (MBtu) | 0 | 0 | 0.00 | $0 | $0 | $0.00000 |
| SCR Catalyst ($m^3$) | w/equip. | 0.40 | 8,938.80 | $0 | $1,123,146 | $0.00027 |
| Emission Penalties | 0 | 0 | 0.00 | $0 | $0 | $0.00000 |
| **Subtotal Other** | | | | **$0** | **$1,123,146** | **$0.00027** |
| **Waste Disposal** | | | | | | |
| Fly Ash (ton) | 0 | 0 | 25.11 | $0 | $0 | $0.00000 |
| Bottom Ash (ton) | 0 | 882 | 25.11 | $0 | $6,869,485 | $0.00168 |
| **Subtotal Waste Disposal** | | | | **$0** | **$6,869,485** | **$0.00168** |
| **By-products & Emissions** | | | | | | |
| Gypsum (tons) | 0 | 67 | 0.00 | $0 | $0 | $0.00000 |
| **Subtotal By-products** | | | | **$0** | **$0** | **$0.00000** |
| **TOTAL VARIABLE OPERATING COSTS** | | | | **$167,186** | **$34,517,654** | **$0.00843** |
| **Fuel (ton)** | 0 | 5,918 | 68.60 | **$0** | **$125,949,425** | **$0.03075** |

Exhibit 5-4 shows the breakdown for the cost of electricity (COE) (first-year, without transport and storage [T&S]) for the two CLC power plants and compares them against the conventional PC power plant with amine-based carbon capture. Even though the $Fe_2O_3$ oxygen carrier CLC power plant has higher thermal efficiency and lower capital cost than the $CaSO_4$ oxygen carrier CLC power plant, the COE is lower for the $CaSO_4$ CLC power plant due to the high cost of makeup oxygen carrier in the $Fe_2O_3$ CLC power plant.

**Exhibit 5-4 Cost of electricity breakdown comparison**

| Cost | $Fe_2O_3$ ($/MWh) | $CaSO_4$ ($/MWh) | Conventional PC BBR Case 12 |
|---|---|---|---|
| Capital | 49.6 | 53.4 | 73.1 |
| Fixed | 11.3 | 12.2 | 15.7 |
| Variable | 25.7 | 8.4 | 13.2 |
| Maintenance materials | 3.2 | 3.5 | 4.7 |
| Water | 0.4 | 0.4 | 0.9 |
| Carrier makeup* | 18.7 | 1.1 | N/A |
| Other chemicals & catalyst | 1.9 | 1.7 | 6.4 |
| Waste disposal | 1.5 | 1.7 | 1.3 |
| Fuel | 28.6 | 30.8 | 35.3 |
| Total | 115.2 | 104.7 | 137.3 |

*$Fe_2O_3$ oxygen carrier makeup: 123 tons/day @ $2,000 per ton; Limestone carrier makeup: 425 tons/day @ $33.5 per ton

# 6 Chemical Looping Combustion Reference Plant Performance and Cost Sensitivity

There are a host of parameters used in the design of the CLC power plant that can influence the CLC power plant performance and cost. There are also significant uncertainties associated with the design and performance parameters. Selected sensitivity evaluations have been performed to understand the influence of the key parameters on the CLC plant performance and cost.

The key Reducer performance parameters are listed below, and their reference values are listed in Exhibit 6-1.

- Steam and recycled-$CO_2$ feed rates

- Cyclone recycle ratio (solids rate re-circulated to the Reducer/total solids collection rate) – the non-recycled material is transported to the Oxidizer
- Oxygen carrier Reducer outlet extent of conversion
- Reducer temperature
- Reducer gas velocity
- Reducer overall carbon conversion efficiency

The first two parameters are fixed at the Reference plant values. The last four parameters have been assessed in sensitivity evaluations. These factors influence the Reducer characteristics:

- Pressure drop
- Total vessel height
- Vessel shell diameter
- Outlet $H_2$ and CO gas content
- Overall carbon capture efficiency for the plant

Likewise, the Oxidizer performance parameters are listed below, and their reference plant values are listed in Exhibit 6-2.

- Oxygen carrier feed rate and its inlet extent of conversion
- Outlet excess $O_2$
- $H_2$ and CO fed from the fuel recovery/$CO_2$ purification system, and the carbon sent from the Reducer
- Cyclone recycle ratio (solids rate re-circulated to the Oxidizer/total solids collection rate) – the non-recycled material is transported to the Reducer
- Oxygen carrier outlet extent of conversion
- Oxidizer temperature
- Oxidizer gas velocity

The first five parameters are fixed at the Reference plant values. The last two parameters have been assessed. These factors influence the Oxidizer characteristics:

- Pressure drop
- Total vessel height
- Vessel shell diameter

Two important plant cost sensitivities are:

- Rate of oxygen carrier makeup and the makeup oxygen carrier delivered price
- Cost of char-carrier separation equipment

These two items influence the plant cost of electricity and are included in sensitivity studies.

**Exhibit 6-1 Reducer parameters**

| Parameter | $Fe_2O_3$ Case Base Values | $CaSO_4$ Case Base Values |
|---|---|---|
| **Base Plant Fixed Parameters** | | |
| Steam feed rate (moles/mole carbon) | 0.44 | 0.44 |
| Recycled-$CO_2$ feed rate (moles/mole carbon) | 0.031 | 0.044 |
| Oxygen carrier feed rate (moles/mole carbon) | 10.1 | 0.55 |
| Oxygen carrier Reducer inlet extent of conversion (%) | 6.9 | 0.0 |
| Cyclone recycle ratio | 4:1 | 4:1 |
| **Sensitivity Parameters Base Plant Values** | | |
| Oxygen carrier outlet extent of conversion (%) | 68.7 $Fe_3O_4$ | 17.7 CaS |
| Reducer temperature (°F) | 1,745 | 1,800 |
| Reducer outlet gas velocity (ft/s) | 30 | 29 |
| Reducer overall carbon conversion (%) | 96 | 96 |
| **Plant Performance Sensitivity Variables Base Values** | | |
| Reducer pressure drop (psi) | 21.4 | 2.9 |
| Reducer vessel height (ft) | 115 | 87 |
| Reducer vessel shell diameter (ft) | 39 | 41 |
| Reducer outlet $H_2$ and CO gas content (mole%) | 0.05 | 1.5 |
| Overall carbon capture efficiency for the plant (%) | 95.8 | 91.4 |

**Exhibit 6-2 Oxidizer parameters**

| Parameter | $Fe_2O_3$ Case Base Values | $CaSO_4$ Case Base Values |
|---|---|---|
| **Base Plant Fixed Parameters** | | |
| Oxygen carrier inlet extent of conversion (%) | 31.3 | 0.0 |
| Cyclone recycle ratio | 3:1 | 3:1 |
| Outlet excess $O_2$ (mole%) | 3.5 | 3.5 |
| Oxygen carrier outlet extent of conversion (%) | 93.1 $Fe_2O_3$ | 100 $CaSO_4$ |
| **Sensitivity Parameters Base Plant Values** | | |
| Oxidizer temperature (°F) | 1800 | 2000 |
| Oxidizer outlet gas velocity (ft/s) | 32 | 30 |
| **Plant Performance Sensitivity Variables Base values** | | |
| Oxidizer pressure drop (psi) | 1.8 | 0.4 |
| Oxidizer vessel height (ft) | 39 | 54 |
| Oxidizer shell diameter (ft) | 52 | 63 |
| Oxidizer FD-Fan power (kW) | 6,450 | 4,410 |

## 6.1 Reactor Temperature Sensitivity

The Reducer temperature sensitivity results are displayed in Exhibit 6-3. The top chart shows results for the $Fe_2O_3$ Reducer and the bottom chart shows results for the $CaSO_4$ Reducer. The Reducer vessel height and off-gas $H_2$ and CO are shown as a function of the Reducer temperature. For the highly reactive $Fe_2O_3$ oxygen carrier the Reducer can operate at relatively low temperatures where char gasification is slow. Increasing the temperature greatly reduces the vessel height needed to gasify the coal char. This reduction in vessel height, though, results in an increase in the Reducer off-gas $H_2$ and CO content by a factor of five. This increase will have little impact on the plant performance and cost so long as the $H_2$ and CO content remains small at less than 0.1 mol%, so it is concluded that it would be beneficial to increase the Reducer temperature to the highest level that can be operated without secondary operating issues, such as oxygen carrier reactivity loss due to sintering, of fluid bed particle agglomeration.

In the $CaSO_4$ oxygen carrier Reducer, the oxygen carrier has low reactivity and the Reducer must operate at higher temperatures where char gasification rates are also higher. Increasing the Reducer temperature results in a reduction in the Reducer vessel height and the off-gas $H_2$ and CO content, the off-gas $H_2$ and CO content ranging from 1 to 2 mol%. Again, it is concluded that it would be beneficial to increase the Reducer temperature to the highest level that can be operated without secondary operating issues, such as oxygen carrier reactivity loss due to sintering, or fluid bed particle agglomeration.

The Oxidizer temperature sensitivity results are displayed in Exhibit 6-4. Increase in the Reducer temperature will demand an increase in the Oxidizer temperature just due to the solid circulation heat balance. The exhibit shows that for both the $Fe_2O_3$ and $CaSO_4$ oxygen carriers, increased temperature results in reduced Oxidizer vessel height and reducer FD fan auxiliary power consumption, though these improvements are very small for the high-reactivity $Fe_2O_3$ oxygen carrier. While these are helpful trends, the improvements will not result in significant improvements in the CLC plant performance or cost. It is concluded that the best operating temperature for the Reducer and Oxidizer vessels with respect to operational reliability and oxygen carrier durability needs to be identified experimentally, and the benefits of temperature increases above this temperature need to be considered relative to the detrimental impacts of these increases.

**Exhibit 6-3 Reducer temperature sensitivity**

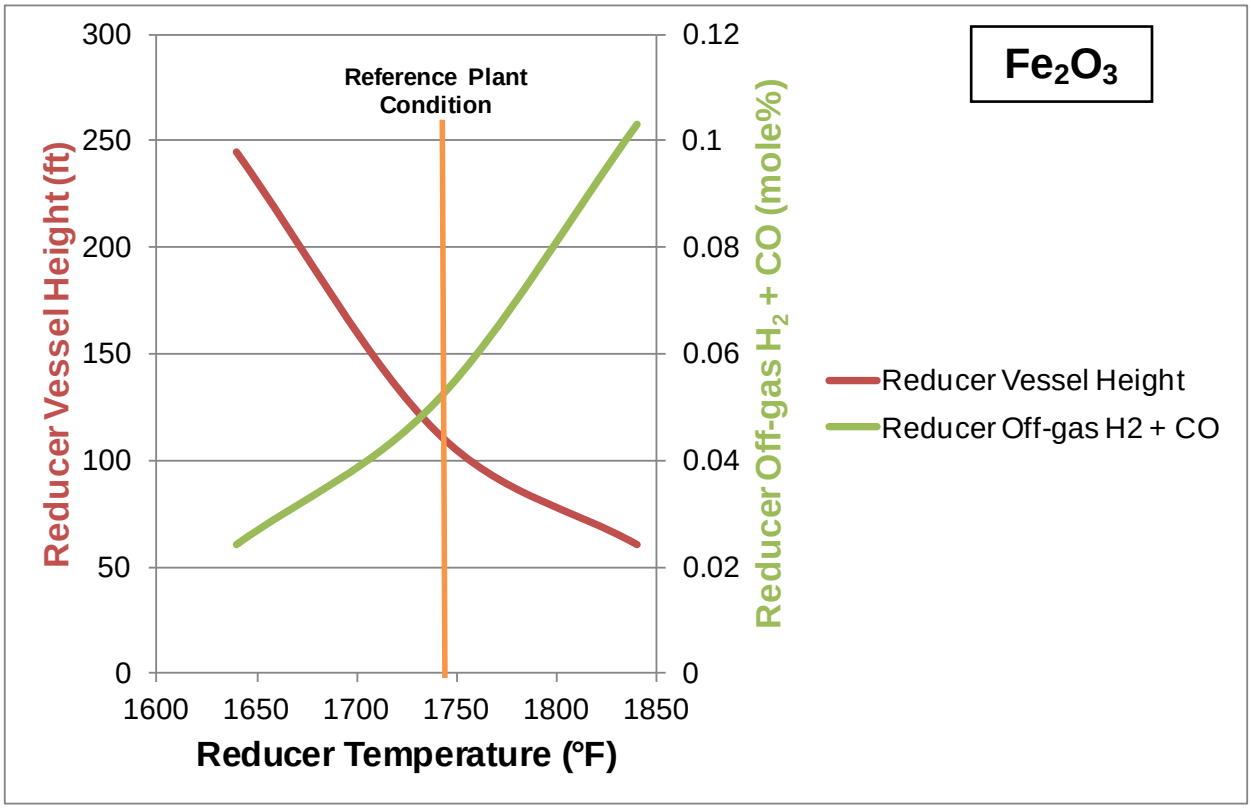


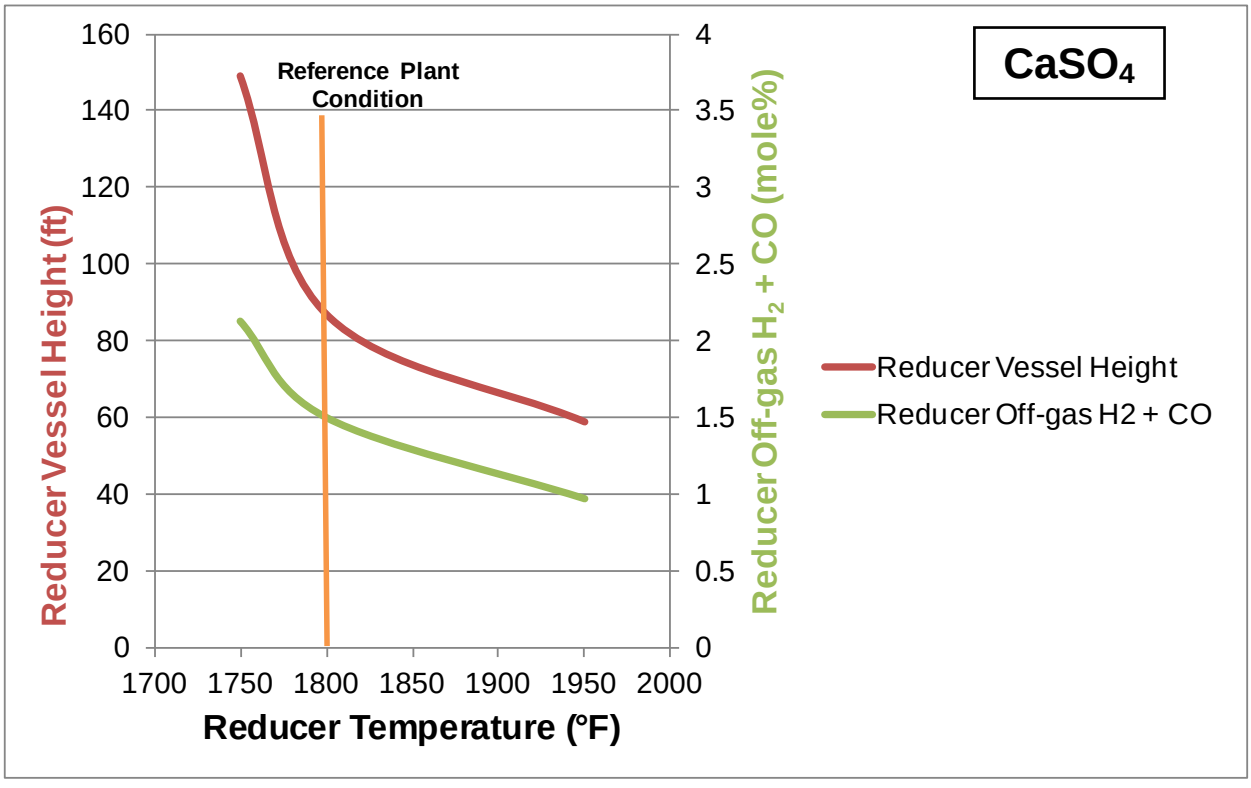

**Exhibit 6-4 Oxidizer temperature sensitivity**

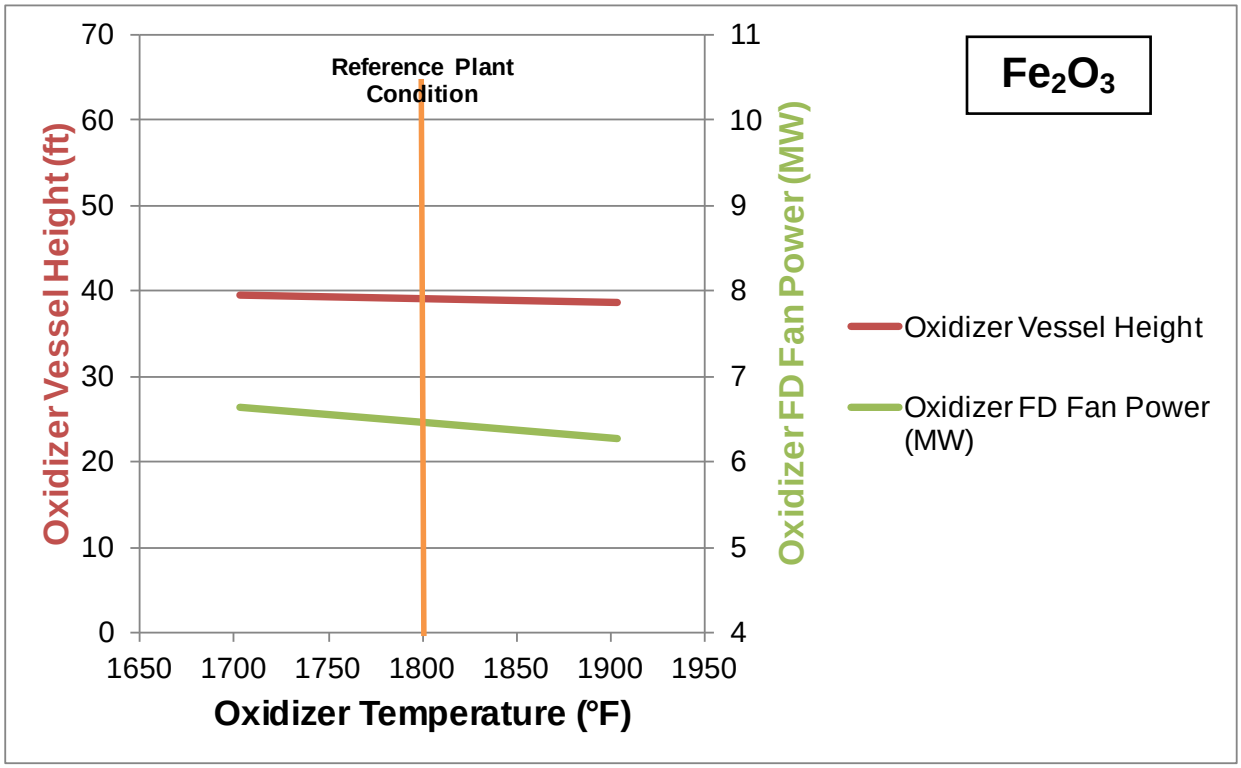


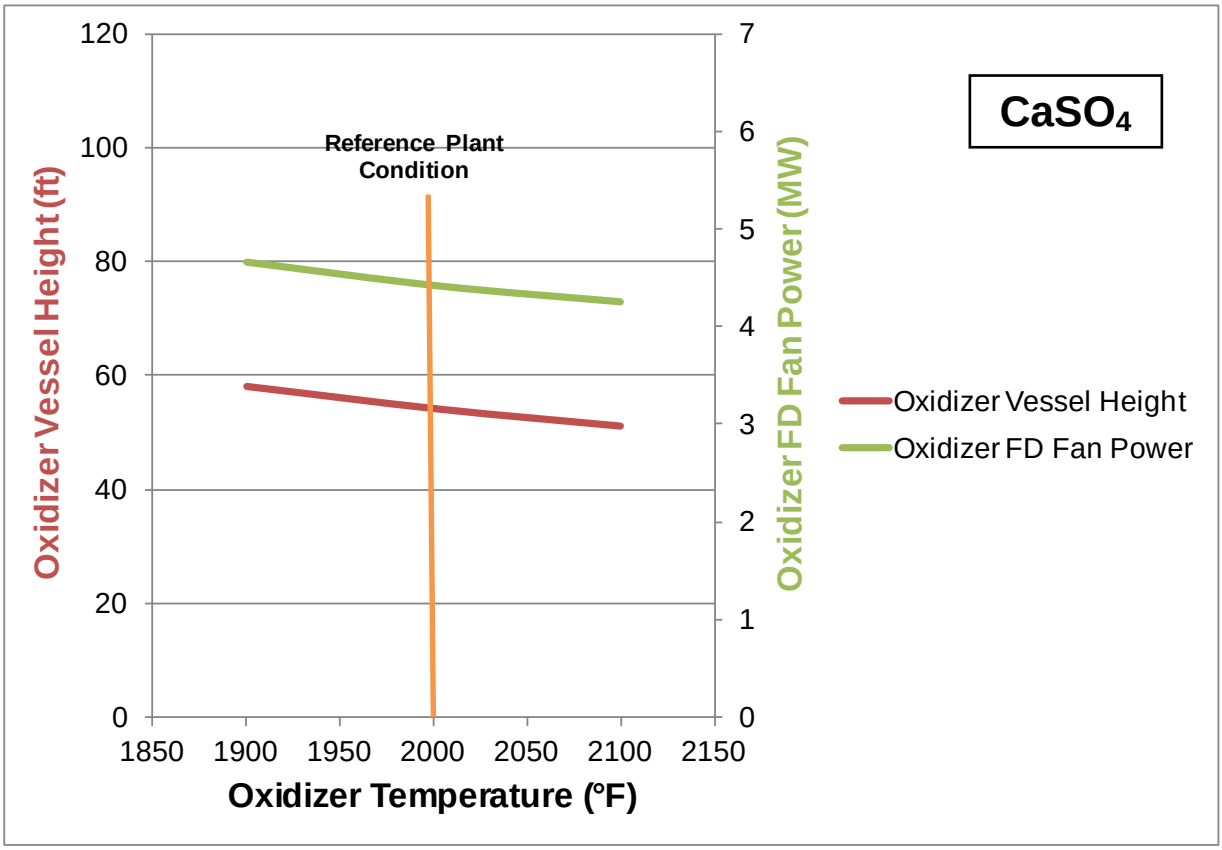

## 6.2 Reactor Velocity Sensitivity

The Reducer velocity sensitivity results are displayed in Exhibit 6-5. Again, the top chart shows results for the $Fe_2O_3$ oxygen carrier, and the bottom chart shows results for the $CaSO_4$ oxygen carrier. Reducer vessel height, Reducer shell inner diameter, and off-gas $H_2$ and CO content are plotted against the Reducer outlet velocity. As the velocity increases, the vessel shell diameter decreases, but does not approach a vessel size that could be shop fabricated. Increasing velocity also results in greatly increased Reducer vessel height with a more moderate increase in the off-gas $H_2$ and CO content. There is certainly no clear benefit resulting from increased Reducer velocity for either of the two oxygen carrier types. The impact of reactor footprint versus reactor vessel height needs to be assessed for given plant sites to provide further perspective and a basis for judging the sensitivity results.

The Oxidizer velocity sensitivity results are displayed in Exhibit 6-6. A similar trend is shown for the Oxidizer velocity sensitivity. Increasing the Oxidizer velocity for both oxygen carriers yields a reduction in the Oxidizer shell diameter, which is beneficial. The is accompanied by an increase in the Oxidizer vessel height and the Oxidizer FD fan power consumption due to higher Oxidizer vessel pressure drop. Again, it is concluded that there is no clear benefit to be shown for increasing the Oxidizer velocity. It should also be noted that operating velocities above 30 ft/s enter a region of limited commercial circulating fluid bed operational experience and would require significant development effort.

**Exhibit 6-5 Reducer velocity sensitivity**

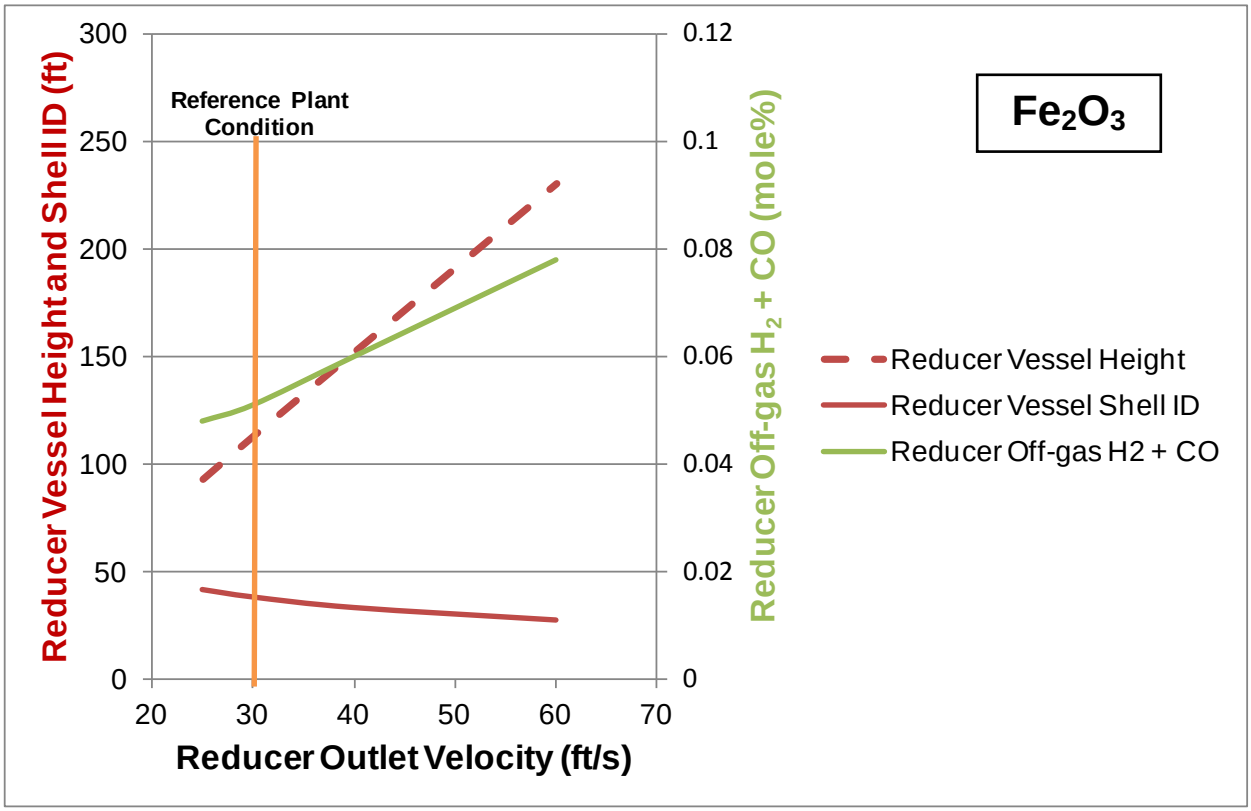


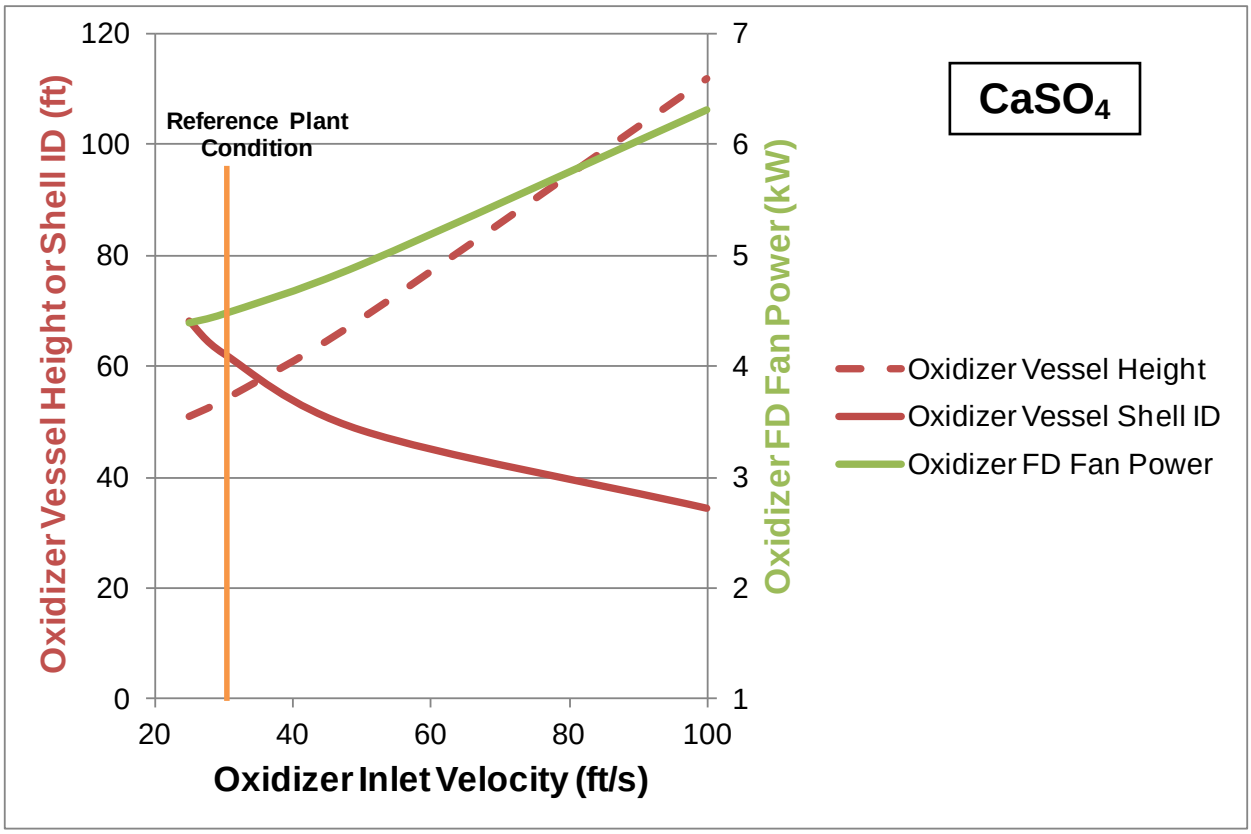

**Exhibit 6-6 Oxidizer velocity sensitivity**

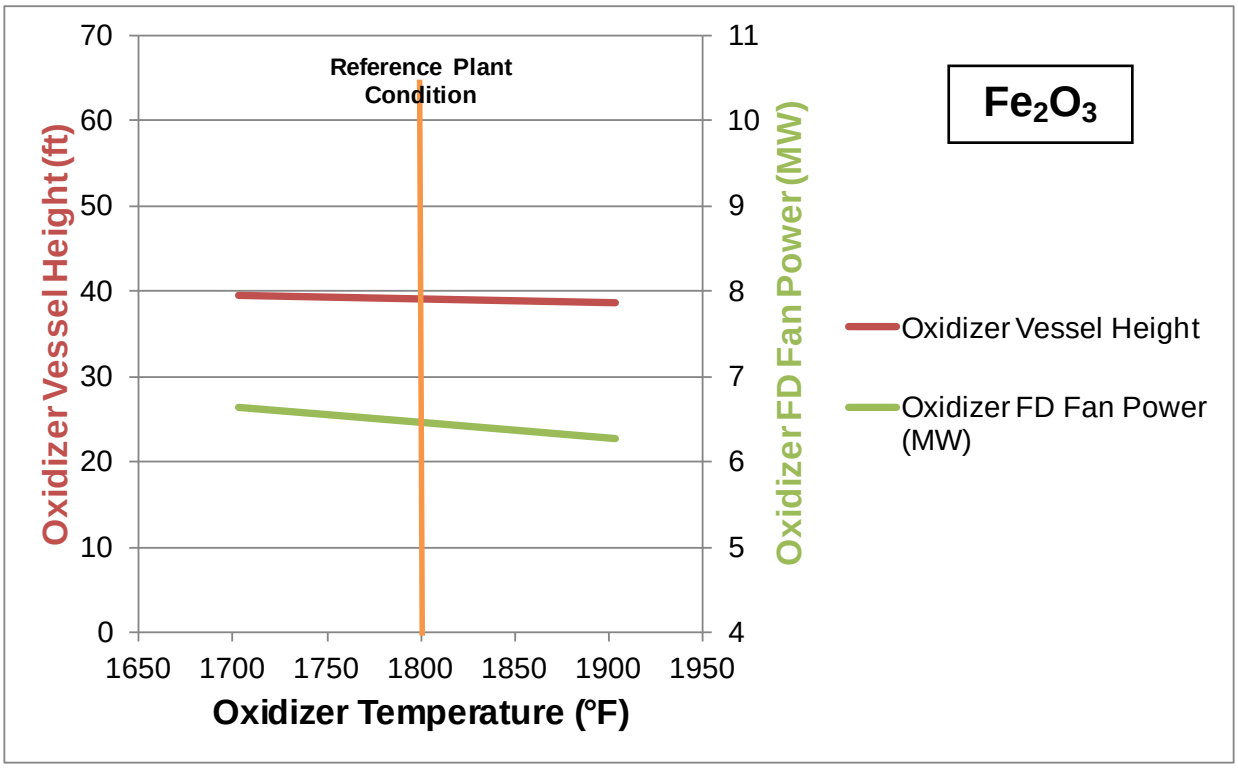


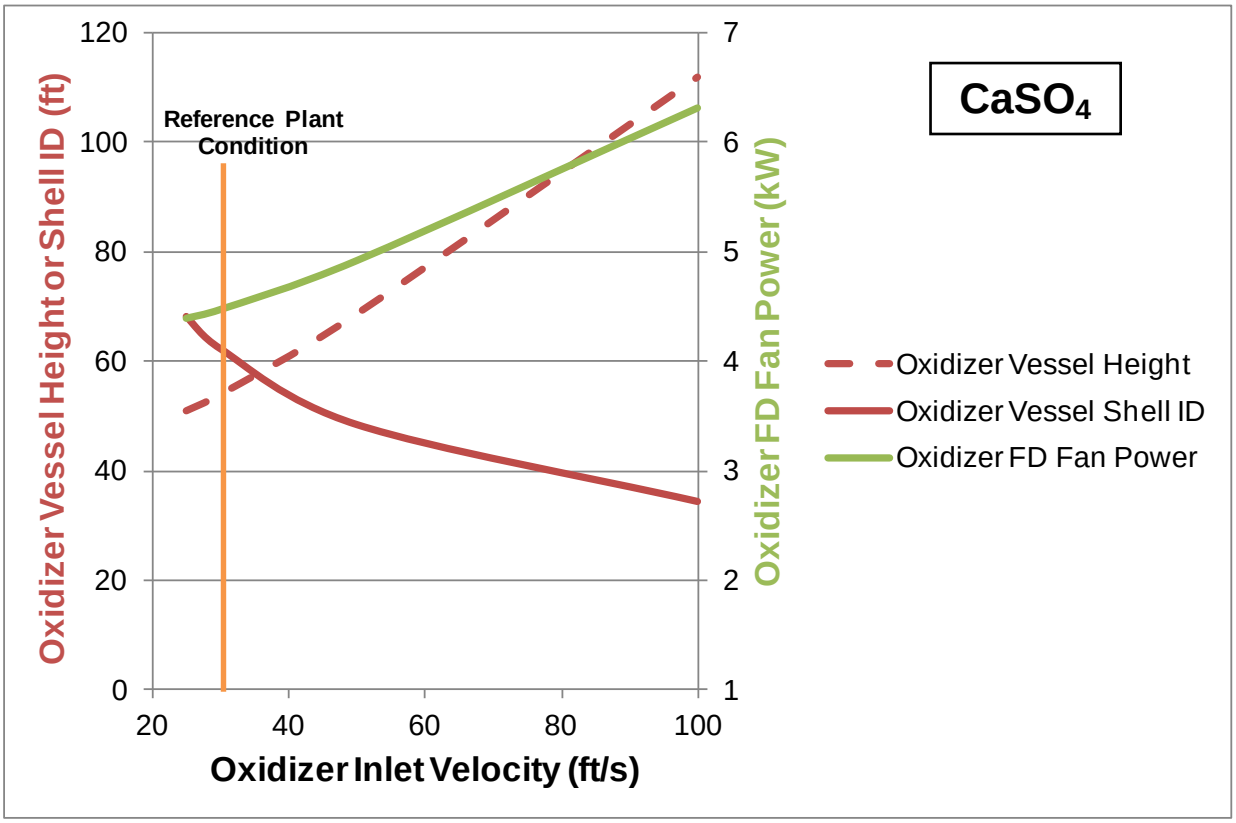

## 6.3 Carbon Gasification Efficiency Sensitivity

The Reducer carbon gasification efficiency sensitivity results are displayed in Exhibit 6-7. Plots are shown of the Reducer vessel height, cost, and off-gas $H_2$ and CO content as a function of the carbon gasification efficiency for Reducers with and without char-oxygen carrier separators. For the $Fe_2O_3$ oxygen carrier, the off-gas $H_2$ and CO content curves are not shown, because the $H_2$ and CO content remains low with this highly reactive oxygen carrier. In this report, the carbon gasification efficiency is defined as the total coal carbon conversion rate to CO and $CO_2$, over the total coal carbon feed rate. The Reducer model provides estimates of how the carbon gasification efficiency might be increased by increasing the reducer temperature or by increasing the effectiveness of the char-oxygen carrier separation system.

The benefit of the char-oxygen carrier separation system appears to be clear from these plots. Without char-oxygen carrier separation the Reducer, vessel height and vessel cost are dramatically increased to a point where the Reducer would not be a feasible reactor. Simultaneously, the Reducer off-gas $H_2$ and CO content would be reduced to very low levels due to the greatly increased gas residence time, but not to sufficient benefit to counter the greatly increased vessel height.

When using char-oxygen carrier separation, increased carbon gasification efficiency results in moderately greater Reducer vessel heights and vessel costs with slightly decreased off-gas $H_2$ and CO content. Increased carbon gasification efficiency will only serve to increase the plant $CO_2$ capture efficiency and will not impact the power plant thermal efficiency significantly since all of the carbon not gasified in the Reducer will be burned in the Oxidizer reactor. There appears to be little need for Reducer carbon gasification efficiency greater than that needed to achieve 90 percent carbon capture efficiency.

The real need is to develop technically feasible and affordable char-oxygen carrier separation approaches for achieving even this level of carbon gasification efficiency. The challenge is the very high rate of solids flow, having very small content of char that is characteristic of these CLC processes.

**Exhibit 6-7 Carbon gasification efficiency sensitivity**

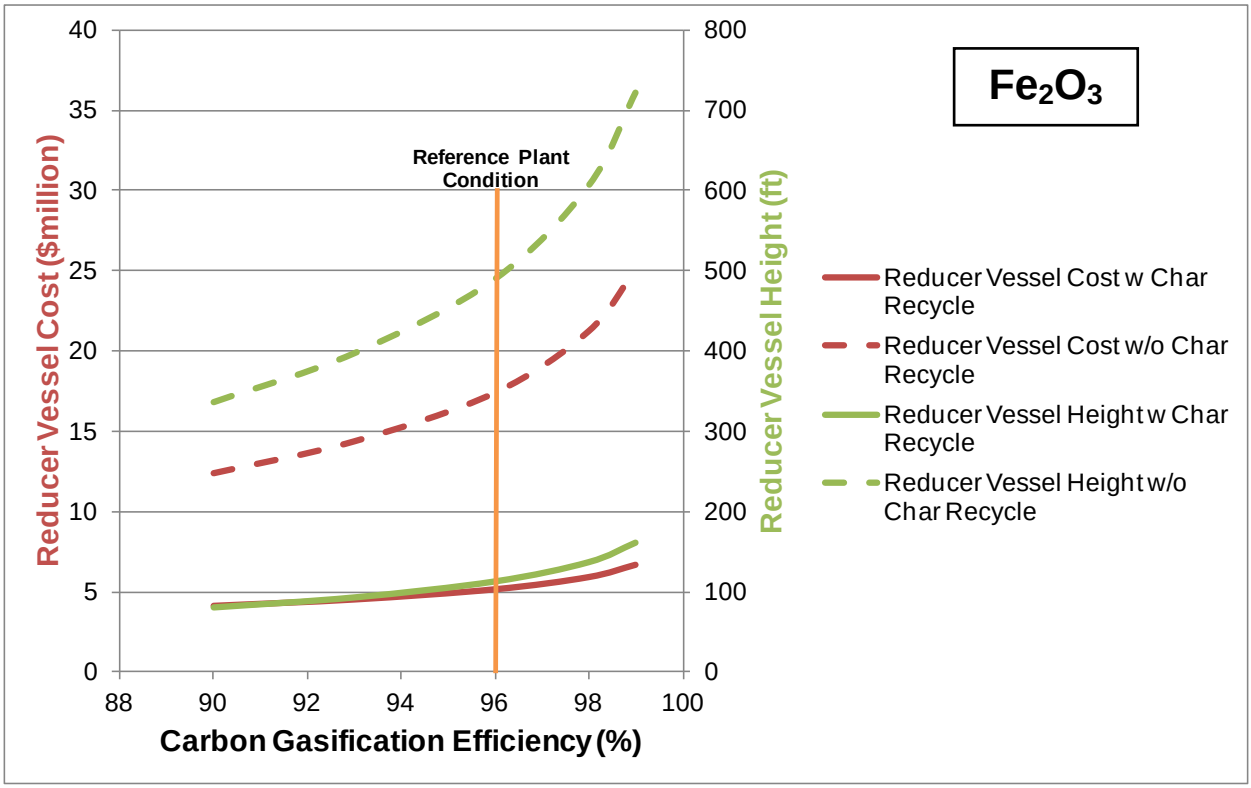


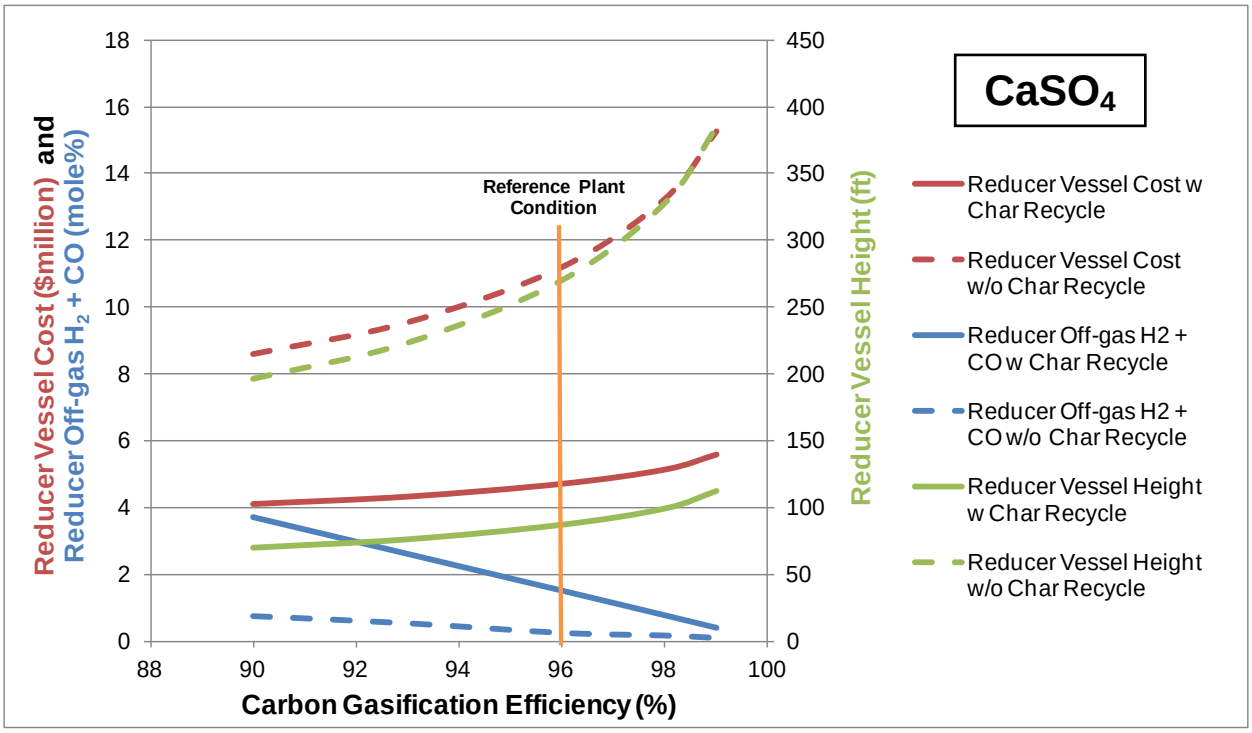

## 6.4 Reducer Oxygen Carrier Conversion Sensitivity

The Reducer oxygen carrier conversion sensitivity results are displayed in Exhibit 6-8**.** The graphs plot the oxygen carrier circulation rate, the Reducer off-gas $H_2$ and CO content, and the Oxidizer FD fan power against the Reducer outlet oxygen carrier fractional conversion. Lower levels of oxygen carrier conversion will result in higher reactivity oxygen carrier, and lower Reducer off-gas $H_2$ and CO contents. Lower levels of oxygen carrier conversion also result in moderately higher Oxidizer FD fan power consumption and a very large increase in the oxygen carrier circulation rate.

With the $Fe_2O_3$ oxygen carrier, the oxygen carrier is inherently of high reactivity, and higher conversions can be applied to avoid the huge oxygen carrier circulation rates that would result at low oxygen carrier conversion. The reference plant conversion level of about sixty-nine percent appears to be a good design choice.

The $CaSO_4$ oxygen carrier is a low reactivity material, with inherently low oxygen carrier circulation rates. Operating at lower levels of oxygen carrier conversion results in a relatively high reactivity in the Reducer, and also gives oxygen carrier circulation rates that are low compared to those found for the $Fe_2O_3$ oxygen carrier. Again, the $CaSO_4$ oxygen carrier reference plant conversion of about nineteen percent appears to be a good design choice.

Large oxygen carrier circulation rates are relatively easy to accommodate when using circulating fluidized bed reactors, because the Reducer and Oxidizer off-gases are the transport gases for the circulating solids and can generate high circulation rates if required. High rates are more costly and consume more auxiliary power with other reactor types, such as bubbling fluidized beds or moving beds. In these types of reactors the oxygen carrier circulation system is a completely independent equipment system, and a separate transport gas system is needed.

**Exhibit 6-8 Reducer oxygen carrier conversion sensitivity**

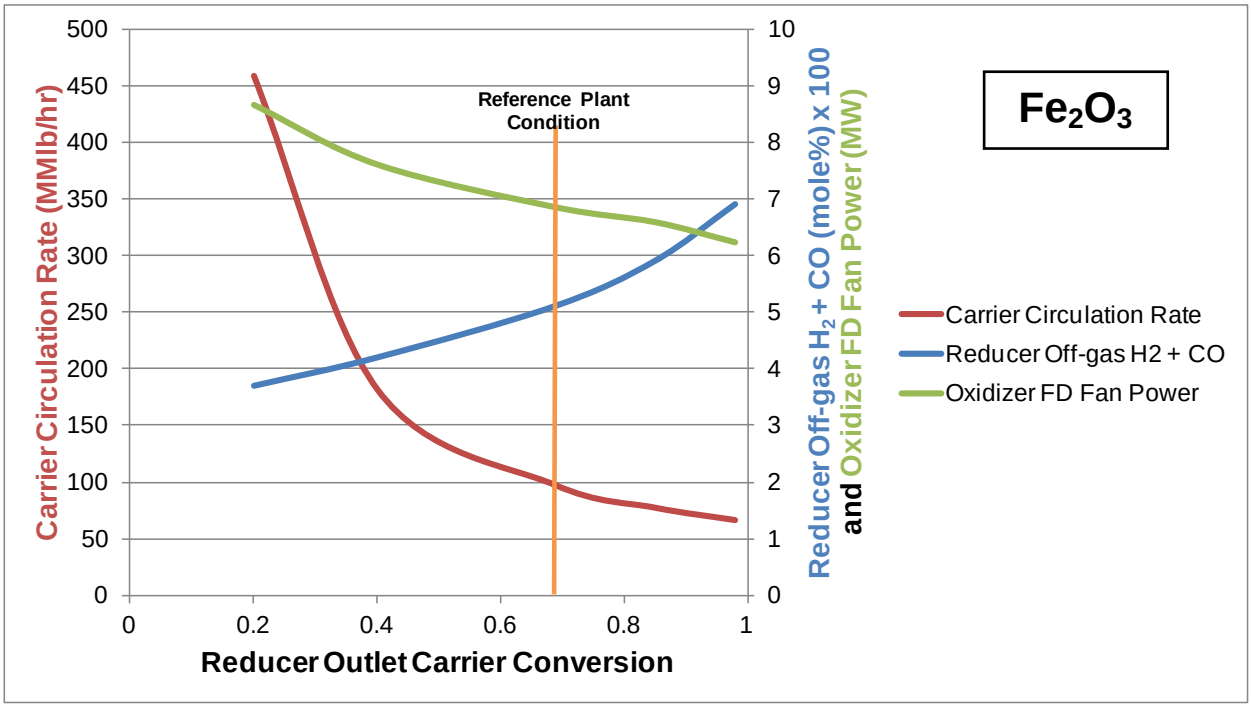


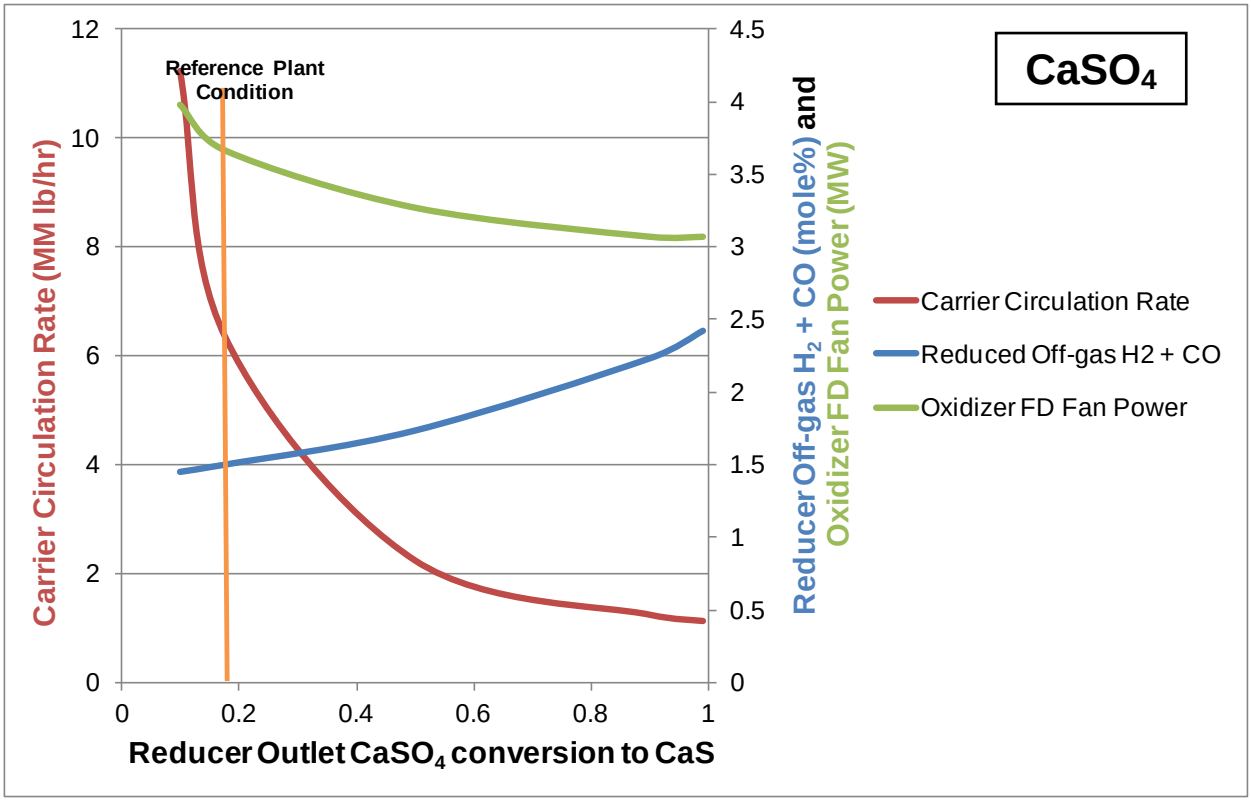

## 6.5 COE Sensitivity to Oxygen Carrier Makeup Rate and Price

The oxygen carrier makeup rate and price sensitivity results are displayed in Exhibit 6-9**.** In this report, the COE for the CLC power plant is shown as a function of the oxygen carrier makeup rate and the price of the makeup material. The COE for the conventional PC power plant with amine-based $CO_2$ absorption is superimposed on the plots.

The $Fe_2O_3$ oxygen carrier has an expected price of $1/lb to $5/lb, and with high makeup rates the COE could exceed the COE of the conventional PC plant. For the $Fe_2O_3$ oxygen carrier CLC power plant to have lower COE than the $CaSO_4$ oxygen carrier CLC power plant the $Fe_2O_3$ makeup rate will need to be quite low. The dashed lines on the $Fe_2O_3$ oxygen carrier plot represent oxygen carrier prices for cheaper $Fe_2O_3$ materials, for example raw ores or waste materials. While these materials may have lower reactivity than the reference plant supported $Fe_2O_3$ oxygen carrier; their lower price makes them candidates for development consideration. Minimizing $Fe_2O_3$ oxygen carrier losses is a priority for process development.

The $CaSO_4$ oxygen carrier, even if at a relatively high limestone price in the range of $100/ton to $200/ton, can accommodate high makeup rates and maintain a COE significantly lower than that in the conventional PC plant. At the lower price assumed in the reference plant design, $33.5/ton, the limestone makeup rate is not a significant consideration.

**Exhibit 6-9 Oxygen carrier makeup and price sensitivity**

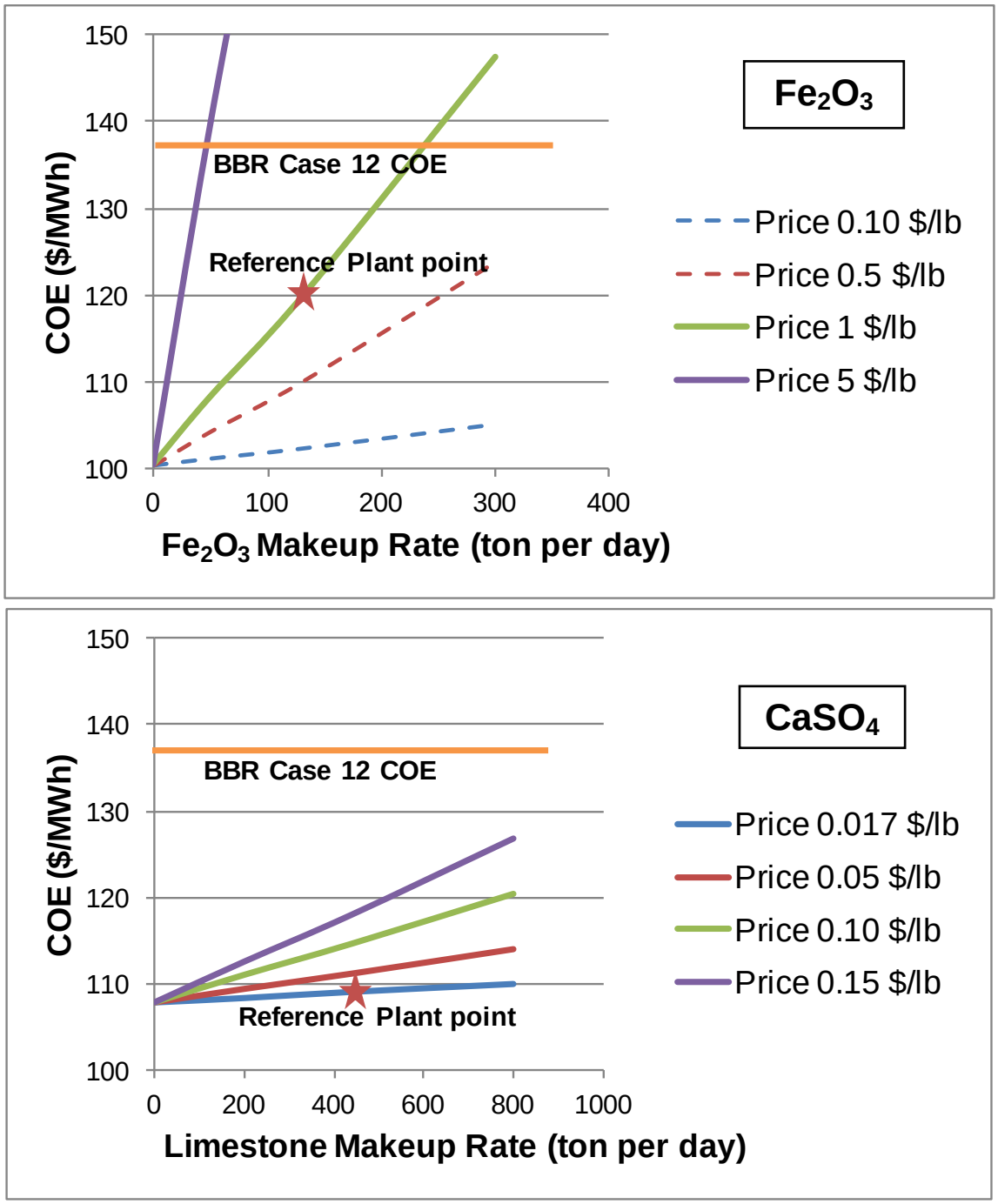

## 6.6 COE Sensitivity to Char-Oxygen Carrier Separator Cost

In the reference plant evaluations, the hypothetical char-oxygen carrier separation system was assumed to have zero cost. To understand how sensitive the CLC plant COE is to the potential capital cost of the char-carrier separation system, a range of char-carrier costs has been applied that are equivalent to as much as ten-times the cost of the Reducer reactor. The characteristic duty of the reference plant char-carrier-ash separation device is also shown in the exhibit, with very large solids flow rates having very small char content. The COE sensitivity to the char-carrier separator cost results are displayed in Exhibit 6-10. Parallel lines for the two oxygen carriers result, with an increase in the CLC plant COE of as much as three $/MWh over the separator cost range considered. It is concluded that the capital cost of the char-carrier separation system is not likely to have a significant impact on the CLC power plant COE. The performance and reliability of the char-carrier separation system, though, will be critically important.

**Exhibit 6-10 Char-carrier separator device cost sensitivity**

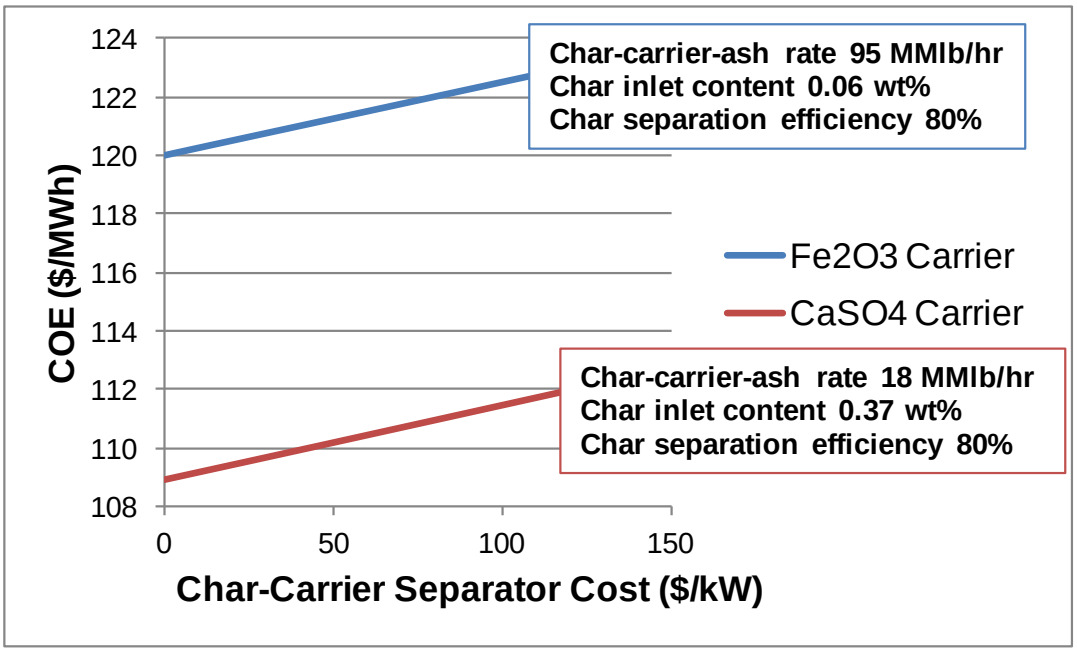

# 7 CLC Circulating Fluid Bed Reactor Modeling

The circulating fluid bed CLC modeling is performed for metal oxide oxygen carriers and calcium sulfate oxygen carrier. While iron-based carrier is used in the model development for metal oxide oxygen carriers, the models are easily adjusted for use with any metal oxide carrier, except those that actually generate a significant elemental oxygen release into the gas phase. The modeling relates specifically to near atmospheric-pressure operation, with many aspects of the reaction kinetics and fluidized bed dynamics changing with elevated pressure operation.

The modeling applies previously proposed circulating fluid bed reactor models that represent the structure of the circulating fluid bed and the various mass transfer resistances within the fluid bed. These models have very uncertain behavior and are based primarily on small-scale test observations and contain several parameters. The oxygen carrier reaction kinetics that are used are taken from laboratory testing reported in the open literature for both iron-based and $CaSO_4$-based oxygen carriers. Many aspects of the oxygen carrier behavior in the circulating fluid bed are uncertain, including the durability and reactivity degradation in this reaction system. The resulting reactor models can only be expected, at best, to represent approximate performance trends for the Reducer and Oxidizer reactors and to be an initial step in understanding the CLC system.

## 7.1 Reducer Reactor

The Reducer reactor must be designed and operated so that coal and oxygen carrier particles will react to simultaneously gasify coal to near complete carbon conversion while producing an outlet gas high in $CO_2$ and $H_2O$ content, and low in $H_2$ and CO content. These two desired results will not be possible with all oxygen carrier types and at all operating conditions. Past experience with coal gasification indicates that coal gasification is relatively slow at typical Reducer temperatures and may limit the performance of the Reducer.

Numerous metal oxides have been considered as candidates for oxygen carriers in CLC applications. $Fe_2O_3$-based oxygen carriers are used in this document to illustrate the modeling principles for metal oxide oxygen carriers, and alternative metal oxide oxygen carriers can be substituted for $Fe_2O_3$ if comparable reaction kinetics are available. The modeling principles for an alternative oxygen carrier class, $CaSO_4$-based oxygen carriers, are also described.

Several primary chemical conversions occur in the Reducer reactor that must be incorporated into the Reducer model. These primary reactions are described below.

### 7.1.1 Metal Oxide Oxygen Carrier Reactions

Metal oxide oxygen carriers are reduced to a lower oxygen form, $Fe_3O_4$, by $H_2$ and CO that are generated by coal gasification reactions in the Reducer:

$$H_2 + 3\ Fe_2O_3 = 2\ Fe_3O_4 + H_2O$$

$$CO + 3\ Fe_2O_3 = 2\ Fe_3O_4 + CO_2$$

Even lower oxide levels of iron, FeO, and Fe, are not considered in fluidized bed reactors, because the rates of the reduction reactions to these oxide levels at feasible operating temperature are very slow and may be limited by equilibrium constraints.

Other possible metal oxide reactions neglected here are interaction reactions with coal-based contaminants such as halides (e.g., HCl) and sulfur in the form of $H_2S$ and COS. Such contaminant reactions may adversely influence the metal oxide oxygen carrier performance.

In essence, oxygen is released by

$$3\ Fe_2O_3 = 2\ Fe_3O_4 + O$$

For the mixture of $Fe_2O_3$ and $Fe_3O_4$, the "conversion" of $Fe_2O_3$ to $Fe_3O_4$ is given by

$$\mathbf{X_S = 3/2\ M_{Fe3O4} / [M_{Fe2O3} + 3/2\ M_{Fe3O4}] = 3/2\ M_{Fe3O4} / M_T}$$

where M represents the molar flow rate, and the denominator is an invariant equal to the total molar flow rate of oxygen carrier, $M_T$. In terms of the mole fractions in the mixture,

$$\mathbf{X_S = x_{Fe3O4} / 2 / [x_{Fe3O4} / 2 + x_{Fe2O3} / 3]}$$

where $x_{Fe3O4}$ and $x_{Fe2O3}$ are mole fractions of $Fe_3O_4$ and $Fe_2O_3$ in reacted oxygen carrier mix.

The apparent molar rate of $O_2$ generation is given by

$$\mathbf{M_{O2} = (X_{Sout} - X_{Sin}) \bullet M_T / 6}$$

### 7.1.2 $CaSO_4$-Based Oxygen Carrier Reactions

$CaSO_4$ is reduced to CaS by $H_2$ and CO that are generated by coal gasification reactions in the Reducer:

$$H_2 + 1/4\ CaSO_4 = 1/4\ CaS + H_2O$$

$$CO + 1/4\ CaSO_4 = 1/4\ CaS + CO_2$$

It is also possible that a portion of the $CaSO_4$ may reductively decompose to CaO and $SO_2$, and, in the Reducer environment, this $SO_2$ may be converted to $H_2S$:

$$CaSO_4 + H_2 / CO = CaO + SO_2 + H_2O / CO_2$$

$$SO_2 + 3\ H_2 = H_2S + 2\ H_2O$$

Of course, sulfur species released from the coal in the Reducer will also react with the $CaSO_4$-based oxygen carrier:

$$CaO + H_2S = CaS + H_2O$$

and carbonation of CaO to $CaCO_3$ may also occur in the Reducer with its high partial pressure of $CO_2$.

Limestone is the cheapest $CaSO_4$-based oxygen carrier makeup source, although a sulfated limestone from some other application or from a fabricated $CaSO_4$ material could be used and may have better reaction kinetics. Limestone will always undergo calcination within the

Reducer reactor. Several classes of limestone and numerous quarry sources are available, and their reactivity and durability can vary significantly.

In essence, oxygen is released by

$$CaSO_4 = CaS + 2\ O_2$$

For the mixture of $CaSO_4$ and CaS, with CaO and $CaCO_3$, where the secondary impacts of $CaSO_4$ decomposition and CaO sulfidation are neglected, the "conversion" of $CaSO_4$ to CaS is given by

$$\mathbf{X_{Ca} = M_{CaS} / [M_{CaSO4} + M_{CaS}] = M_{CaS} / M_T}$$

where M represents the molar flow rate, and the denominator is an invariant equal to the total molar flow rate of oxygen carrier, $M_T$. In terms of the mole fractions in the mixture,

$$\mathbf{X_{Ca} = x_{CaS} / [x_{CaSO4} + x_{CaS}]}$$

The apparent molar rate of $O_2$ generation is given by

$$\mathbf{M_{O2} = 2 \bullet (X_{Caout} - X_{Cain}) \bullet M_T}$$

### 7.1.3 Coal Gasification

The coal particles injected near the base of the Reducer reactor undergo rapid heating and conversion, with coal volatile release, formation of char particles, and volatile species conversions to lower hydrocarbons by reactions with injected steam and $CO_2$ in the lower portion of the Reducer:

$$\text{coal} \rightarrow \text{volatiles} + \text{tars/oils} + \text{char}$$

$$\text{volatiles} + \text{tars/oils} + H_2O / CO_2 \rightarrow H_2 / CO + H_2S / COS / HCl / NH_3$$

Slow conversion of char carbon throughout the bulk of the Reducer reactor will control the required dimensions of the Reducer and its performance:

$$C + H_2O = CO + H_2$$

$$C + CO_2 = 2CO$$

### 7.1.4 Reaction Kinetics in the Reducer

The coal transformations to char and lighter hydrocarbons are assumed to be fast due to rapid mixing with hot solids in the high steam and $CO_2$ content near the base of the reactor. It is assumed that about 0.5 second gas residence time, or about 10 ft of reactor depth is needed to complete these conversions. This assumption is based on test observations showing that devolatilization is initiated at relatively low temperature and proceeds very rapidly with the rapid heating that occurs within the fluidized bed and provides some contingency for the vessel height to accommodate these phenomena. [9]

The conversions of oxygen carrier and char carbon in the bulk of the Reducer reactor are highly interdependent. The oxygen carrier consumes $H_2$ and CO and produces $H_2O$ and $CO_2$. The char carbon conversion consumes $H_2O$ and $CO_2$ and generates $H_2$ and CO. This interaction, as illustrated by the chemical reactions listed above, and the relative rates of these reactions, are critical to estimating the dimensions and performance of the Reducer reactor. The secondary oxygen carrier reactions, such as oxygen carrier calcination and decomposition, and various gas-phase reactions such as the water-gas-shift, are modeled by imposing thermodynamic equilibrium estimates.

#### *7.1.4.1 Metal Oxide Oxygen Carrier Reduction*

The reaction kinetics for different metal oxide oxygen carriers depend on a variety of factors, for example, metal oxide type, oxygen carrier processing (e.g., natural ore, or fabricated, supported metal oxide), particle size, particle voidage distribution, and particle grain size distribution. Other environmental factors, such as reactor temperature, gas-particle velocities in the reactor, and equilibrium constraints, are also important. Over the potential operating ranges of these variables it is possible for different reaction resistances to dominate: for example, diffusion of the reactive gas species from the gas phase to the oxygen carrier particle surface, diffusion of the reactive gas species through the particle pores, diffusion of the reactive gas species through the reaction product layer to the reaction interface, the chemical reaction rate itself, diffusion of the reaction products out of the grains and pores and back to the bulk gas phase.

It is assumed that in the fluidized bed environment, with the particle sizes characteristic of high-velocity fluidized beds, at the reactor temperatures selected, and with metal oxide oxygen carriers typical of those described in the literature, equilibrium constraints will be insignificant, and the reaction kinetics can be described by a form suggesting the reaction gas species diffusion through the particle grain product layer dominate the gas-particle reaction resistances:

$$\mathbf{d\,X_S\,/dt = 3\,/\tau \bullet (1 - X_S)^{2/3} = 3 \bullet b_j \bullet k_j \bullet C_j^{\,Nj}\,/(\,\rho_m \bullet r_g) \bullet (1 - X_S\,)^{2/3}}$$

$X_S$ is the fraction of the metal oxide converted, $\tau$ is the time for complete carrier particle reaction with fixed reaction gas concentration $C_j$, $b_j$ is the reaction coefficient (moles of metal oxide converted per mole of gas species j, ($H_2$ or CO), $k_j$ is the kinetic rate constant as determined by experimentation at representative conditions in reactant gas j, $N_j$ is the reaction order in gas species j, $\rho_m$ is the molar density of the carrier particle (moles of reactive oxide per particle volume), and $r_g$ is the representative particle grain radius within the oxygen carrier particle.

Literature data is available for many metal oxide oxygen carrier types that fit this rate expression, as well as other closely associated rate expressions. Thermogravimetric apparatus (TGA) tests may be performed to generate data that can provide an empirical fit of reaction rate versus conversion level ($X_S$) over a range of temperatures, reactant gas compositions, particle sizes, etc., and generate an empirical expression that can be used for engineering estimates without identifying specific reaction mechanisms.

Such test data was reported by Abad [3] and others for several metal oxide oxygen carriers. In general, at the reaction conditions of interest, it is observed that the reaction rate is not sensitive to particle size or gas pressure. For a supported $Fe_2O_3$ oxygen carrier, the kinetic terms are:

$$\mathbf{k_{H2}(m/s) = 0.0023 \bullet \exp\{-24/(R \bullet T)\}}$$

$$\mathbf{k_{CO}(m/s) = 0.00062 \bullet \exp\{-20/(R \bullet T)\}}$$

R is the gas constant, equal to 0.008314 kJ/mol-K

T is the reactor temperature in K

$r_g(m) = 2.6\times10^{-7}$

$\rho_m$ (mole/$m^3$) = 32,811

$N_{H2}$ = 0.8

$N_{CO}$ = 1

As shown by the chemical reactions for an $Fe_2O_3$ oxygen carrier, the value of $b_j$ is 3 in either $H_2$ or CO.

For perspective, most metal oxide oxygen carriers have relatively high reactivity, and the time for total reduction, $\tau$ , of this $Fe_2O_3$-based oxygen carrier to $Fe_3O_4$, in 100 percent reductant and with temperature of 1681°F, would be, from the kinetic parameters,

$\tau$ = 2.2 seconds in $H_2$

$\tau$ = 3.4 seconds in CO

### *7.1.4.2 $CaSO_4$ Oxygen Carrier Reduction*

The $CaSO_4$-based oxygen carrier could be a fabricated, supported material, or a natural mineral such as limestone or dolomite. Most development work with $CaSO_4$-based oxygen carrier has used sulfated limestone. [4] The reduction kinetics of $CaSO_4$ to CaS in $H_2$ and CO has been characterized to only a limited extent in the literature, so the reaction kinetics basis applied here is very uncertain. The reaction rate for this conversion is dependent on the $CaSO_4$ source used, as well as its particle size and the reaction conditions in the Reducer.

Song, et al, tested natural anhydrite ore for reduction to CaS in a small fluidized bed reactor with $H_2$, CO, and mixtures of $H_2$ plus CO. [6] They observed that the reaction rate is first order in both $H_2$ and CO concentration and that the reaction rate is greater in $H_2$ than in CO, and is slightly greater in $H_2$ + CO mixtures than it is in $H_2$ alone. While the Song work estimated kinetic factors for the conversion reaction, it did not account for the significant fluidized bed resistances that would have been present, and thus the presented kinetic factors underestimated the actual reaction kinetics.

Tian and Guo [7] presented test data and analyses done with a TGA system that provides direct kinetic results. They tested analytically pure calcium sulfate in CO reaction gas. The particle diameter of this material was about 9 microns, so the tested material was not truly representative of limestone-based material have sizes in the 100 to 300 μm range needed for this application. It is assumed that the reaction rate form can be expressed as:

$$\mathbf{d\,X_{Ca}/dt = 3 \bullet b \bullet k \bullet C/(\rho_{Ca} \bullet r_g) \bullet (1 - X_{Ca})^{2/3}}$$

$$\mathbf{k = A \bullet \exp\{ - Ea / (R \bullet T)\}}$$

Here, $X_{Ca}$ is the fraction of the $CaSO_4$ converted to CaS. For a test condition with CO at $CO_T$ and a total reaction time of $\tau_T$

$$\mathbf{k_T = \rho_{Ca} \bullet r_g / (b \bullet \tau_T \bullet C_T)}$$

With about 1,200 second total reaction time at 1800°F and 20 mole% CO, the data analysis by Tian and Guo reported an $E_a$ of 280.45 kJ/mole. From this it can be estimated that

$$k_T = 0.00044 \text{ (m/s)}$$

and

$$A = 1.41 \times 10^8 \text{ (m/s)}$$

It is assumed here that reaction in $H_2$ + CO mixture would show similar rate behavior:

$$\mathbf{k_{H2 + CO} (m/s) = 1.41x10^8 \bullet \exp\{-280.45/(R \bullet T)\}}$$

Since the rate data is from tests with analytical grade anhydrite, not representative of a natural limestone source, a rate adjustment factor is also incorporated into the rate constant to use for sensitivity studies and was set in the reference design to double the above test data rate value.

These reaction rate expressions indicate that under similar reaction conditions, the rate of $Fe_2O_3$ oxygen carrier reduction, and other metal oxide oxygen carriers, would be at least 100 times greater than the estimated rate of $CaSO_4$ oxygen carrier reduction used here, depending on the Reducer operating temperature selected.

### *7.1.4.3 Char Carbon Gasification*

It is observed that char carbon reacts in $H_2O$ and $CO_2$ as

$$\mathbf{d X_C / dt = k_C \bullet Y_j \bullet (1 - X_C)}$$

almost to complete conversion. $X_C$ is the fraction of char carbon reacted, $k_C$ (1/s) is the reaction rate constant, and $Y_j$ is the reaction gas mole fraction (j being $H_2O$ or $CO_2$). Test data in the temperature range of interest indicate that the rate of char carbon reaction is almost identical in $H_2O$ and $CO_2$.

Test data presented by Johnson [9] for Illinois No. 6 char indicated that

$$\mathbf{d X_C / dt = 129{,}599 \bullet \exp\{-21{,}731 / T(K)) \} \bullet Y_j \bullet (1 - X_C)}$$

It is also observed that

- the char gasification rate was nearly independent of particle size for particle less than 2 mm diameter, with chemical reaction rate control prevailing
- the rate decreased with increased product concentrations of CO and $H_2$

- increased gas pressure increased the rate only about 50 percent over an increase in pressure from atmospheric to 5 atmospheres, showing no influence at higher pressures, at the temperature range of interest to CLC

This reaction rate expression indicates that the rate of char carbon reaction is lower than the rate of $CaSO_4$ reduction, maybe a factor of five to ten times slower. In contrast, the rate of char carbon reaction is much slower than the rate of $Fe_2O_3$, or most other metal oxides, reduction. These relative reaction rates have important consequences for the overall Reducer reactor behavior and performance.

### 7.1.5 Fluidized Bed Reducer Assumptions and Conversion Expressions

The fluidized bed Reducer can range in operating velocity from levels that generate bubbling bed behavior (i.e., 3 ft/s) to fast, circulating bed behavior (i.e., greater than 25 ft/s). These two operating regimes for fluidized bed reactors are characterized by differing voidages within the bed and differing gas-solids mixing rates that influence their reaction performance and vessel dimensions. Most of the gas phase passes through the bed within the bubble phase, because this phase has very small particulate content. Gas transfer, convective and diffusive, from the bubble phase to the dense emulsion phase represents a major resistance to gas-solid reactions in chemical looping combustion reactors. Both regimes are considered in this section.

The following general assumptions suitable for fluidized bed reactors are applied:

- the bed temperature is uniform throughout
- coal is fed near the base of the fluidized bed and coal volatile are quickly released and char is quickly formed as the particle temperatures increase rapidly
- steam and $CO_2$ are fed at the base of the fluidized bed in sufficient quantity to convert the volatiles and tars rapidly to light hydrocarbons, mainly $H_2$ and CO
- the major portion of the Reducer reactor is devoted to the relatively slow reactions related to char carbon conversion and oxygen carrier reduction
- above the volatile release and conversion zone the only significant gas phase constituents for reaction modeling purposes are $H_2$, $H_2O$, CO, and $CO_2$
- the solids (char particles. ash particles, and oxygen carrier particles) are uniformly mixed within the fluidized bed reactor, meaning that the solids outlet stream has an average conversion of char and oxygen carrier ($\underline{X}_C$ for char, and $\underline{X}_S$ for metal oxide oxygen carriers, or $\underline{X}_{Ca}$ for $CaSO_4$ oxygen carriers) that is equal to the average char conversion and oxygen carrier conversion within the fluidized bed reactor
- the average reaction rate of char carbon within the fluidized bed reactor is proportional to a reaction rate expression based on the average char carbon conversion, $(1 - \underline{X}_C)$
- the average reaction rate of oxygen carrier within the fluidized bed reactor is estimated using the integral average of the rate expression, resulting in the average rate being proportional to $3/5 \cdot [ (1-X_1)^{5/3} - (1-X_2)^{5/3}]/(X_2-X_1)$. $X_1$ is the inlet oxygen carrier average conversion to the reactor product form, and $X_2$ is the outlet oxygen carrier average conversion for either $Fe_2O_3$ or $CaSO_4$ based carriers

The fluidized bed reactor consists of gas voids, or bubbles, that contain very little particulate and that pass upward at relatively high velocity through the bed. Most of the reaction gas is contained within this bubble phase, and the reaction gas species are transported from the bubble phase to the particulate phase by various convective and diffusional processes that contribute

large resistances to the overall rate of reaction conversions. Overall reaction rate constants that account for these resistances can be defined and estimated using correlations and models in the literature. A conceptual drawing of the circulating fluid bed structure is shown in Exhibit 7-1.

**Exhibit 7-1 Conceptual picture of circulating reducer reactor**

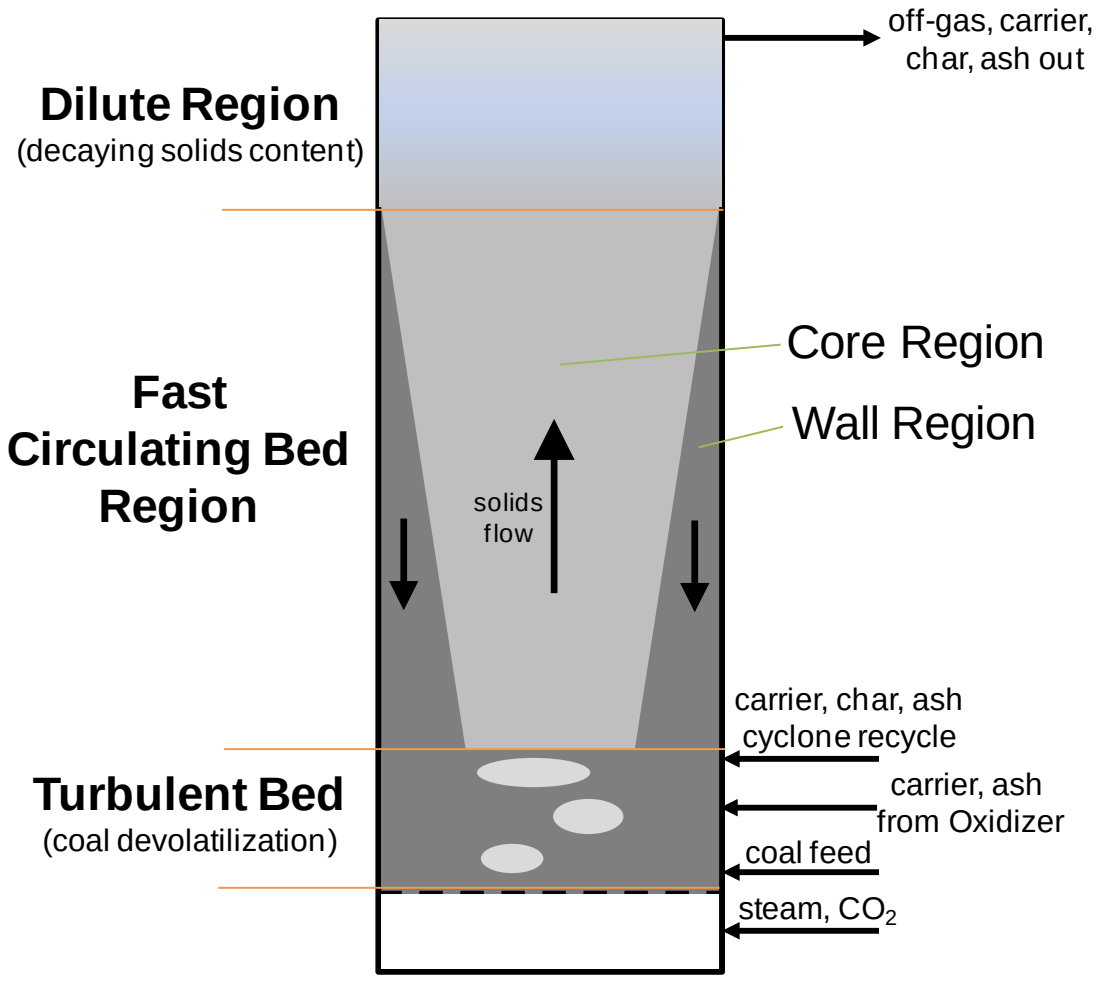


Within the fluidized bed reactor, gas species reaction rate constants are defined that express the rate per unit volume of reactive solids. For the metal oxide oxygen carriers, these are for $H_2$ and CO conversions:

$$k''_{H2}(1/s) = 3\, k_{H2} / r_g \bullet V_s \bullet (1 - \underline{X}_S)^{2/3}$$

$$k''_{CO}(1/s) = 3\, k_{CO} / r_g \bullet V_s \bullet (1 - \underline{X}_S)^{2/3}$$

For the $CaSO_4$ oxygen carrier, this is for a $H_2$ and CO mixture:

$$k''_{H2+CO}(1/s) = 3\, k_{H2+CO} / r_g \bullet V_s \bullet (1 - \underline{X}_S)^{2/3}$$

In general, the oxygen carrier rate constant with be designated $k''_{H2}$ in the following derivations.

For char gasification in $H_2O$ and $CO_2$:

$$k''_C \text{ (moles/s-m}^3\text{)} = k_c \bullet \rho_c \bullet V_c \bullet (1 - \underline{X}_C)$$

Here, $V_s$ is the volume fraction of oxygen carrier solids within the particulate mixture of ash, char and oxygen carrier, and $V_c$ is the volume fraction of char particles within the mixture. $\rho_c$ is the initial char particle moles of carbon per unit volume. The solids mixture consists of oxygen carrier particles, char particles, and ash particles fed from the Oxidizer reactor to the Reducer.

A differential $H_2$ balance on a horizontal plane cutting through the Reducer reactor is given by

$$d(U \bullet Y_{H2})/dz = - K_{H2} \bullet Y_{H2} + K_c/C^* \bullet Y_{H2O}$$

U is the superficial velocity through the bed at elevation z above the base, $K_{H2}$ is the overall fluidized bed reaction constant for oxygen carrier reaction with $H_2$, $K_c$ is the overall reaction constant for char carbon conversion, $Y_{H2}$ is the $H_2$ mole fraction at elevation z, $Y_{H2O}$ is the $H_2O$ mole fraction at elevation z, and $C^*$ is the total gas concentration at the reactor temperature and atmospheric pressure.

An analogous differential CO balance on the horizontal plane through the reactor is given by

$$d(U \bullet Y_{CO})/dz = - K_{CO} \bullet Y_{CO} + K_c/C^* \bullet (2 \bullet Y_{CO2} + Y_{H2O})$$

Adding these two expressions

$$d(U \bullet Y_{H2} + U \bullet Y_{CO})/dz = - K_{H2} \bullet Y_{H2} - K_{CO} \bullet Y_{CO} + 2 \bullet K_c/C^* \bullet (Y_{CO2} + Y_{H2O})$$

The following assumptions are applied:

- $Y_{H2} + Y_{CO} + Y_{H2O} + Y_{CO2} = 1$
- $K_{H2} \approx K_{CO}$
- the gas velocity through the Reducer reactor increases significantly from bottom to top, and a mean velocity, $U_m$ , is defined and applied to simplify the differential equations

Then

$$d\{U \bullet (Y_{H2} + Y_{CO})\}/dz = - \{K_{H2} + 2 \bullet K_c/C^*\}/ U_m \bullet U \bullet (Y_{H2} + Y_{CO}) + 2 \bullet K_c/C^*$$

The above differential equation can be solved to find an expression for the mole fraction of $H_2$ and CO at the bed exit. A bubbling bed reactor can be treated as a single zone reactor, with the splash zone above the bubbling bed contributing little to the reactor conversion. The circulating fluidized bed has a dense zone at the bottom and a dilute zone at the top, with the dilute zone making enough contribution to the overall reactor performance that it generally is considered.

Bubbling fluidized bed and circulating fluid bed dense region

At the top of the bubbling bed, or the top of the circulating bed dense zone

$$U_o \bullet (Y_{oH2} + Y_{oCO}) = B_{C1} \bullet U_m + [U_i \bullet (Y_{iH2} + Y_{iCO}) - B_{C1} \bullet U_m] \bullet \exp\{-2 \bullet K_c/C^*/B_{C1} \bullet H_d/U_m\}$$

where

$$B_{C1} \equiv 2 \bullet K_c/C^* /( K_{H2} + 2 \bullet K_c/C^*)$$

The terms $Y_{iH2}$ and $Y_{iCO}$ are the mole fractions of $H_2$ and CO at the top of the coal devolatilization zone near the base of the fluidized bed. $U_i$ is the gas superficial velocity at the top of the devolatilization zone, and $U_o$ is the gas superficial velocity at the top of the dense fluidized bed reactor, or at the top of the circulating bed dense region. $H_d$ is the height of the dense fluidized bed above the top of the devolatilization zone.

This relationship indicates that, for a bubbling fluidized bed, the minimum value of the mole fraction of $H_2$ plus CO, and thus the maximum value of the $CO_2$ and $H_2O$ gas content will be achieved when the bed height, $H_d$, approaches infinity, and

$$\mathbf{(Y_{oH2} + Y_{oCO})_{min} = U_m/U_o \ / \{ K_{H2} / (2 \bullet K_C/C^*) + 1 \}}$$

If the overall oxygen carrier reaction rate constant in the fluid bed, $K_{H2}$, is much greater than the overall rate constant for char carbon gasification, $2 \bullet K_c/C^*$, then the bubbling fluid bed Reducer outlet gas mole fraction of $H_2$ plus CO will approach zero, and the bulk of the gas phase should consist of $CO_2$ and $H_2O$ throughout most of the reactor. On the other hand, if the overall fluid bed rates of oxygen carrier reduction and char carbon gasification are comparable, the bubbling fluid bed minimum outlet $H_2$ plus CO mole fraction will be significant, and the Reducer performance will be limited. In this case, through much of the reactor the concentration of $H_2$, CO, $H_2O$, and $CO_2$ will remain nearly constant even through the oxygen carrier and char carbon continue to react. The chemical looping combustion process cannot be effective if this latter situation exists.

Circulating fluid bed dilute region

Additional conversion in the dilute region above the dense circulating bed is also considered, because of the potential considerable height of this region and its relatively high content of solids compared to the splash zone above a bubbling fluidized bed. The height of the dilute zone is selected so that the flux of solids at the top of the dilute zone, entering the gas outlet, results in the required solids circulation rate being carried to the cyclones, and circulated back to the base of the reactor with a portion being transported to the Oxidizer reactor. The height of this lean zone is estimated by. [5, 10]

$$\mathbf{H_l = 1/a \bullet Ln \{ (f_d - f^*) / (f_{ex} - f^*) \}}$$

Here, "a" is the decay constant for solids in the lean zone, an empirical constant estimated to be 0.1524, $f_d$ is the estimated solids volume fraction in the dense phase, $f_{ex}$ is the solids volume fraction in the entrained solids from the reactor needed to achieve the required circulation rate, and $f^*$ is the solids volume fraction at saturation in an equivalent pneumatic transport line.

In the dilute zone, with the gas velocity constant at $U_o$, this region acts like a reactor with linear, unmixed flow of gas and solids, and the solids have a decaying volume content with increased height. These assumptions lead to the relationship below:

$$\mathbf{Y_{oH2} + Y_{oCO} = B_1 + [Y_{iH2} + Y_{iCO} - B_1] \bullet \exp\left\{-2 \bullet \frac{k''_C}{B_1 \bullet C^*} \bullet \left[\frac{f^*}{U_o} \bullet B_2 + \frac{(f_d - f^*)}{U_o} \bullet B_3\right]\right\}}$$

where $B_1$, $B_2$, and $B_3$ are defined as

$$B_1 \equiv 2\bullet k''_C/C^* /( k''_{H2} + 2\bullet k''_C /C^*)$$

$$B_2 \equiv H_l - (1-\eta_d)/b \bullet \{1-\exp(-b \bullet H_l)\}$$

$$B_3 \equiv [1-\exp(-a \bullet H_l) ] /a - (1- \eta_d) / (a+b) \bullet [1-\exp(-(a+b) \bullet H_l) ]$$

In this equation, $\eta_d$ is the conversion efficiency of the lean phase reactor compared to a plug flow reactor, and b is the decay constant for the gas-particle contact inefficiency within the lean phase. Similar to the bubbling fluid bed, the circulating fluid bed Reducer performance is sensitive to the relative rates of oxygen carrier reduction and char carbon gasification:

$$(Y_{oH2} + Y_{oCO})_{min} = B_1 = 1 / \{ k''_{H2} / (2\bullet k''_C/ C^*) + 1 \}$$

Again, the oxygen carrier reaction rate constant, $k''_{H2}$, must be significantly larger than the char carbon gasification rate constant, $2\bullet k''_C/ C^*$, if the chemical looping combustion process is to be successful.

### 7.1.6 Fluidized Bed Overall Reaction Rate Constant Estimates

Kunii and Levenspiel [10] present expressions for overall reaction rate constants for bubbling and fast, circulating fluidized bed reactors. These overall rate terms are very uncertain and are based on small-scale, empirical evidence for their conceptual formulations and for the development of mass transfer coefficients and fluid bed phase distributions.

Bubbling fluid bed

The overall reaction rate constant in a bubbling fluid bed, $K_{H2}$ and $K_C$, are in the form of mass transfer resistances in series between the bubble, cloud, and emulsion phases. They are broken down here to make its components more easily understood. For the oxygen carrier overall reaction rate constant:

$$K_{H2} = [ f_b \bullet k''_{H2} + 1/(G + H) ]$$

with the following definitions:

$$G \equiv 1/(\delta_{BB} \bullet K_{bc})$$

$$H \equiv 1 / ( f_c \bullet k''_{H2} + J )$$

$$J \equiv 1 / [ 1/(\delta_{BB} \bullet K_{ce}) + 1 /(f_e \bullet k''_{H2}) ]$$

Similarly, for the char carbon overall reaction rate constant:

$$K_C = [ f_b \bullet k''_C + 1/(G + H_C) ]$$

$$G \equiv 1/(\delta_{BB} \bullet K_{bc})$$

$$H_C \equiv 1 / ( f_c \bullet k''_C + J_C )$$

$$J_C \equiv 1 / [ 1/(\delta_{BB} \bullet K_{ce}) + 1 /(f_e \bullet k''_C) ]$$

The fluidization terms in these equations are defined as

- $f_b$ = volume of total solids in the bubble phase per total volume of reactor
- $\delta_{BB}$ = volume fraction of the bubble phase within the bubbling bed reactor
- $K_{bc}$ = gas exchange coefficient between bubble phase and cloud phase, volume of gas transferred/s divided by the bubble volume, seconds
- $f_c$ = volume of total solids in the cloud phase per total volume of reactor
- $K_{ce}$ = gas exchange coefficient between cloud phase and emulsion phase, volume of gas transferred/s divided by the bubble volume, seconds
- $f_e$ = volume of total solids in the emulsion phase per total volume of reactor

In reality, these all would be functions of height within the reactor, but it is assumed here that average values representative of the entire bed can be used.

Circulating fluid bed dense region

The overall reaction rate constant in a fast, circulating fluid bed, $K_{H2}$ and $K_c$, are in the form of mass transfer resistances in series between a "core" region and a "wall" region. For the oxygen carrier overall reaction rate constant:

$$\mathbf{K_{H2} = f_{core} \bullet k"_{H2} + 1/ \{ 1/( \delta_{core} \bullet K_{cw}) + 1/ (f_{wall} \bullet k"_{H2}) \}}$$

Similarly, for the char carbon overall reaction rate constant:

$$\mathbf{K_{C} = f_{core} \bullet k"_{C} + 1/ \{ 1/( \delta_{core} \bullet K_{cw}) + 1/ (f_{wall} \bullet k"_{C}) \}}$$

The fluidization terms in these equations are defined as

- $f_{core}$ = volume of total solids in the core region per total volume of reactor
- $\delta_{core}$ = volume fraction of the core region within the fast bed reactor
- $K_{cw}$ = gas exchange coefficient between core and wall regions, volume of gas transferred/s divided by the core volume, seconds
- $f_{wall}$ = volume of total solids in the wall region per total volume of reactor

Kunii and Levenspiel [10] and others (e.g., Abba [5]) offered suggested values and correlations for the various fluidization terms in these equations. These terms are functions of the carrier, char, and ash particle characteristics (density, particle diameter, particle shape factor, mixture bulk density, and bulk voidage), the gas properties at the Reducer temperature (density, viscosity, diffusivity of reacting species $H_2$, CO, $H_2O$, and $CO_2$), the basic fluidization factors at the Reducer conditions (minimum fluidization velocity, particle terminal velocity, Archimedes Number), the Reducer operating conditions (temperature, velocity), and the Reducer vessel diameter. Some of the terms are simply provided by judgments based on expectations. To reduce the uncertainty associated with the estimation of these terms, experimental values generated under sub-scale, pilot simulation conditions are needed.

# 7.2 Oxidation Reactor

## 7.2.1 Chemical Reactions

### *7.2.1.1 Metal Oxide Reactions*

The main reaction for $Fe_3O_4$ oxidation is

$$O_2 + 4\ Fe_3O_4 = 6\ Fe_2O_3$$

### *7.2.1.2 $CaSO_4$ Reactions*

The oxidation of CaS can result in $CaSO_4$ or the decomposition to CaO and $SO_2$.

$$O_2 + 1/2\ \ CaS = 1/2\ \ CaSO_4$$

$$3/2\ O_2 + CaS = CaO + SO_2$$

### *7.2.1.3 Combustible Reactions*

Combustibles such as char carbon from the Reducer, or $H_2$ and CO from the fuel recovery/$CO_2$ purification system have the following reactions:

$$O_2 + C = CO_2$$

$$1/2\ O_2 + H_2 / CO = H_2O / CO_2$$

## 7.2.2 Reaction Kinetics in the Oxidizer

### *7.2.2.1 Metal Oxide Oxygen Carrier Oxidation*

The reaction kinetics expression for different metal oxide carriers depends on a variety of factors: metal oxide type, particle size, particle voidage distribution, particle grain size distribution, reactor temperature, gas-particle velocities in the reactor, equilibrium constraints, etc. Over the ranges of the variables it is possible for different reaction resistances to dominate: diffusion of the reactive gas species from the gas phase to the carrier particle surface, diffusion of the reactive gas species through the particle pores, diffusion of the reactive gas species through the reaction product layer to the reaction interface, chemical reaction rate itself, diffusion of the reaction products out of the grains and pores.

It is assumed that in the fluidized bed environment, with the particle sizes characteristic of high-velocity fluidized beds, at the reactor temperatures selected, and with metal oxide carriers typical of those described in the literature, the equilibrium constraints will be insignificant, and the kinetics can be described by a form suggesting the gas species diffusion through the particle grains dominate the reaction resistances:

$$\mathbf{d\ X_S\ /dt = 3\ /\tau \bullet (1 - X_S)^{2/3} = 3 \bullet b \bullet k \bullet C_{O2}^{\ N} /(\ \rho_m \bullet r_g) \bullet (1 - X_S\ )^{2/3}}$$

where $X_S$ is the fraction of the metal oxide converted, $\tau$ is the time for complete carrier particle reaction with fixed reaction gas concentration $C_{O2}$, b is the reaction coefficient (moles of metal oxide converted per mole of $O_2$), k is the kinetic rate constants as determined by experimentation

at representative conditions in reactant gas, $C_{O2}$ is the molar concentration of gaseous reactant, N is the empirical reaction order, $\rho_m$ is the molar density of the carrier particle (moles of reactive oxide per particle volume), and $r_g$ is the representative particle grain radius. For $Fe_2O_3$ the value of b is 4.

Literature data is available for many metal oxide types that fit this expression. TGA tests may be performed to generate data that can provide an empirical fit of reaction rate versus conversion level ($X_S$) over a range of temperatures, reactant gas compositions, and particle sizes and generate an entirely empirical expression that can be used for engineering estimates without identifying specific reaction mechanisms. In general, at the reaction conditions of interest, it is observed that the reaction rate is not sensitive to particle size or gas pressure.

Test data reported by Abad [3] for the oxidation of $Fe_3O_4$ to $Fe_2O_3$ is

$$\mathbf{k(m/s) = 0.00031 \bullet \exp\{-14/(R \bullet T)\}}$$

where the gas constant R has a value of 0.008314 kJ/mol-K.

T is the reactor temperature in K

$$r_g(m) = 2.6 \times 10^{-7}$$

$$N = 1$$

In applications, $Fe_2O_3$ particles having undergone partial reduction to $Fe_3O_4$ will be oxidized back to near total $Fe_2O_3$ in the oxidizer.

#### *7.2.2.2 $CaSO_4$ Oxygen Carrier Oxidation*

The oxidation of CaS to $CaSO_4$ in $O_2$ has been characterized to only a limited extent in the literature. The reaction rate for this conversion is dependent on the limestone source used, as well as the limestone particle size and the reaction conditions.

Song, et al [6] tested natural anhydrite ore, 0.15 to 0.2 mm diameter, for multi-cyclic reduction to CaS in a small fluidized bed system. From this data the average conversion rates of reduction and oxidation are estimated and are used for estimating the relative rate of the reduction and oxidation reactions:

$dX_S/dt$ (average reduction) = 0.0002 1/s with conditions 950°C, and 75% $H_2$ + CO mixture

$dX_S/dt$ (average oxidation) = 0.0004 1/s with conditions 950°C, and 5% $O_2$

From these values, the time for complete oxidation of a CaS particle in 100 percent oxygen is estimated to be 524 seconds at 950°C.

It is assumed that a similar reaction rate form to that used by Abad [3] for metal oxide carriers could be used:

$$\mathbf{d\,X_{Ca}/dt = 3/\tau_{Ca} \bullet (1 - X_{Ca})^{2/3} = 3 \bullet b \bullet k_{O2} \bullet C_{O2}^{\,N}/(\rho_m \bullet r_g) \bullet (1 - X_S)^{2/3}}$$

Here, $\tau_{Ca}$ is the complete reaction time at the reactant gas concentration used in the original reaction test, and $X_{Ca}$ is the fraction of the CaS converted to $CaSO_4$, assuming the particle was initially 100 percent CaS.

Analysis of the Song, et al data [6] gives:

$$\mathbf{d\ X_{Ca}\ /dt = A \bullet exp\{ - E_a / (R \bullet T)\} \bullet ( 1- X_{Ca} )^{2/3} \bullet Y_{O2}}$$

$A = 32.5$ 1/s

$E_a = 70.1$ kJ/mole

### 7.2.3 Fluidized Bed Oxidizer Assumptions and Conversion Expressions

The fluidized bed Oxidizer can range in operating velocity for levels that generate bubbling bed behavior to fast, circulating bed behavior. These two operating regimes for fluidized bed reactors are characterized by differing solids voidages and gas-solids mixing rates that influence their reaction performance and vessel dimensions. Both regimes are considered in this report.

The following general assumptions suitable for fluidized bed reactors are applied:

- bed temperature is uniform throughout
- air is fed at the base of the fluidized bed in sufficient quantity convert the $Fe_3O_4$ and all other combustibles with an appropriate excess $O_2$ content at the reactor top
- the major portion of the Oxidizer reactor is devoted to the slow reactions related to oxygen carrier oxidation, with char carbon and injected $H_2$ and CO being quickly consumed
- $O_2$, $H_2$, $H_2O$, CO, $CO_2$, Q, and Ar are the only significant gas phase constituents
- solids (ash particles and oxygen carrier particles) are uniformly mixed within the fluidized bed reactor, meaning that the solids outlet stream has an average conversion of ash and oxygen carrier ($\underline{X}_S$ or $\underline{X}_{Ca}$ ) that is equal to the average oxygen carrier conversion within the fluidized bed reactor
- the average reaction rate of oxygen carrier within the fluidized bed reactor is estimated using the integral average of the rate expression, resulting in the average rate being proportional to $3/5 \bullet [ (1-X_1)^{5/3} – (1-X_2)^{5/3}]/(X_2-X_1)$. $X_1$ is the inlet oxygen carrier average conversion to the reactor product form, and $X_2$ is the outlet oxygen carrier average conversion, for either $Fe_2O_3$ or $CaSO_4$ based carriers.

The fluidized bed reactor consists of gas voids, or bubbles, that contain very little particulate and pass upward through the bed. Most of the reaction gas is contained within this bubble phase, and the reaction gas species are transported from the bubble phase to the particulate phase by various convective and diffusional processes that contribute large resistances to the overall rate of reaction conversions. Overall reaction constants can be defined and estimated using correlations in the literature.

Within the fluidized bed reactor, oxidation reaction rate constants are defined that express the rate per unit volume of solids:

$$\mathbf{k''_{O2},\ 1/s = 3\ k_{O2}\ /r_g \bullet Vs \bullet\ (1 – \underline{X}_S)^{2/3}}$$

Here, Vs is the volume fraction of oxygen carrier solids within the particulate mixture. The solids mixture consists of oxygen carrier particles, and ash particle fed from the Reducer reactor.

Bubbling bed or circulating bed dense region

A differential $O_2$ balance on the horizontal plane through the reactor is given by

$$\mathbf{d(U \bullet Y_{O2})/dz = - K_{O2} \bullet Y_{O2}}$$

U is the superficial velocity through the bed at elevation z above the base, $K_{O2}$ is the overall fluidized bed reaction constant for oxygen carrier reaction with $O_2$, $Y_{O2}$ is the $O_2$ mole fraction at elevation z.

The gas velocity through the Oxidizer reactor decreases slightly from top to bottom, and is assumed constant in the differential equations

then

$$\mathbf{d\{U \bullet Y_{O2}\}/dz = - K_{O2} \bullet Y_{O2}}$$

where U is the inlet gas velocity within the reactor. The above differential equation can be solved: at the top of the bubbling bed or circulating bed dense zone

$$\mathbf{Y_{oO2} / Y_{iO2} = exp\{ - K_{O2} \bullet H_d / U \}}$$

The term $YiO_2$ is the mole fractions of $O_2$ at the base of the fluidized bed. U is the gas superficial velocity at the base of the dense fluidized bed reactor. $H_d$ is the height of the dense fluidized bed.

Circulating fluid bed dilute region

Additional conversion in the dilute region above the dense circulating bed is also considered, because of the considerable height of this region and its high content of solids compared to the splash zone above a bubbling fluidized bed. The height of the dilute zone is selected so that the flux of solids at the top of the dilute zone, entering the gas outlet, results in the required solids circulation rate being recirculated through cyclones to the base of the reactor and being transported to the Reducing reactor. This height is given by

$$\mathbf{H_l = 1/a \bullet Ln \{(f_d - f^*)/(f_{ex} - f^*)\}}$$

Here, "a" is the decay constant for solids in the lean zone, an empirical constant estimated to be 0.1524, $f_d$ is the estimated solids fraction in the dense phase, $f_{ex}$ is the solids volume fraction in the entrained solids from the reactor needed to achieve the required circulation rate, and $f^*$ is the solids volume fraction at saturation in an equivalent pneumatic transport lime.

In the dilute zone, with the gas velocity constant at U and this region acting like an reactor with linear, unmixed flow of gas and solids, the solids having a reduced volume content with increased height,

$$\mathbf{Ln\left(\frac{Y_{iO2}}{Y_{oO2}}\right) = k''_{O2} \bullet \frac{f^*}{U} \bullet \left[ H_l - \frac{(1-\eta_d)}{b} \bullet \{1 - exp(-b \bullet H_l)\} \right]}$$

$$+k''_{O2} \bullet \frac{f_d - f^*}{U} \bullet \left[ \frac{\{1 - \exp(-a \bullet H_l)\}}{a} - \frac{(1 - \eta_d)}{a + b} \bullet \{1 - \exp(-(a + b) \bullet H_l)\} \right]$$

### 7.2.4 Fluid Bed Overall Reaction Rate Estimates

Kunii and Levenspiel [10] present expressions for overall reaction rate constants for bubbling and fast, circulating fluidized bed reactors. These overall rate terms are very uncertain and are based on small-scale, empirical evidence for both their conceptual descriptions and the development of mass transfer coefficients and phase distributions.

Bubbling fluid bed

The overall reaction rate constant in a bubbling fluid bed, $K_{O2}$ is in the form of mass transfer resistances in series between the bubble, cloud, and emulsion phases. They are broken down here to make its components more easily understood. For the oxygen carrier overall reaction rate constant:

$$K_{O2} = [\, f_b \bullet k''_{O2} + 1/(G + H) \,]$$

$$G = 1/(\delta_{BB} \bullet K_{bc})$$

$$H = 1 / (\, f_c \bullet k''_{O2} + J \,)$$

$$J = 1 / [\, 1/(\delta_{BB} \bullet K_{ce}) + 1 /(f_e \bullet k''_{O2}) \,]$$

The fluidization terms in these equations are defined as

- $f_b$ = volume of total solids in the bubble phase per total volume of reactor
- $\delta_{BB}$ = volume fraction of the bubble phase within the bubbling bed reactor
- $K_{bc}$ = gas exchange coefficient between bubble phase and cloud phase, volume of gas transferred/s divided by the bubble volume, seconds
- $f_c$ = volume of total solids in the cloud phase per total volume of reactor
- $K_{ce}$ = gas exchange coefficient between cloud phase and emulsion phase, volume of gas transferred/s divided by the bubble volume, seconds
- $f_e$ = volume of total solids in the emulsion phase per total volume of reactor

Strictly, these all would be functions of height within the reactor, but it is assumed that average value representative of the entire bed can be used.

Circulating fluid bed dense region

The overall reaction rate constant in a fast, circulating fluid bed, $K_{O2}$, is in the form of mass transfer resistances in series between the core and wall regions. For the oxygen carrier overall reaction rate constant:

$$K_{O2} = f_{core} \bullet k''_{O2} + 1/ \{\, 1/(\, \delta_{core} \bullet K_{cw}) + 1/ (f_{wall} \bullet k''_{O2}) \,\}$$

The fluidization terms in these equations are defined as

- $f_{core}$ = volume of total solids in the core region per total volume of reactor
- $\delta_{core}$ = volume fraction of the core region within the fast bed reactor

- $K_{cw}$ = gas exchange coefficient between core and wall regions, volume of gas transferred/s divided by the core volume, seconds
- $f_{wall}$ = volume of total solids in the wall region per total volume of reactor

Kunii and Levenspiel [10] and others (e.g., Abba [5]) offered suggested values and correlations for the various fluidization terms in these equations. These terms are functions of the carrier, and ash particle characteristics (density, particle diameter, particle shape factor, mixture bulk density, and bulk voidage), the gas properties at the Oxidizer temperature (density, viscosity, diffusivity of reacting species $O_2$, and $CO_2$), the basic fluidization factors at the Oxidizer conditions (minimum fluidization velocity, particle terminal velocity, Archimedes Number), the Oxidizer operating conditions (temperature, velocity), and the Oxidizer vessel diameter. Some of the terms are simply provided by judgments based on expectations. To reduce the uncertainty associated with the estimation of these terms, experimental values generated under sub-scale, pilot simulation conditions are needed.

# 8 Summary, Recommendations, and Conclusions

An emerging, coal-fired power plant technology, CLC, is assessed in this report. CLC technology is, in essence, an oxycombustion technology being developed with focus on its perceived potential for improved performance and reduced cost. Its benefits are measured against performance and cost of the conventional PC power plant using amine-based $CO_2$ absorption for post-combustion carbon capture.

In CLC, the oxygen carrier particles replace the oxygen source, air or air separation unit (ASU)-derived oxygen, used in the conventional PC plant or in the oxycombustion PC plant. A key variable in the CLC technology is the type of oxygen carrier applied in the process reactors. CLC reference plant configurations for two types of oxygen carriers are assessed in this document. The two oxygen carrier types considered are an iron-based carrier, $Fe_2O_3$ supported on alumina, and $CaSO_4$ generated by limestone sulfation. These two oxygen carriers represent alternative approaches to CLC, the first using highly reactive, but expensive, metal oxide applied on a fabricated particle structure, and the second using lower-reactivity, but cheaper, oxygen carrier material.

Several CLC process concepts were considered for the reference plant design including bubbling fluidized beds, circulating fluidized beds, and moving beds. A circulating fluid bed CLC process design was selected. The Reducer and Oxidizer reactors are circulating fluidized beds operated with high gas velocities and with temperatures, pressure drops, solids circulation rates, and off-gas compositions characteristic of the oxygen carrier properties. The significance of these characteristics is described in this document.

Reference CLC power plant performance and cost have been estimated for these two oxygen carriers by means of process simulation to generate power plant energy and material balances. The reference CLC plant concept includes supercritical steam cycle and conventional carbon dioxide compression technology. Plant material and energy balance results are reported in Section 4. Integrated with the process simulation has been CLC reactor modeling to estimate main reactor performance and dimensions, as outlined in Section 7.

The results indicate that:

- The $Fe_2O_3$ oxygen carrier CLC power plant has higher plant efficiency and lower plant capital cost, but the $CaSO_4$ oxygen carrier CLC power plant has lower cost of electricity
- This lower COE is a direct result of the expected higher price of the makeup $Fe_2O_3$ oxygen carrier relative to the lower price for a $CaSO_4$ oxygen carrier makeup limestone
- Both CLC reference power plants show a sizable COE advantage over the comparable conventional PC power plant with amine-based carbon capture
- The carbon capture efficiency of the $CaSO_4$ oxygen carrier CLC plant, at 91.4 percent, is less than that of the $Fe_2O_3$ oxygen carrier CLC plant due to $CO_2$ losses in the CLC processing that ensures that fuel constituents (CO and $H_2$) are not lost and the $CO_2$ product stream is sufficiently pure
- Alternative processing can be applied that will produce a lower purity $CO_2$ product stream while yielding lower $CO_2$ losses

The CLC reference plant assessments have identified the status and potential issues associated with the CLC technology:

- The development status of CLC power generation is at a laboratory/bench-scale; insufficient test data and data correlation is available to project plant performance and cost with any degree of certainty.
- The Reducer reactor is complex and is the major developmental component in the CLC process.
- The Reducer reactor is a simultaneous coal gasifier and oxygen carrier reducer, and it operates at temperatures where char gasification reaction rates are relatively slow.
- The Reducer reactor char gasification efficiency may limit the CLC power plant performance.
- To minimize the Reducer reactor size and meet the carbon capture requirement, a char-oxygen carrier separation process must also be developed as part of the Reducer system.
- The char-oxygen carrier separation process requires processing very large amounts of solids, an 18 to 100 million lb/hr mixture of coal ash and oxygen carrier particles having a small content of char particles, to extract and recycle at least eighty percent of the char.
- The Reducer off-gas (the raw $CO_2$ stream) may contain substantial $H_2$ and CO, and purification with fuel recovery may be needed to maintain the plant efficiency and to meet $CO_2$ product purity specifications.
- $CO_2$ capture efficiency as high as ninety percent may be difficult to achieve, depending on how high the Reducer reactor carbon gasification efficiency can be maintained and how low the Reducer off-gas $H_2$ and CO content will be.

There is significant uncertainty in the CLC process performance and cost for the initial set of operating conditions and design parameters selected, and sensitivity studies have been performed to assess how sensitive the CLC power plant performance and cost is to the major operating conditions and design parameters. Sensitivity studies around the CLC reference plant designs have been completed, showing that:

- Increased temperature results in reduced Oxidizer vessel height and reduced FD fan auxiliary power consumption. While these are helpful trends, these improvements will not result in significant improvements in the CLC plant performance or cost. It is concluded that the best operating temperature for the Reducer and Oxidizer vessels with respect to operational reliability and oxygen carrier durability needs to be identified experimentally. The benefits of temperature increases above this best-temperature can then be considered relative to the detrimental impacts of these increases.
- As the Reducer velocity increases, the vessel shell diameter decreases, but does not approach a vessel size that could be shop fabricated. Increasing velocity also results in greatly increased Reducer vessel height with a moderate increase in the off-gas $H_2$ and CO content.
- There is certainly no clear benefit resulting from increased Reducer velocity for either of the two oxygen carrier types. The impact on reactor footprint versus reactor vessel height needs to be assessed for given plant sites to provide further perspective and a basis for judging these sensitivity results.
- A similar trend is shown for the Oxidizer velocity sensitivity. Increasing the Oxidizer velocity for both types of oxygen carriers yields a reduction in the Oxidizer shell

diameter, which is beneficial. This is accompanied by an increase in the Oxidizer vessel height and the Oxidizer FD fan power consumption due to higher Oxidizer vessel pressure drop. Again, it is concluded that there is no clear benefit to be shown for increasing the Oxidizer velocity.

- It should also be noted that operating velocities above 30 ft/s enter a region of limited commercial operational experience in circulating fluid beds and would require significant development effort.
- The benefit of the char-oxygen carrier separator appears to be clear. Without char-oxygen carrier separation the Reducer vessel height and vessel cost are dramatically increased to a point where the Reducer would not be a feasible reactor to construct and install.
- When using char-oxygen carrier separation, increased carbon gasification efficiency results in moderately greater Reducer vessel heights and vessel costs, with slightly decreased off-gas $H_2$ and CO content. Increased carbon gasification efficiency will only serve to increase the plant $CO_2$ capture efficiency and will not impact the power plant thermal efficiency significantly since all of the carbon not gasified in the Reducer will be burned in the Oxidizer reactor.
- There appears to be little need for Reducer carbon gasification efficiency greater than that needed to achieve 90 percent carbon capture efficiency.
- The greatest need is to develop technically feasible and affordable char-oxygen carrier separation approaches for achieving even this limited level of carbon gasification efficiency. The technology challenge is the very high rate of solids flow having very small content of char that are characteristic of these CLC processes.
- Lower levels of oxygen carrier conversion will result in higher reactivity oxygen carrier, and lower Reducer off-gas $H_2$ and CO contents. Lower levels of oxygen carrier conversion also result in moderately higher Oxidizer FD fan power consumption, and a very large increase in the oxygen carrier circulation rate.
- With the $Fe_2O_3$ oxygen carrier, the oxygen carrier is inherently of high reactivity, and higher conversions can be applied to avoid the huge oxygen carrier circulation rates that would result at low oxygen carrier conversion. The reference plant conversion level of about sixty-nine percent appears to be a good design choice.
- The $CaSO_4$ oxygen carrier is a low reactivity material, with inherently low oxygen carrier circulation rates. Operating at lower levels of oxygen carrier conversion results in a relatively high reactivity in the Reducer, and also gives oxygen carrier circulation rates that are low compared to those found for the $Fe_2O_3$ oxygen carrier. Again, the $CaSO_4$ oxygen carrier Reference plant conversion of about nineteen percent appears to be a good design choice.
- Large oxygen carrier circulation rates are relatively easy to accommodate when using circulating fluidized bed reactors, because the Reducer and Oxidizer off-gases are the transport gases for the circulating solids and can generate high circulation rates if required. High rates are more costly and consume more auxiliary power with other reactor types of reactors, such as bubbling fluidized beds or moving beds. In these types of reactors the oxygen carrier circulation system is a completely independent equipment system, and a separate transport gas system is needed.
- The $Fe_2O_3$ oxygen carrier has an expected price of \$1/lb to \$5/lb, and with high makeup rates the COE could exceed the COE of the conventional PC plant. For the $Fe_2O_3$ oxygen

carrier CLC power plant to have lower COE than the $CaSO_4$ oxygen carrier CLC power plant the $Fe_2O_3$ makeup rate will need to be quite low. Minimizing $Fe_2O_3$ oxygen carrier losses is a priority for process development.

- The $CaSO_4$ oxygen carrier, even if at a relatively high limestone price, can accommodate high makeup rates and maintain a COE significantly lower than the conventional PC plant. At the lower price assumed in the reference plant design, the limestone makeup rate is not a significant consideration.
- In the reference plant evaluations, the hypothetical char-oxygen carrier separation system was assumed to have zero cost. It is found that the capital cost of the char-carrier separation system is not likely to have a significant impact on the CLC power plant COE. The performance and reliability of the char-carrier separation system, though, will be critically important.

At this early stage of development of CLC technology the uncertainties in its performance and cost are great. The process simulations in this report have shown the possibility that CLC could provide sizable performance and cost advantages over conventional PC power plants using conventional, amine-based $CO_2$ capture technology. These findings may be optimistic given that the CLC plant operability and availability are assumed in this report to be the same as that of the conventional PC power plant. Operability and reliability issues are likely to represent the major challenges to be dealt with in continued, larger-scale development of CLC technology and may limit the technology's ultimate feasibility.

# 9 References


1. U.S. Department of Energy (DOE), National Energy Technology Laboratory (NETL). (November 2010). *Cost and Performance Baseline for Fossil Energy Plants, Volume 1: Bituminous Coal and Natural Gas to Electricity* (DOE/NETL-2010/1397). Pittsburgh, Pennsylvania.
2. U.S. Department of Energy (DOE), National Energy Technology Laboratory (NETL). (January 2012). *QGESS: Process Modeling Design Parameters.* (DOE/NETL-341/081911). Pittsburgh, Pennsylvania.
3. Abad, A., et al. (2007) "Mapping of the Range of Operational Conditions for Cu-, Fe-, and Ni-Based Oxygen Carriers in Chemical Looping Combustion," *Chem. Eng. Sci.,* 62,533-549.
4. Andrus, et al. (June 2006). *Hybrid Combustion-Gasification Chemical Looping Coal Power Technology Development, Phase II - Final Report*. Report # PPL-06-CT-27.
5. Abba, A., J. R. Grace, H. T. Bi, and M. L. Thompson. (2003). "Spanning the Flow Regimes: Generic Fluidized-Bed Reactor Model." *AIChE Journal*, 49(7), 1838-1848.
6. Song, et al. (2008). "$CaSO_4$ Reduction Kinetics from Effect of Temperature on Reduction of $CaSO_4$ Oxygen Carrier in Chemical Looping Combustion of Simulated Coal Gas in a Fluidized Bed Reactor." *Ind. Eng. Chem*. Res. 47, 8148 – 8159.
7. Tian, H., and Q. Guo. (2009). "Investigation into the Behavior of Reductive Decomposition of Calcium Sulfate by Carbon Monoxide in Chemical-Looping Combustion," *Ind. Eng. Chem.* Res., 2009, 48, 5624-5632.
8. Qilei Song, Rui Xiao, Zhongyi Deng, Wenguang Zheng, Laihong Shen, and Jun Xiao. (2008). "Multicycle Study on Chemical-Looping Combustion of Simulated Coal Gas with a $CaSO_4$ Oxygen Carrier in a Fluidized Bed Reactor." *Energy & Fuels*, 22, 3661–3672.
9. Johnson, J. L. (1981). "Fundamentals of Coal Gasification." Chapter 23 in *Chemistry of Coal Utilization*, editor M. A. Elliott: John Wiley & Sons, New York.
10. Kunii, D., and O. Levenspiel. (1997). "Circulating Fluidized Bed Reactors." *Chemical Engineering Science*, 52(15), 2471-2482.
11. White, V. (January 2007). *Purification of Oxyfuel Derived $CO_2$ for Sequestration or EOR*. International Oxy-Combustion Research Network, Windsor, Connecticut.
12. Moran, P. P., Solex Thermal Science. (2012). *Energy Recovery Using Indirect Heat Exchange: High Temperature Mineral Applications*. Enermin 2012, 2nd Int. Seminar on Energy Management in the Mining Industry.

Robert Stevens
Robert.Stevens@netl.doe.gov

Mark Woods
Mark.Woods@contr.netl.doe.gov


**www.netl.doe.gov**
Pittsburgh, PA • Morgantown, WV • Albany, OR • Sugar Land, TX • Anchorage, AK
(800) 553-7681